

(d) Gross Structure in Reactions with ^{40}Ca on ^{40}Ca G.M. Crawley, D.K. Scott and H. Toki

The recent experiments of Frascaria et al¹⁾ have shown resonance-like structures in the energy spectra of outgoing projectile-like heavy nuclei from reactions of ^{40}Ca on ^{40}Ca at incident energies of 284 and 400 MeV, corresponding to excitation energies in the residual nuclei of approximately 25, 50, 80 and 120 MeV.

Several theoretical models, including sequential excitation and decay²⁾ and the excitation of giant resonances^{3,4)} have been proposed to explain the data. The evaporation model does not, however, seem adequate to explain the results of more recent coincidence measurements.⁵⁾ Van Giai has shown³⁾ that the mean energies of the strength distribution of giant resonances of high angular momentum appear to converge to a small value, and that giant resonance excitations are unlikely to account for the high lying structures. Calculations in the framework of TDHF suggest, however, that higher harmonics of the normal modes of giant resonances might correspond to the observed structures.⁴⁾

Recently Toki and Matsushita have considered⁵⁾ the possibility that quasi-free scattering of the incident heavy ion on light clusters in the target (p,d,t, α) might explain some of the data. Using a Fermi momentum distribution in three dimensions for the nucleons in the target, the energy distribution of each quasi-free particle is integrated from the kinematically allowed maximum angle to an empirical minimum angle. The results for $^{40}\text{Ca} + ^{40}\text{Ca}$ at 400 MeV are shown in Fig. 1, where a close correspondence with excitations observed experimentally is obtained. There is, however, at present an adjustable parameter in the calculation through the choice of the minimum angle of scattering of the quasi-free particles.

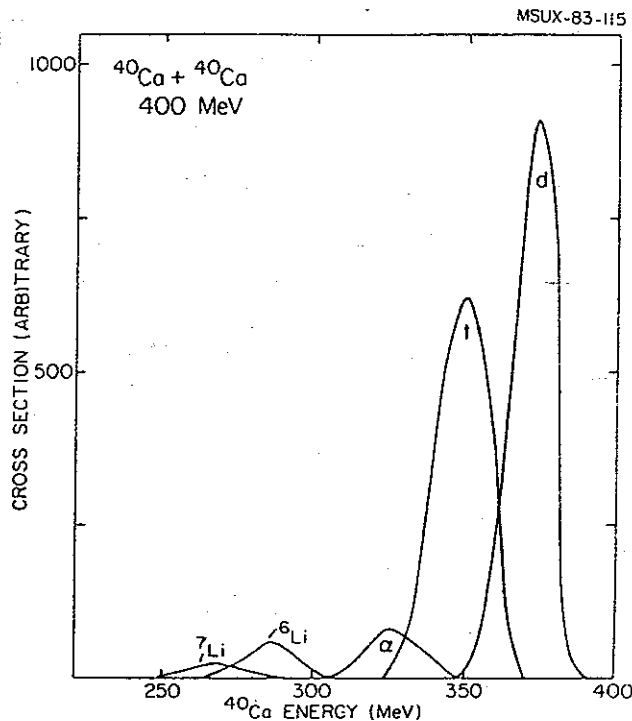


Fig. 1. Predicted energy spectrum for Ca+Ca at an incident energy of 400 MeV, producing Ca residual nuclei by quasi-free scattering on light target constituents.

Calculations have also been carried out at 800 MeV bombarding energy. According to this model, the structures should be found at different effective excitations; the observation of this effect would constitute a good test of the model. On the other hand, if the observed structures originate from giant resonance excitations, they should remain at fixed excitations when the incident energy is increased from 10 to 20 MeV/nucleon.

The experiments will be carried out using the S320 Magnetic Spectrometer, with a focal plane detection system of two position sensitive detectors, an ion chamber and focal plane scintillator. A time-zero detector is under construction which will be used in conjunction with the scintillator to measure time-of-flight, a knowledge of which is essential to resolve ambiguities in identification of heavy ions when several charge states may be present.

Depending on the outcome of these experiments we shall plan further coincidence measurements, in which the quasi-

free scattered particle is also detected. Although the quasi-free scattering model developed so far is very schematic, it serves to focus attention that some structures from this process could be present in the experimental spectra. It may well be that structures due to giant resonances and to sequential excitation and decay are also present. Experiments at different incident energies between 10 and 20 MeV/nucleon should be valuable in elucidating further the nature of these intriguing observations.

References

1. N. Frascaria, P. Colombani, A. Gamp, J.P. Garron, M. Riou, J.C. Roynette, C. Stephan, A. Ameaume, C. Bizard, J.L. Laville and M. Louvel, Z. Phys. A294, 167 (1980) and references therein.
2. D. Hilscher, J.R. Birkelund, A.D. Hoover, W.U. Schroder, W.W. Wilcke, J.R. Huizenga, A.C. Mignerey, K.L. Wolf, H.F. Breur and V. E. Viola, Phys. Rev. C20, 556 (1979).
3. N. Van Giai, Phys. Lett. 105B, 11 (1981).
4. H. Flocard and M.S. Weiss, Phys. Lett. 105B, 14 (1981).
5. J.C. Roynette, N. Frascaria, Y. Blumenfeld, J.C. Jacmart, E. Plagnol, J.P. Garron, A. Gamp and H. Fuchs, Z. Phys. A299, 73 (1981).
6. N. Matsushita and H. Toki, to be published.

B 2. CHARGE EXCHANGE REACTIONS

- (a) The (${}^6\text{Li}$, ${}^6\text{He}$), (${}^{12}\text{C}$, ${}^{12}\text{B}$) and (${}^{12}\text{C}$, ${}^{12}\text{N}$) Reactions**
- (b) Search for Pion Precursor Phenomena**

(a) The (${}^6\text{Li}, {}^6\text{He}$), (${}^{12}\text{C}, {}^{12}\text{B}$)
and (${}^{12}\text{C}, {}^{12}\text{N}$) Reactions

N. Anantaraman, S.M. Austin, A. Galonsky, L.H. Harwood

and A.F. Zeller

(i) Previous Work

Ever since the discovery, in 1975, of the giant Gamow-Teller (GT) resonance in (p,n) reactions at this laboratory,¹⁾ an active program of following up the consequences of that discovery has been under way. Among the charge-exchange experiments performed in the final years of the old (K50) cyclotron was a detailed study^{2,3)} of the ${}^{24,25,26}\text{Mg}(p,n)$ reactions, from which a variety of information was extracted. Fig. 1 shows a ${}^{26}\text{Mg}(p,n)$ spectrum measured at 25 MeV. From the variation with bombarding energy of cross sections measured for several 1^+ levels and for the 0^+ isobaric analogue state, the energy dependence of the spin-flip ($V_{\sigma\tau}$) and no spin-flip (V_{τ}) parts of the effective interaction was obtained. The integrated (p,n) cross sections for the stronger spin-flip transitions showed a general correlation with the $B(M1)$ values of the analogous M1 transitions, thereby demonstrating the similarity of the operators for the two processes. The correlation is not exact because the two operators are not identical, and the consequences of this have been explored in a recent paper by Anderson et al.⁴⁾

The availability of high-energy proton beams has resulted, in the last few years, in a dramatic advance in our knowledge of such spin excitations. Both the (p,n) and the (p,p') reactions have made significant contributions to this advance.^{5,6)} In these reactions, the dominance of the spin-transferring part of the effective interaction at high bombarding energies ($E > 100$ MeV) and low momentum transfer (small angles) allows one to cleanly observe $\Delta S = 1$

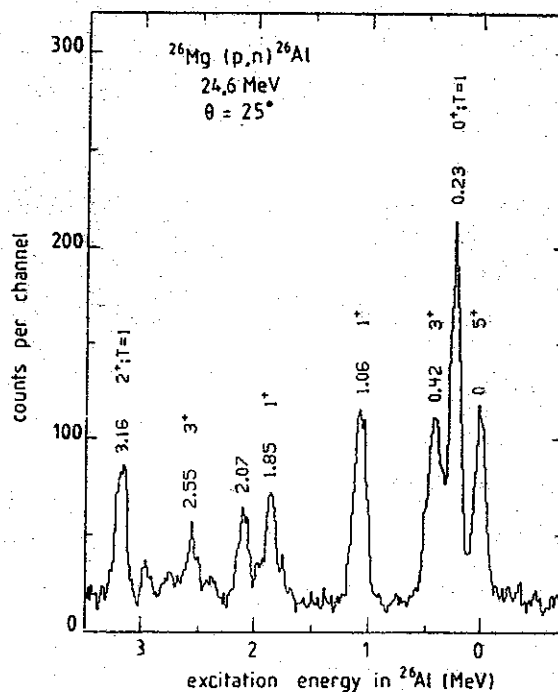


Fig. 1. Spectrum of $^{26}\text{Mg}(p,n)^{26}\text{Al}$ at 25° at a bombarding energy of 24.6 MeV.

excitations. For example, Fig. 2 shows a neutron time-of-flight spectrum at 0° for the $^{26}\text{Mg}(p,n)$ reaction measured at 135 MeV at IUCF.⁷⁾ In comparison with Fig. 1, the dominance of $0^+ \rightarrow 1^+$ transitions at the higher energy is remarkable. This makes it possible to determine the locations and strengths of all components of the Gamow-Teller excitation, and allows an important test of shell-model calculations. For example, the sharp peak seen in Fig. 2 at 13.7 MeV excitation probably corresponds to the lowest 1^+ , $T=2$ state containing a major part of the $T=2$ strength as predicted by Wildenthal.⁸⁾ The potential of such measurements for spectroscopy in the continuum is obvious. The distribution of strength with isospin is found to be unusually sensitive to the details of the configuration mixing and should help clarify the relationship of quenching observed in M1 and GT transitions.

The (p,n) and (p,p') reactions have been used to complement each other in a study of the even Ni isotopes, where the higher resolution achieved in the (p,p') reaction⁹⁾ was

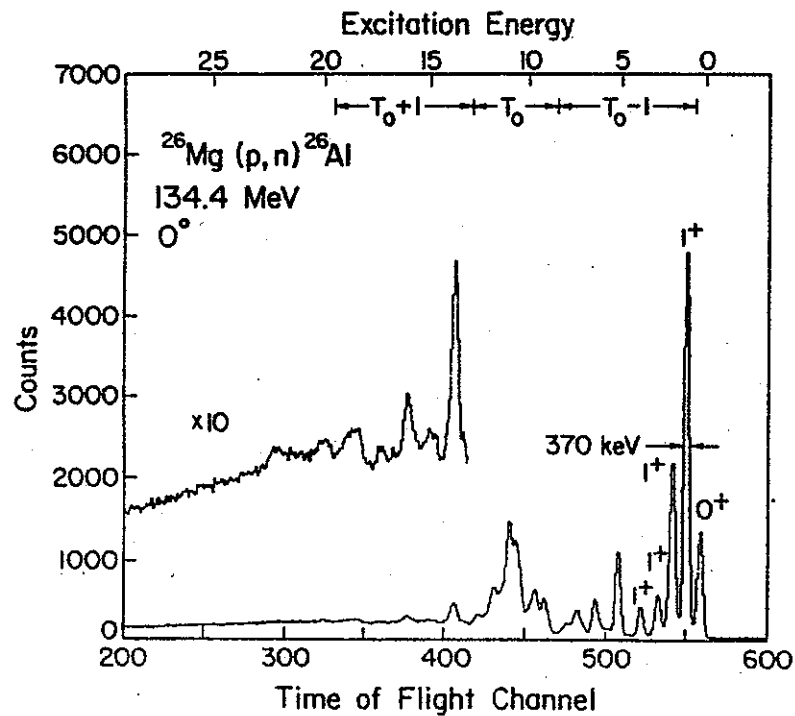


Fig. 2. Neutron time-of-flight spectrum of the $^{26}\text{Mg}(p,n)^{26}\text{Al}$ reaction at 0° at a bombarding energy of 134 MeV.

used to make isospin assignments to the rather broad structures seen in the (p,n) spectra,¹⁰⁾ as shown in Fig. 3. This made it possible to study the isospin distribution of the GT strength and compare it with model predictions. When yields of relatively sharp structures are extracted using the "experimentalist's" background shown by the solid lines in Fig. 3, a uniform reduction of the theoretical $B(\text{GT})$ values to about 0.35 of the prediction is required to bring agreement between experiment and theory for the T_0-1 and T_0 components for all four of the even Ni isotopes (Fig. 4). This is consistent with the observed quenching for sharp states excited in (p,p') reactions.⁶⁾ For the weak T_0+1 component, there are large fluctuations between experiment and (reduced) theory, presumably at least partly due to the uncertainties in the extraction of the experimental values. When all the $L=0$ strength in the background is

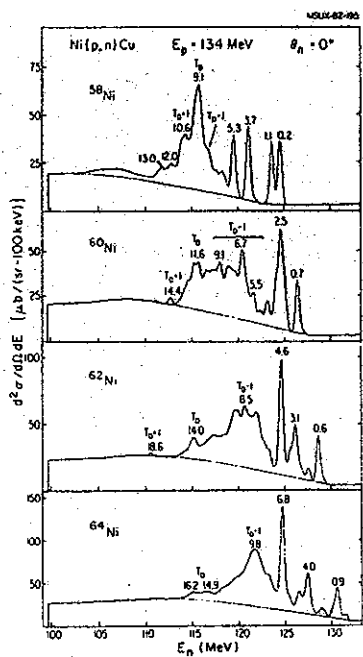


Fig. 3. Spectra of neutrons from $^{58,60,62,64}\text{Ni}(p,n)$ reactions at 0° .

included, the overall "reduction factor" rises from 0.35 to 0.54, consistent with other results.¹¹⁾

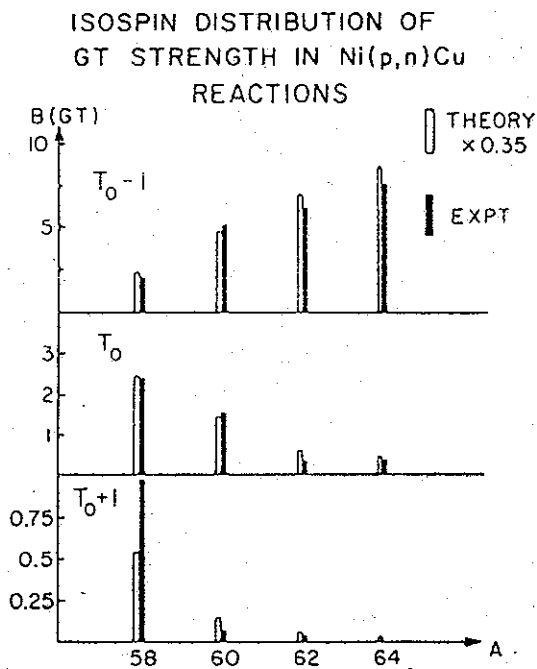


Fig. 4. Comparison of experimental and theoretical isospin distributions of Gamow-Teller strength in Ni(p,n) Cu reactions.

The calcium isotopes provide another excellent ground for studying the dependence of the spin-isospin strength on the neutron excess. Data taken at IUCF at 120 MeV (Fig. 5) are being analyzed by the thesis student of one of us (S.M. Austin).¹²⁾

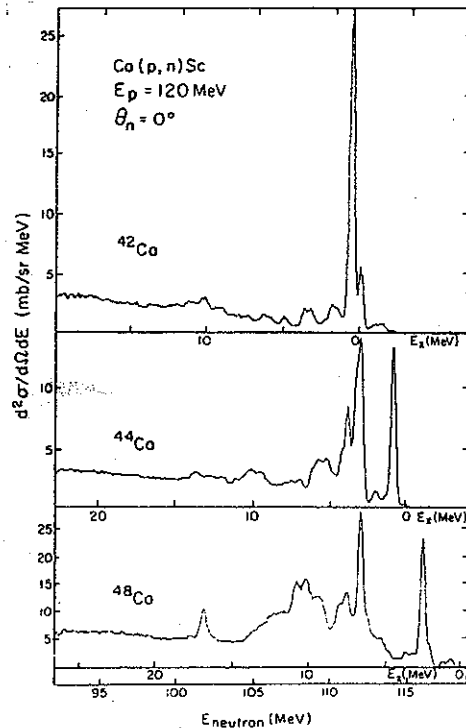


Fig. 5. Spectra of neutrons from $^{42,44,48}\text{Ca}(p,n)$.

(ii) Future Research

Perhaps the most important problems involving spin transfer strength are:

- (1) Obtaining better estimates of the $L=0$ strength above the main GT peak so as to elucidate the mechanisms responsible for quenching the GT strength;
- (2) Obtaining information about the location and strength of the higher multipolarity spin resonances; and
- (3) Investigating reactions analogous to β^+ decay.

It appears that heavy-ion induced charge exchange reactions may, for reasons outlined below, make substantial contributions to these problems. The early stages of the research will of necessity be devoted to establishing the

validity of the heavy-ion probe.

In charge-exchange reactions involving heavy ions, the possibility exists of satisfying the selection rule $\Delta S=1$ absolutely, in addition to the selection rule $\Delta T=1$. An example is the (${}^6\text{Li}, {}^6\text{He}$) reaction. Since the ground state spin-isospin combination is $(1^+, T=0)$ for ${}^6\text{Li}$ and $(0^+, T=1)$ for ${}^6\text{He}$, to first order the reaction excites only those isovector transitions in which there is a spin flip. Other examples are the (${}^{12}\text{C}, {}^{12}\text{B}$) and (${}^{12}\text{C}, {}^{12}\text{N}$) reactions. We propose studying all three of these reactions. If the results obtained in these studies suggest additional (p,n) measurements, we shall perform them at IUCF.

(a) The (${}^6\text{Li}, {}^6\text{He}$) Reaction

It appears that the high energy, high intensity ${}^6\text{Li}^{++}$ beam from the K500 cyclotron, coupled with the S320 spectrograph, has many advantages for studying spin transfer strength via the (${}^6\text{Li}, {}^6\text{He}$) reaction. Since the reaction transfers one unit of spin and isospin, only unnatural parity states can be reached from $J^\pi=0^+$ targets, and only the V_{ot} component of the effective interaction (and possibly the tensor component at high momentum transfer) contributes to the cross section in first order. Thus the background due to no-flip transitions will be absent. One hopes that general three-body background will also be smaller, as is observed for excitation of isoscalar giant resonances with heavy ions, so the presence of $L=0$ strength in the continuum will be more easily observed. Moreover, only the ground state of ${}^6\text{He}$ is particle stable; the double excitation process, so common in heavy ion reactions, will not be detected. Finally, ${}^6\text{He}$ will be the most magnetically rigid reaction product. This may make it possible to take data at 0° , a great advantage in enhancing sensitivity to $L=0$ transitions.

A number of considerations enter into the choice of energy. It must be high enough to ensure that higher order processes do not dominate the reaction mechanism. It has

been shown recently that $^{14}\text{C}(^6\text{Li}, ^6\text{He})^{14}\text{N}$ data at 34 and 62 MeV are well described by the direct one-step charge exchange process.¹³⁾ The increasing importance of V_{ot} with energy should increase the dominance of first order processes. On the other hand, the resolution will be worse at higher energies. It appears, overall, that the incident energy range from 30 to 40 MeV/u is the probable best choice. The maximum ^6He energy that can be bent in the spectrograph is about 35 MeV/u. With a 35 MeV/u ^6Li beam, a resolution of ~ 100 keV can be achieved by reducing the solid angle of the spectrograph to half its full value. This resolution is about 3 times better than has been obtained in (p,n) reactions at IUCF energies.

Compared to the (p,n) reaction, then, the ($^6\text{Li}, ^6\text{He}$) reaction is expected to have a lower background and a better resolution. Both these features should help in studying (1) weaker GT transitions than possible with (p,n) reactions and (2) higher multipole spin-flip transitions, such as spin dipole and spin quadrupole, and (3) searching for high-lying $L=0$ strength. Thus the reaction should bring new capabilities to the study of spin-flip transitions. In connection with (2) above, it is interesting to note that in a recent study of the $^{27}\text{Al}(^6\text{Li}, ^6\text{He})^{27}\text{Si}$ reaction at 93 MeV, a giant resonance with a multipolarity between 3 and 5 was found in the excitation energy range of 10-18 MeV.¹⁴⁾

When one wishes to extract quantitative information from a reaction of complex projectiles, it seems better to calibrate the reaction empirically rather than to rely on a priori DWBA calculations. A comparison will be made of the measured cross sections, corrected for obvious distortion effects, with known β -decay matrix elements for nuclei ranging from ^6Li to ^{144}Sm . The hope is to establish a calibration curve from which the β -decay matrix can be read, given the observed ($^6\text{Li}, ^6\text{He}$) cross section. We note in passing that since the isobaric analog state, so prominent in Fig. 1, should be absent, its intensity will monitor contributions

from higher order processes.

Following these measurements, should the probe prove viable, we shall search for GT strength above the main GT resonance in a variety of medium and heavy nuclei, beginning with ^{90}Zr and ^{208}Pb , and also try to find the higher L spin resonances in these nuclei. We shall also attempt to observe the weak low-lying GT strength. This strength often occurs in isolated states, and the resolution afforded by (^6Li , ^6He) will be important. In nuclei where the neutron excess is reasonably small (<10), one should see resonances having isospin T as well as T-1. Estimates of the symmetry potential and of the location of M1 strength in the target nucleus will then be straightforward.

(b) The (^{12}C , ^{12}B) and (^{12}C , ^{12}N) Reactions

The (^{12}C , ^{12}B) and (^{12}C , ^{12}N) reactions, should they proceed by a one-step process, will be a useful, and in some respects a unique probe for the study of GT transitions for the following reasons:

(1) The selection rules involved in the one-step process imply $\Delta S = 1$ and $\Delta T = 1$ (valid when the ejectiles, ^{12}B and ^{12}N , are left in their ground states, with $J^\pi = 1^+$). Then, in the limit of small momentum transfer, the reactions proceed via the $V_{\sigma\tau}$ component of the nucleon-nucleon force.

(2) The one-step operator mediating the (^{12}C , ^{12}N) reaction has a strong analogy to the operator for β^+ decay and therefore probes the β^+ strength in nuclei. Of the few available probes which sample this strength over a broad range of excitation, only the (n,p) reaction is likely to be more tractable theoretically and it presents a formidable experimental challenge at energies above 100 MeV where $\Delta S = \Delta T = 1$ is dominant in the reaction.

(3) Since the fundamental processes, $^{12}\text{B}(\text{g.s.}) \rightarrow ^{12}\text{C}(\text{g.s.})$ and $^{12}\text{N}(\text{g.s.}) \rightarrow ^{12}\text{C}(\text{g.s.})$, have "allowed" strengths ($\log ft \sim 4.0$), the GT transitions will involve a favorable light-ion vertex.

Before the (^{12}C , ^{12}B) and (^{12}C , ^{12}N) reactions can be

used as spectroscopic tools for the study of spin-dependent transitions, their reaction mechanism must be established. In this connection, we note that preliminary data on the $^{58}\text{Ni}(^{13}\text{C}, ^{13}\text{N})$ reaction at an energy of about 10 MeV/nucleon show that the final states are very selectively populated; only 1^+ and 2^- states are observed.¹⁵⁾ Our first objective will be to investigate whether a ^{12}C energy of 42 MeV/u, which will be the highest available during the initial operation of the cyclotron, is high enough to make the reactions proceed predominantly via a simple one-step mechanism, similar to that operating in (p,n) reactions at energies above 25 MeV. For this purpose, angular distributions will be measured for transitions to several low-lying, resolved states and their shapes and magnitudes will be compared with both one-step and two-step calculations. Alternatively, if one finds a simple correspondence between measured ($^{12}\text{C}, ^{12}\text{B}$) cross sections and known β -decay matrix elements, then the one-step nature of the ($^{12}\text{C}, ^{12}\text{B}$) and ($^{12}\text{C}, ^{12}\text{N}$) reactions (or at least the spectroscopic utility of the reactions) can be established without recourse to detailed calculations. Our initial list of targets includes ^{24}Mg , ^{26}Mg and ^{42}Ca .

If its one-step nature is established, the ($^{12}\text{C}, ^{12}\text{N}$) reaction may turn out to be a uniquely useful probe for β^+ strength, since it is probably easier experimentally than (n,p) and is more selective regarding angular momentum transfer than such lighter probes reactions as ($^7\text{Li}, ^7\text{Be}$). The last reaction suffers experimentally from the presence of ^7Be in both its ground and first excited states. Since ^{12}N has no particle-stable excited states, the ($^{12}\text{C}, ^{12}\text{N}$) reaction should be clean in this regard.

The β^+ strengths are of interest in astrophysics in connection with the production of light elements in explosive nucleosynthesis and the detailed evolution of supernova explosions.¹⁶⁾ In nuclear physics, one of the interests is in evaluating the β -decay sum rule¹⁷⁾ $S_-(\text{GT}) - S_+(\text{GT}) = 3(N-Z)$, where S_- is the strength for β^- and S_+ is the

strength for β^+ decay. This sum rule will be substantially modified if "quenching", e.g. due to Δ degrees of freedom,¹⁸⁾ is important. Having data on both the β^- and β^+ branches will help in determining the extent of this quenching. In a very recent paper,¹⁹⁾ it has been pointed out that the same Δ -hole mechanism which quenches the GT strength in (p,n) reactions will substantially enhance (n,p) transitions at very forward angles. Similar quenching and enhancement might be expected in ($^{12}\text{C}, ^{12}\text{B}$) and ($^{12}\text{C}, ^{12}\text{N}$) reactions, respectively.

For the same reasons as with the ($^6\text{Li}, ^6\text{He}$) reaction, the ^{12}C -induced charge exchange reactions might be useful for studying both weaker GT transitions than possible with (p,n) and higher-multipole spin-flip transitions. In particular, the kinematic matching conditions governing the reactions might favor the higher multipoles.

References

1. R.R. Doering, A. Galonsky, D.M. Patterson and G.F. Bertsch, Phys. Rev. Lett. 35, 1691 (1975).
2. W.A. Sterrenburg, S.M. Austin, U.E.P. Berg and R. DeVito, Phys. Lett. 91B, 337 (1980).
3. U.E.P. Berg, S.M. Austin, R. DeVito, A.I. Galonsky and W.A. Sterrenburg, Phys. Rev. Lett. 45, 11 (1980).
4. B.D. Anderson, R.J. McCarthy, M. Ahmad, A. Fazely, A.M. Kalenda, J.N. Knudson, J.W. Watson, R. Madey and C.C. Foster, Phys. Rev. C26, 8 (1982).
5. C.D. Goodman, Nucl. Phys. A374, 241 (1982).
6. G.M. Crawley, N. Anantaraman, A. Galonsky, C. Djalali, N. Marty, M. Morlet, A. Willis, J.-C. Jourdain and P. Kitching, in "Spin Excitation in Nuclei: 1982", ed. F. Petrovich (Plenum Press, to be published).
7. R. Madey, B.D. Anderson, J.W. Watson, A.R. Baldwin, C. Lebo, B.S. Flanders, C.C. Foster, S.M. Austin, A. Galonsky and B.H. Wildenthal, to be published.

8. B.H. Wildenthal and W. Chung, in "The (p,n) Reaction and The Nucleon-Nucleon Interaction", eds. C.D. Goodman et al., (Plenum Press, 1980), p. 89; and B.H. Wildenthal, Bull. Am. Phys. Soc. 27, 725 (1982).
9. C. Djalali, N. Marty, M. Morlet, A. Willis, J.-C. Jourdain, N. Anantaraman, G.M. Crawley, A. Galonsky and P. Kitching, Nucl. Phys. A388, 1 (1982).
10. N. Anantaraman, S.M. Austin, G.M. Crawley, A. Galonsky, H. Toki, B.D. Anderson, A.R. Baldwin, C. Lebo, R. Madey, J.W. Watson, C.C. Foster and A.G.M. van Hees, MSU 1981-82 Annual Report, and to be published.
11. J. Rapaport, Proc. Workshop on the Interaction Between Medium Energy Nucleons in Nuclei, IUCF (1982).
12. J. Narayanaswami et al., to be published.
13. A. Cunsolo, A. Foti, G. Imme, G. Pappalardo, G. Raciti, N. Saunier and B.T. Kim, Nucl. Phys. A355, 261 (1981).
14. A. Gutermann, G. Ciangaru, C.C. Chang, J.D. Silk, D.L. Hendrie, T.J.M. Symons and J. Mahoney, Phys. Rev. C27 (1983), in press.
15. W. von Oertzen, Nucl. Phys. A387, 93 (1982).
16. G.M. Fuller, W.A. Fowler and M.J. Newman, Astrophysics Journal 252, 715 (1982); G.M. Fuller, ibid 252, 741 (1982); and priv. comm.
17. C. Gaarde, J.S. Larsen, M.N. Harakeh, S.Y. van der Werf, M. Igarashi and A. Muller-Arnke, Nucl. Phys. A334, 248 (1980).
18. M. Rho, Nucl. Phys. A231, 497 (1974); A. Bohr and B.R. Mottelson, Phys. Lett. 100B, 10 (1981).
19. V.R. Brown, S. Krewald and J. Speth, Phys. Rev. Lett. 50, 658 (1983).

(b) Search For Pion Precursor Phenomena

S.M. Austin and H. Toki

It was first pointed out by Migdal¹⁾ that nuclear matter at sufficiently high density would be characterized by a pion condensed phase, the source of which is a long range ordering of nuclear spin and isospin under the influence of the tensor force. It now seems clear that such a condensation does not occur at normal nuclear densities. Hence there is no long range order, but there may be intermediate range fluctuations in the nuclear spin-isospin fields which correspond to domains of spin-isospin order; these precursor phenomena can in principle affect strongly transitions to unnatural parity states²⁾ for momentum transfers near $q=(2-3)m_{\pi}$ (Note $m_{\pi} \approx 0.7 \text{ fm}^{-1} \approx 140 \text{ MeV}/c$).

Searches for precursor phenomena have been carried out by several groups;³⁾ a measurement of ours⁴⁾ is shown in Fig. 1 and is typical of results to date. While the cross section in the region of interest somewhat exceeds the theoretical predictions, the enhancement is not strong enough to constitute an unambiguous observation of the precursor phenomenon; uncertainties in the nucleon-nucleon t -matrix and in the wave functions for such large q are of at least the same magnitude. Nor are these and other results yet a proof that precursor phenomena are not of substantial size. The uncertainties noted above prevent conclusions from factor-of-two effects. But more fundamentally, the interaction affecting the spin-isospin ordering can be described by pion exchange (longitudinal, $\sigma \cdot q$, coupling), and rho exchange (transverse, $\sigma \times q$, coupling); the tensor components of these two couplings have opposite signs and hence tend to cancel at large q . The overall effect might then be small in spite of the relatively significant effects of π exchange.

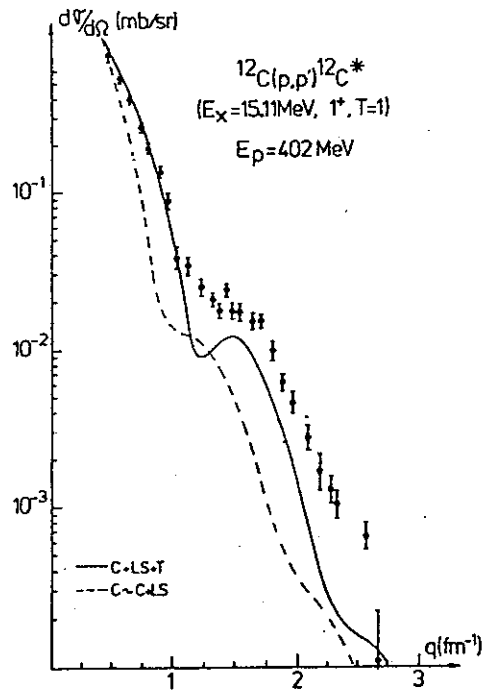


Fig. 1. Cross sections for the $^{12}\text{C}(p,p')$ reaction at $E_p=402\text{MeV}$ leading to the 1^+ states at 15.1 MeV ($T=1$) and 12.7 MeV ($T=0$). A theoretical DWIA calculation with central + spin orbit + tensor two-body t matrix is shown as a solid line.

However, $\sigma x q$ coupling cannot contribute to the ordering describing transitions to 0^- states; if pion induced ordering is large, then precursor phenomena should appear clearly in isovector transitions to such states. Indeed the DWBA reproduces the 35 MeV $^{16}\text{O}(p,n)^{16}\text{F}(0^-)$ cross sections measured recently⁵⁾ for small q , but underestimates them by more than a factor of 20 at large q . One interpretation is that precursor effects are responsible for this enhancement.

We propose to examine this possibility further by studying the $S=1$ selective $^{14}\text{C}(^6\text{Li}, ^6\text{He})^{14}\text{N}$ reaction near 35 MeV/nucleon using the S320 spectrograph (see section B2(a)); close lying but resolvable states with spins 0^- , 1^+ , 1^- , 2^- are known in ^{14}N (see Table I).

Table I

Low Lying States of ^{14}N

E_x	J_π	T
0.0	1^+	0
2.31	0^+	1
3.95	1^+	0
4.92	0^-	0
5.11	2^-	0
5.69	1^-	0
5.83	3^-	0
6.20	1^+	0

From F. Ajzenberg-Selove, Nuclear Phys. A360,1 (1981)

If precursor effects exist, the 0^- cross section should be enhanced relative to DWBA near $q \approx 2m_\pi$; other states should be less affected since the cancelling $\sigma \cdot q$ and $\sigma x q$ effects both contribute. Such a relative comparison might be less sensitive to assumptions about the t-matrix and the wave functions than an absolute comparison to theory. If a qualitatively large enhancement is observed, we will also investigate transitions to this state using the (p,n) reaction at sufficiently low energy to obtain the necessary resolution.

References

- 1) A.B. Migdal, J.E.P.T. 34, 1184 (1972).
- 2) H. Toki and W. Weise, Phys. Rev. Lett. 42, 1034 (1979).
- 3) J.R. Comfort, R.E. Segal, G.L. Moake, D.W. Miller and W.G. Love, Phys. Rev. C23, 1858 (1981) and references therein.
- 4) J.-L. Escudie, S.M. Austin, A. Boudard, G. Bruge, A. Chaumeaux, L. Farvacque, D. Legrand, J.C. Lugol, B. Mayer, P. Belery, P.T. Debevec, T. Dalbar, J. Deutsch, G. Gregoire, R. Prieels, J.M. Cameron, C. Glashausser and C.A. Whitten, Phys. Rev. C24, 792 (1981).
- 5) H. Orihara, S. Nishihara, K. Furukawa, T. Nakagawa, K. Maeda, K. Miura and H. Ohnuma, Phys. Rev. Lett. 49, 1318 (1982).

B 3. GAMMA-RAY EXPERIMENTS

(a) Discrete Line γ -ray Spectroscopy

Appendix (A): A Proposed Gamma-Ray Facility at NSCL

Appendix (B): Improvements and Innovations to Gamma-Ray Detectors

(b) Continuum γ -ray Studies

(c) The Nuclear Josephson Effect



(a) Discrete Line γ -ray Spectroscopy

R.A. Blue, Wm. C. McHarris, R.M. Ronningen and A.F. Zeller

The field of discrete line spectroscopy has advanced greatly in the last five years. One very important reason for this is that a theory, the cranked shell model¹⁾, has become a spectroscopic tool. This has stimulated a renewed interest in Compton suppression techniques and the use of large detector arrays. Currently, the mutual growth of both experimental and theoretical efforts is allowing nuclear levels with spins over $I=30\hbar$ to be observed in discrete line γ -ray spectra, along with many side bands, and interpreted in terms of the underlying shell model structure. A beautiful example of such experimental efforts is shown²⁾ in Fig. 1 where five Ge detectors with anti-Compton shields were employed.

As in the past this laboratory will try to provide the facilities for such state-of-the art experiments. (An Appendix (A) to this section describes a proposal submitted to the NSF³⁻⁶⁾ for an array of six large anti-Compton shielded Ge detectors surrounding an array of detectors which measure γ -ray multiplicity and total energy (MEHRACS)). The use of bismuth germanate (BGO) for the shields and multiplicity detector array provides a most efficient, high quality data collection facility for high spin studies. We can hope to extend our knowledge of high spin states via discrete line spectroscopy into the realm of $I > 40\hbar$. In this region one expects, for example, transitions from prolate to oblate shapes⁷⁾ in light rare earth nuclei.

The study of heavy nuclei above, in, and below the rare earth region has been a major program at MSU. High spin states and isomers in the Hf-Pb region⁸⁻¹⁴⁾ have helped identify the role of specific quasiparticles involving high-j orbitals, such as $i_{13/2}$ neutrons. This work continued to the Yb

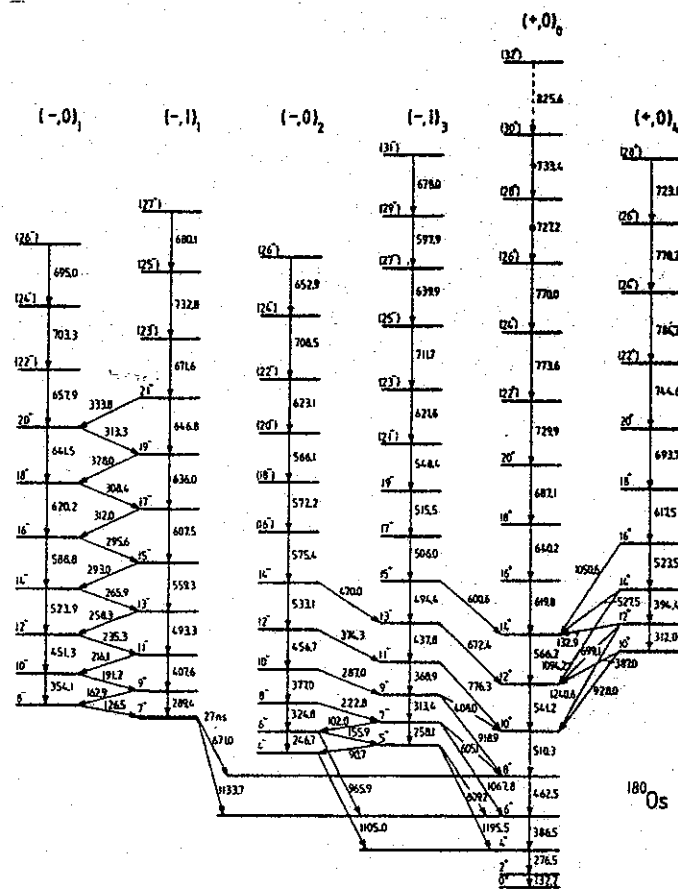


Fig. 1. Partial level scheme of ^{180}Os from Ref.2.

nuclei $^{15-20})$ in which the effects of rotational alignment on high- j particles to produce side-band structure were studied. Work has also been done and is continuing in the lighter rare earths and below, which we now discuss. These γ -ray studies complement mass measurement $^{21,22})$ and shell model studies $^{23})$ at this laboratory.

The discrete γ -ray spectroscopy of odd-mass and odd-odd nuclei, particularly those near closed shells, places stringent demands on resolution and Compton rejection because of the complexity of the spectra and because the deexcitation feeding tends to be dispersed over a multitude of states. In addition, models to describe such nuclei tend not to be so straightforward and satisfying as the collective model with its rotors, Coriolis decouplings, and back-bendings. However, odd-mass nuclei near closed shells are

receiving more attention now, and more complete shell-model calculations, together with phenomenological models such as the triaxial model and group-theoretical models such as the interacting boson model, are proving considerable insight into their structures.

One example of a systematic study of odd-mass nuclei near a closed shell is our recently completed²⁴⁻²⁶⁾ investigation of the $N=80$ nuclei, ^{143}Eu , ^{141}Pm , and ^{139}Pr . A wide variety of states is excited, and many of the lower-lying states can be explained by the simple shell model. But for states above 1 MeV this becomes increasingly difficult. (One improvement would be to perform shell-model calculations that include the $h_{11/2}$ proton in the basis set, but these are not readily available at this time.) We have just completed calculations using the triaxial model of Meyerter-Vehn²⁷⁾, and we present an illustration of this in Fig. 2 for ^{141}Pm with the $d_{5/2}$ and $g_{7/2}$ protons coupled to a triaxial core--these are compared with the experimental positive-parity states. The agreements with experiment can be said only to be adequate or indicative, although somewhat better for the negative-parity states. (There are fewer single-particle states of negative parity available for configuration mixing.) Recently, interacting boson-fermion calculations have been extended to the heavier Eu isotopes by Scholten and Blasi²⁸⁾ and extending these to nuclei below $N=82$ should provide an interesting test of the model.

Relatively little has been done with the study of odd-odd nuclei: For the most part they are not accessible (except for a few low-lying states) to radioactive decay, and their density of states makes in-beam spectroscopy a formidable and cumbersome procedure. That in-beam γ -ray spectroscopy is indeed messy was seen in the results of our just-completed study²⁹⁾ of $^{118}\text{Sb}_{67}$, in which some 41 low-spin states below 1200 keV were excited by the $(p,n\gamma)$ reaction, and the structures (even the J^π values) could be extracted for only a few of the lowest-lying states.

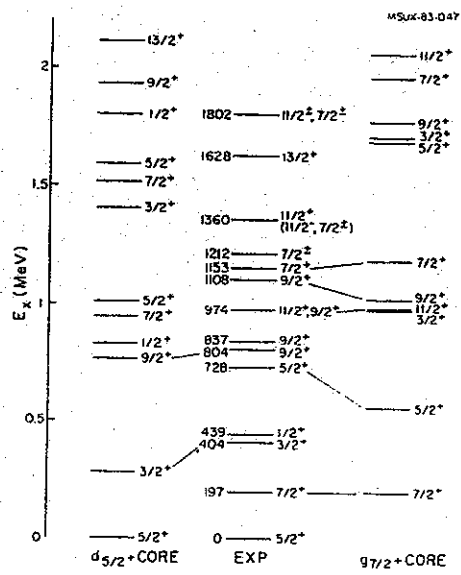


Fig. 2. Triaxial calculations for positive-parity states in ^{141}Pm produced by coupling $d_{5/2}$ and $g_{7/2}$ protons to a $\beta=0.152$, $\gamma=34^\circ$ core.

Contrasted with this is the surprising results one obtains for deformed odd-odd nuclei. In Fig. 3 we show the relatively simple level scheme that results from the $^{181}\text{Ta}(d,3n\gamma)^{182}\text{Re}$ reaction ³⁰⁾. Some 90% of the deexcitation funnels down through only two rotational bands, with most of the rest proceeding through two additional bands. Thus, it appears that only certain selected or "klokast" bands are selected for preferential depopulation ³¹⁾. The explanation for this is actually quite straightforward, the mechanism being similar to backbending ³²⁾ in reverse. A pair (or several) of decoupled particles, usually neutrons in this region, can align itself with the rotation and does so, thus selectively locking in on such bands in the deexcitation path. It can be seen that all of the states going into the rotational bands of Fig. 3 can be highly aligned, but the $9/2^+[624\uparrow]$ neutron, originating from the $i_{13/2}$ spherical state, is a particularly good candidate. In addition to the level spacings, we were able to determine a considerable

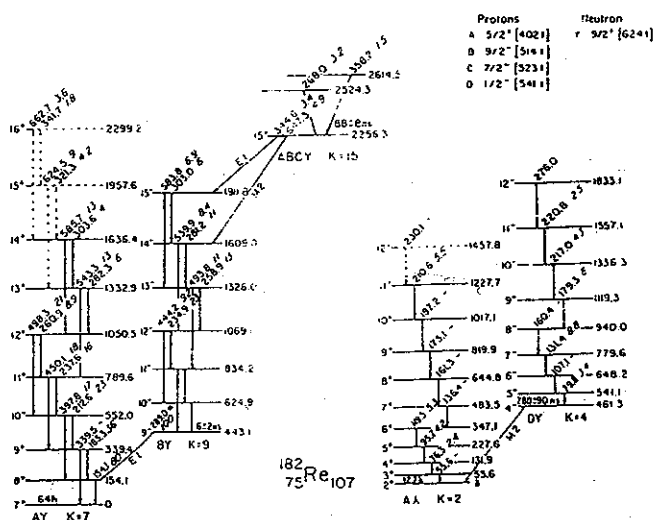


Fig. 3. Levels in deformed odd-odd ^{182}Re produced by the $^{181}\text{Ta}(d, 3n)$ reaction.

amount of information about g-factors and mixing ratios, both from angular distributions and from branching ratios. The rotational bands are quite distorted by Coriolis effects, as expected. We were not able to attain high enough values of R with our d -induced reaction to obtain meaningful information about backbending, although our data are consistent with the aligned pair rather than the pairing collapse model. However, as can be seen in Fig. 4, the moments of inertia have a surprisingly large variation from band to band. In particular, the difference between the 7^+ and 2^+ bands should be noted, for these are merely the triplet and singlet couplings of the same states. Evidently the tendency for alignment with the spin of the rotor is doing severe things to these states. (It should be noted that the relative sizes of the moments of inertia are the reverse of what would be expected from a simple Coriolis-coupling picture.) This is a problem that needs further investigation. Finally, we have identified a four-particle metastable state at 2256.3 keV. This state, although still basically prolate,

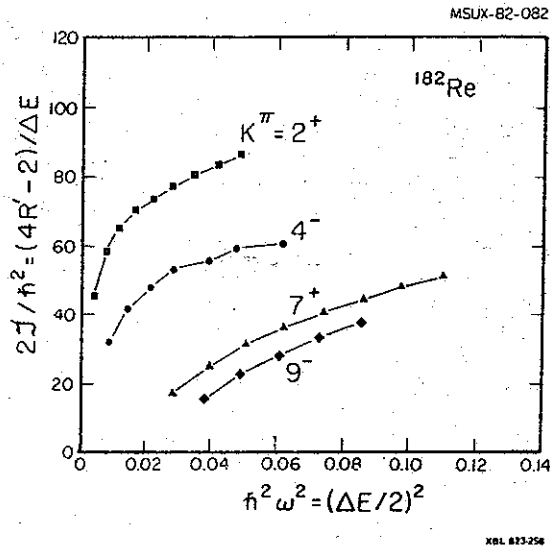


Fig. 4. Plots of the moments of inertia versus the squares of the rotational frequencies for the bands in ^{182}Re .

has an "oblate girdle" around its middle, as depicted in Fig. 5. Thus, it may indicate the beginning of a transition to "oblate-||" pseudo-rotational behavior.

Deformed odd-odd nuclei thus appear to be prime candidates for in-beam studies for a number of reasons: 1) Their spectra are much more amenable to interpretation than had been previously thought because of the selection of the preferred states for deexcitation. 2) Coriolis couplings and distortions are at a maximum, including the self-coupling of the singlet and triplet bands through the $1/2$ states. 3) Odd-odd nuclei have a head start on high-spin states and multi-particle states - one is in the same regime near their ground states as occurs above the pairing gap in other nuclei, yet with less severe collective distortions. However, one pays for these advantages making heavy-ion beams become almost mandatory: As can be seen from Fig. 3, much angular momentum is "soaked up" in single-particle motion, so large values of \vec{R} and other collective variables

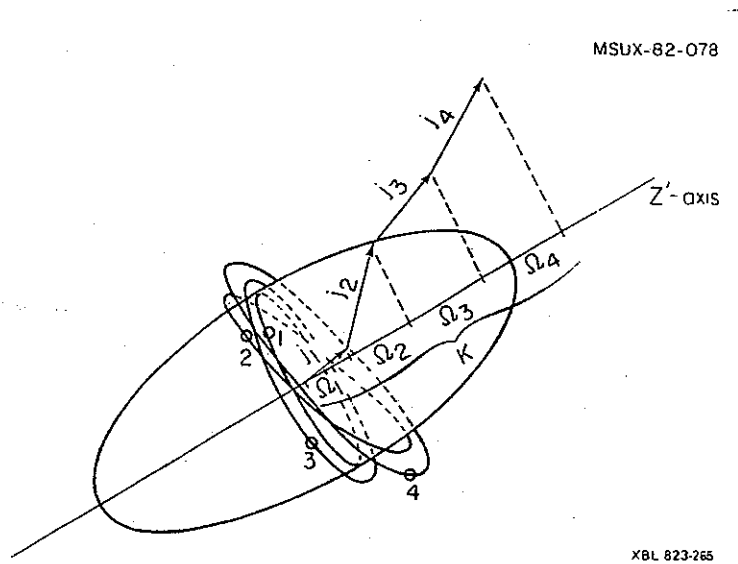


Fig. 5. Stylized representation of the four-particle isomer in ^{182}Re as an "oblate" girdle about the basic prolate core.

were simply not reached in our experiments. We thus propose to make a general, systematic study of deformed odd-odd nuclei with the heavy-ion beams available from Phase I of the NSCL, starting with further studies on ^{182}Re itself, using a ^{14}N beam on a ^{170}Er target, then progressing to the use of heavier beams. In addition, we propose to undertake systematic and complete (using both the singlet and triplet bands, which overlap to give large effects) Coriolis-coupling calculations on the states in these nuclei.

We propose to use the heavy-ion beams from Phase I of the NSCL to extend these studies to higher-spin states, both in nuclei below $N=82$ and in nuclei near other closed shells. Certainly the spectra are going to be quite complex, and calculated model agreements are not in the same stage of sophistication as in the deformed regions. However, by their very state of flux, such experiments should prove to be important in establishing and checking models--and vice versa.

The development of the Cranked Shell Model (CSM) from a theory to a spectroscopic tool has certainly been one of the advances in discrete-line γ -ray spectroscopy and nuclear structure physics in the past five years. The basis of this model is the Nilsson shell model to which pairing interactions have been added. Then the Nilsson potential is rotated and resulting centrifugal and Coriolis forces act on the nucleons moving in this potential. The Hamiltonian for the interaction is

$$h^{\omega} = h_N - \Delta(P^+ + P^-) - \lambda \hat{N} - \omega j_1.$$

Here, h_N is the Nilsson model Hamiltonian, Δ is the pairing correlation energy, P^+ and P^- are pairing operators, λ is the Fermi surface energy, \hat{N} is an average particle number, ω is the rotational frequency, and j_1 is the particle spin along the rotation axis.

The CSM solutions, the quasiparticle energies $e'(\omega)$, are found as a function of $\hbar\omega$. The states are labeled by signature ($d = \pm 1/2$, from rotational invariance 180° about the x-axis) and parity π . An example of such solutions for protons is shown in Fig. 6, from collaborative work at ORNL³³⁾ on ^{128}Ce . To compare the experimentally determined quantities (transition energies, spin and parities in the laboratory frame) to the CSM quantities, one uses the classical procedures of Routh³⁴⁾ for transforming to the rotating frame of reference. The beauty of the CSM is then most evident because there, when referred to a reference state (e.g. the quasiparticle vacuum) or configuration, quasiparticle properties such as excitation energy, angular momentum, and signature are additive. The comparison of experimental and theoretical [Routhians (e') versus $\hbar\omega$] help identify which quasiparticles involved in given quasiparticle structures as well as their excitation energies and the

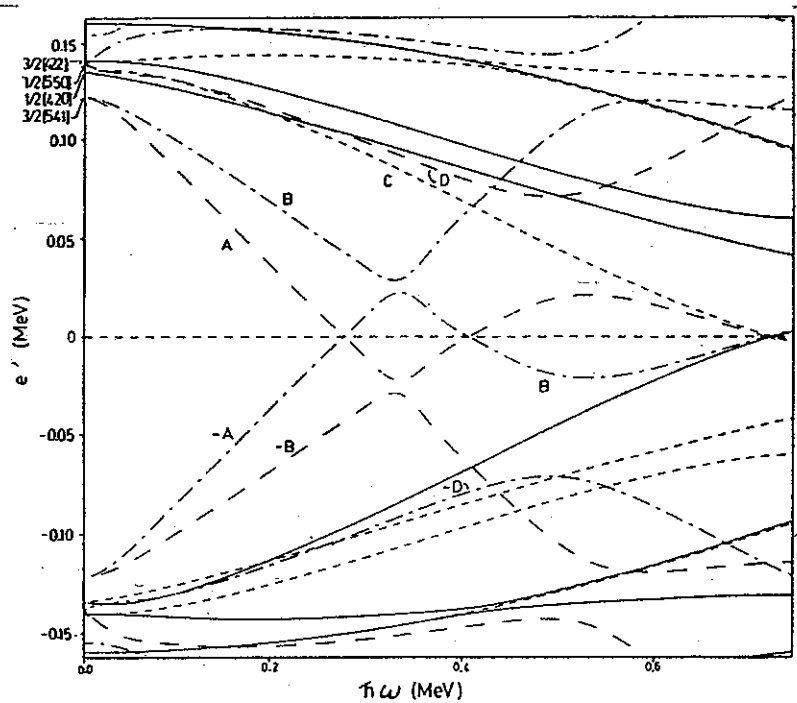


Fig. 6. Theoretical Routhian diagram for protons in ^{128}Ce .

alignment. Furthermore, the rotational frequencies at which two bands cross and the interaction strength between the bands may be obtained.

The rare earth region is now becoming a showcase for the combined power of studies of the systematical behavior of quasiparticle configurations and calculations using the CSM. Garrett et al.³⁵⁾ have identified single- and multi-quasiparticle configurations in $^{160-163}\text{Yb}$ and extracted residual two-body interactions and pairing correlation energies. These are sensitive tests of the independence of particles moving in the rotating potential, indeed the CSM approach. Similarly, because the Routhian depends on the pairing strength, the crossing frequency differences between even and odd neighbors are sensitive to the pairing interaction. These differences have been correlated to the quadrupole moments of specific quasiparticle configurations

and become a test of the multipole composition of the pairing force.³⁶⁾

Recently the Ce-Ba region has been fostering intense activity^{33,37-39)} in testing and using the CSM. High spin properties there are strongly influenced by $h_{11/2}$ proton quasiparticle configurations. And, this region is also one of shape transition where triaxial degrees of freedom may be important.³⁷⁾ The discrete line spectroscopy of ^{128}Ce was studied by us in collaboration³³⁾ with Johnson's group at ORNL. The level structure is shown in Fig. 7. It is seen that the "s-band" crosses the "g-band" at the 10^+ state.

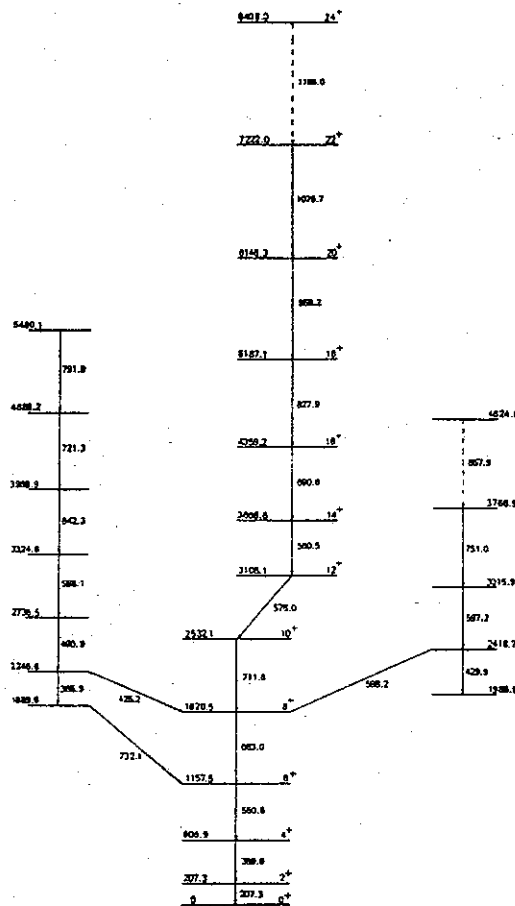


Fig. 7. Level scheme for ^{128}Ce .

The nature of the s-band is that of a decoupled $h_{11/2}$ proton pair and is well known in $^{130,132}\text{Ce}$. The crossing frequency

and alignment carried by those quasiparticles were very well predicted by the CSM. The experimental diagram is shown in Fig. 8. (The theoretical Routhian is given in Fig. 6). The crossing frequency experimentally is about $\hbar\omega = 0.315$ MeV, close to the calculated value (the frequency at which lines A and B approach in Fig. 6) of 0.317 MeV. The alignment gain is $i=8.9 \hbar$ compared to $8.4 \hbar$ from the CSM (since $e' = -\frac{di}{du}$ the alignment is deduced by adding the slopes of lines A and B).

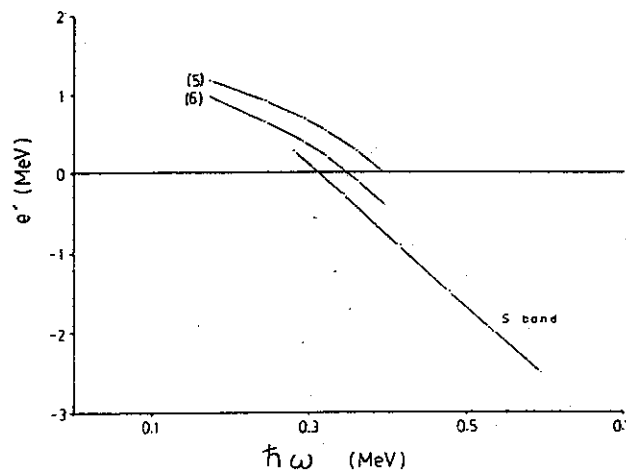


Fig. 8. Experimental Routhian diagram for ^{128}Ce .

It is becoming increasingly clear that the CSM is developing into a powerful tool for the nuclear spectroscopist. The amount of information contained in a typical Routhian as a function of spin is presently only being tested a limited way. Better tests can be made by identifying more of the intrinsic configurations and identifying the respective band members to higher spin. Experimentally this places a greater demand upon the measuring apparatus. The use of Compton suppression techniques has helped identify band crossings at high frequencies. In ^{180}Os crossings at frequencies for which $0.32 < \hbar\omega < 0.38$ are thought due to alignment of proton quasiparticle configurations.²⁾ The neutron configurations have crossings where $0.25 < \hbar\omega < 0.32$.

Currently, one of the most basic pieces of equipment needed in the study of high spin states is a total energy-multiplicity filter. This device can help eliminate low multiplicity events such as from radioactivity and some Coulomb excitation events, thus enhancing the ability to detect high-spin states. Such a filter can help separate reaction channels as well. The latter is particularly important because the emphasis in high spin structure is on nuclei far from stability where many channels can become available after compound nuclear formation. In our study of ^{128}Ce using the $^{20}\text{Ne} + ^{112}\text{Cd}$ at 103 MeV twelve 5-, 4- and 3-particle reaction channels were observed of which only the 4n channel was of main interest to us. Using MEHRACS excellent total energy and multiplicity information will be obtained (see appendix to this section). This laboratory can also provide limited information on total energy or multiplicity by using four existing 3"x3" BGO detectors to surround the target. One obvious way to enhance the exit channel selection is to measure charged particle - γ coincidences. Such experiments are usually limited because of the small γ -ray detection efficiency so that a large number of high efficiency Ge detectors are needed. MEHRACS is compatible with such measurements in that the number of detectors is large and the forward direction is relatively open to installation of charged particle counters.

To take advantage of the high multiplicity of γ -rays in such reactions and to have a large meaningful event rate more than two detectors are desirable; in the ^{128}Ce study we used seven. These detectors did not have shields so that in the beamtime allotted to the experiment, while approximately 240 million coincident pair events were recorded, because the photopeak-to-total ratios of a "bare" Ge detector is about 10% only about 1% of the events were "useful" photopeak coincidences. With MEHRACS the peak-to-total ratios should be about 70%, implying 49% useful data. More importantly, 21% will be useful triple-photopeak

coincidences. Using triple coincidences one can study coincident pairs of γ -rays in coincidence with a particular transition. This would certainly enhance the information on side band structures and side feeding of levels providing important data for testing the CSM.

There is interesting work being carried out in the $A \approx 60-100$ region in terms of both nuclear structure and detection techniques. Along the stability line in this mass region the nuclei are nearly spherical. But when only a few neutrons are removed (or added), dramatic structural changes can occur, sometimes at very low spin. In $^{72,74}\text{Se}$ (Ref. 40) the deformed excited band coexists with the spherical ground band. In $^{74,76}\text{Kr}$, however, the excited band is spherical whereas the ground band transitions are surprisingly collective ($\approx 50-100$ spu)(Ref. 41). Such large deformation effects have previously been observed in this region only for neutron rich nuclei such as ^{100}Sr (Ref. 42). A possible reason⁴¹⁾ for the abrupt structure change between Ge, Se and Kr is that as Z approaches midshell values large deformations can be energetically favorable for neutrons which access the $g_{9/2}$ orbital. The importance of this orbital is already known^{43,44} from irregularities in the yrast sequences at low spin, $I \approx 8\hbar$. Ragnarsson, Nilsson, and Sheline⁴⁵⁾ expect that an island of deformation should exist in this region because $N=Z=40$ (and 60) are magic numbers for a harmonic oscillator single particle potential when $u_x = u_z = 2:1$ ($\leftarrow \approx 0.6$).

Nuclear shapes in this region compared to the rare earth region are not as well understood, and the relevant experiments can be somewhat more difficult. Beyond only a half-dozen or so neutrons from the stability line little is known. Traditional γ -ray coincidence techniques are difficult because many channels are open (x, y, z , where typically $x, y = 0, 1, 2$ and $z = 0, 1, \dots, 6$). Several groups^{41,46,47)} are measuring neutron multiplicities. The high recoil velocities in heavy ion reactions kinematically focus neutrons into the forward direction. Thus, an array of neutron

counters there will have an especially large effective solid angle. The multiplicity will help tag the exit channel. Suppression factors of unwanted channels can be ⁴⁶⁾ 10 to 100. Besides the suppression of undesirable channel photo-peaks, the correlated Compton events will also be suppressed as well so that the sensitivity to small cross sections is enhanced. This laboratory has had a long history of neutron detection and has or is planning experiments on neutron - γ coincidences. An array of neutron counters in the forward direction of MEHRACS enhances an already powerful tool. Such a combination of techniques can go far in providing a better understanding of this region.

The reaction product mass spectrometer (RPMS) may be also used for exit channel selection. In Phase I the mass selection is $M/\delta M=200$. Thus, long lived (>1 msec) residual nuclei may be transported far from the reaction chamber and beam dump to a much cleaner environment in terms of background radiations. Nearly all the spectroscopic devices typically used (γ , x, charged particle detectors) can surround the focal point of the device. The residual nucleus can be studied before and/or after its flight. During its flight the residual nucleus may have cooled to its ground state. By catching it in a lead foil, for example, one can observe Coulomb excitation lines, depending on the energy of the incident residual, providing a new means of high spin state spectroscopy for collective states in nuclei far from stability. If the product is radioactive, its decay may then be studied upon stopping in the foil by a variety of techniques. One can also replace the catcher arrangement by a target and the RPMS can act as an exotic beam facility for standard in-beam γ experiments.

MEHRACS (Appendix A) represents a state-of-the art γ -ray facility. However we also wish to remain open to possibilities of new materials and devices which have the promise of being at the forefront in the future. Some possibilities are described in Appendix B.

References

1. R. Bengtsson and S. Frauendorf, Nucl. Phys. A314, 27 (1979); Nucl. Phys. A327, 139 (1974).
2. A. Neskakis, R.M. Lieder, G. Sletten and G.D. Garrett, Proc. Conf. on High Angular Momentum Properties of Nuclei, Oak Ridge, TN, Nov. 1982, Vol. 4 of Nuclear Science Research Conference Series, to be published by Harwood Academic Publishers, New York.
3. J.X. Saladin, C. Baktash, I.Y. Lee, W. Benenson, R. Blue, R. Ronningen, and R.A. Sorensen, "Proposal for a Multi-Detector Gamma Ray Facility," submitted to the National Science Foundation, March 1982.
4. J.X. Saladin, C. Baktash, I.Y. Lee, R. Blue, R. Ronningen, and R.A. Sorensen, Bull. Am. Phys. 27, 703 (1982).
5. J.X. Saladin, C. Baktash, I.Y. Lee, R. Blue, R. Ronningen, and R.A. Sorensen, International Conference on Nucleus-Nucleus Collisions (Michigan State University, September 26-October 1, 1982).
6. J.X. Saladin, C. Baktash, I.Y. Lee, R. Blue, R. Ronningen, and R.A. Sorensen, International Workshop on Bismuth Germanate Technology, Princeton, N.J., November 1982.
7. I. Ragnarsson, T. Bengtsson, G. Leander, and S. Åberg, Nucl. Phys. A347, 287 (1980).
8. R.A. Warner, F.M. Bernthal, J.S. Boyno, and T.L. Khoo, Phys. Rev. Lett. 31, 835 (1974).
9. T.L. Khoo, F.M. Bernthal, C.L. Dors, M. Piiparinen, S. Saha, P.J. Daly, and J. Meyer-ter-Vehn, Phys. Lett. 60B, 341 (1976).
10. T.L. Khoo, F.M. Bernthal, R.G.H. Robertson, and R.A. Warner, Phys. Rev. Lett. 37, 823 (1976).
11. T.L. Khoo and G. Løvholden, Phys. Lett. 67B, 389 (1977).

12. M. Piiparinen, J.C. Cunnane, P.J. Daly, C.L. Dors, F.M. Bernthal, and T.L. Khoo, Phys. Rev. Lett. 34, 1110 (1975).
13. H. Helppi, S.K. Saha, P.J. Daly, S.R. Faber, T.L. Khoo, and F.M. Bernthal, Phys. Lett. 67B, 279 (1977).
14. T.L. Khoo, R.K. Smither, B. Haas, O. Hausser, H.R. Andrews, D. Horn, and D. Ward, Phys. Rev. Lett. 41, 1027 (1978).
15. P.M. Walker, S.R. Faber, W.H. Bentley, R.M. Ronningen, R.B. Firestone, and F.M. Bernthal, Phys. Lett. 86B, 9 (1979).
16. S.R. Faber, W.H. Bentley, R.M. Ronningen, and R.B. Firestone, Phys. Lett. 87B, 339 (1979).
17. P.M. Walker, S.R. Faber, W.H. Bentley, R.M. Ronningen, and R.B. Firestone, Nucl. Phys. A343, 45 (1980).
18. P.M. Walker, W.H. Bentley, S.R. Faber, R.M. Ronningen, R.B. Firestone, F.M. Bernthal, and J. Borggreen, Nucl. Phys., A365, 61 (1981).
19. P.M. Walker, W.H. Bentley, S.R. Faber, R.M. Ronningen, R.B. Firestone, F.M. Bernthal, J. Borggreen, J. Pedersen, and G. Sletten, Institute of Physics Conference on "Nuclear Structure and Particle Physics", Oxford University, Oxford, England, April 6-8, 1981.
20. J.L.S. Carvalho, P.M. Walker, W.H. Bentley, and S.R. Faber, Bull. Am. Phys. Soc. 25, 604 (1980).
21. R.C. Pardo, S. Gales, R.M. Ronningen, and L.H. Harwood, Phys. Lett. 21B, 41 (1980).
22. B.H. Wildenthal and E. Kashy, Exp. 82026, 82027, approved for NSCL.
23. H. Kruse and B.H. Wildenthal, MSU Cyclotron Laboratory Annual Report, 1981-1982, p.61.
24. R. Aryaeinejad, R.B. Firestone, W.H. Bentley, and Wm.C. McHarris, Phys. Rev. C23, 194 (1981).

25. R. Aryaeinejad, W.H. Bentley, P.M. Walker, R.B. Firestone, and Wm.C. McHarris, submitted to Phys. Rev. C (1983).
26. R. Aryaeinejad, R.B. Firestone, P.M. Walker, and Wm.C. McHarris, in preparation (1983).
27. J. Meyer-ter-Vehn, Nucl. Phys. A249, 11 (1975).
28. O. Scholten and N. Blasi, Nucl. Phys. A380, 509 (1982).
29. Wm. B. Chaffee, Wm. C. McHarris and W.H. Kelly, accepted for publication in Phys. Rev. C (1983).
30. M.F. Slaughter, R.A. Warner, T.L. Khoo, W.H. Kelly and Wm. C. McHarris, submitted to Phys. Rev. C (1983).
31. Wm. C. McHarris and W.H. Kelly, to be submitted to Phys. Lett. B.
32. F.S. Stephens and R. Simon, Nucl. Phys. A183, 257 (1972).
33. J.L.S. Carvalho, R.M. Ronningen, N.R. Johnson, J.S. Hattula, I.Y. Lee, M.P. Fewell, L.L. Riedinger, H. Ower, J.C. Wells, and F.M. Bernthal, International Conference on Nucleus-Nucleus Collisions (Michigan State University, September 26-October 1, 1982).
34. J.J. Routh, in "The Advanced Part of a Treatise on the Dynamics of a System of Rigid Bodies," 6 ed. (Macmillan, London, 1905).
35. J.D. Garrett, O. Andersen, J.J. Gaardhoje, G.B. Hagemann, B. Herskind, J. Kownacki, J.C. Lisle, L.L. Riedinger, W. Walus, N. Roy, S. Jonsson, H. Ryde, M. Guttormsen, and P.O. Tjøm, Phys. Rev. Lett. 47, 75 (1981).
36. J.D. Garrett, G.B. Hagemann, B. Herskind, J. Bacelar, R. Chapman, J.C. Lisle, J.N. Mo, A. Simcock, J.L. Willmott, and H.G. Price, Phys. Lett. 118B, 297 (1982).
37. J. Gizon, R.M. Diamond, and F.S. Stephens, Nucl. Phys. A290, 272 (1979).

38. P.J. Nolen, D.M. Todd, P.J. Smith, D.J.G. Love, P.J. Twin, O. Anderson, J.D. Garrett, G.B. Hagemann, and B. Herskind, *Phys. Lett.* 108B, 269 (1982).
39. P.J. Nolen, G.M. Todd, R. Aryaeinejad, D.J.G. Love, A.H. Nelson, P.J. Smith, P.J. Twin, J.D. Garrett, G.B. Hagemann, and B. Herskind, *Proc. Conf. on High Angular Momentum Properties of Nuclei, Oak Ridge, TN, Nov. 1982, Vol. 4 of Nuclear Science Research Conference Series, to be published by Harwood Academic Publishers, New York.*
40. For a review see J.H. Hamilton, A.V. Ramayya, and R.L. Robinson, *Nuclear Interactions*, edited by B.A. Robson, (Springer-Verlag, Berlin).
41. R.B. Piercey, J.H. Hamilton, R. Soundranayagam, A.V. Ramayya, C.F. Maguire, X.-J. Sun, Z.Z. Zhao, R.L. Robinson, H.J. Kim, S. Frauendorf, J. Doring, L. Funke, G. Winter, J. Roth, L. Cleemann, J. Eberth, W. Neumann, J. Wells, J. Lin, A.C. Rester, and H.K. Carter, *Phys. Rev. Lett.* 47, 1514 (1981).
42. R.E. Azuma, G.L. Borchert, L.C. Carraz, P.G. Hansen, B. Jonson, S. Mattsson, O.B. Nielsen, G. Nyman, I. Ragnarsson, and H.L. Ravn, *Phys. Lett.* 86B, 5 (1979).
43. A.P. de Lima, J.H. Hamilton, A.V. Ramayya, B. van Nooijen, R.M. Ronningen, H. Kawakami, R.B. Piercey, E. de Lima, R.L. Robinson, H.J. Kim, W.K. Tuttle, L.K. Peker, F.A. Rickey, and R. Popli, *Phys. Lett.* 83B, 43 (1979).
44. K.J. Weeks, C.S. Han, and J.P. Draayer, *Nucl. Phys.* A371, 32 (1981).
45. Ingemar Ragnarsson, Sven Gosta Nilsson, and Raymond K. Sheline, *Phys. Rep.* 45, 1 (1978).
46. J. Roth, L. Cleemann, J. Eberth, T. Heck, W. Neumann, M. Nolte, R.B. Piercey, A.V. Ramayya, and J.H. Hamilton, *Proc. of 4th International Conference on Nuclei far from Stability, July 20, 1981, Vol. II, CERN 81-09.*
47. C.J. Lister, B.J. Varley, H.G. Price, and J.W. Olness, *Phys. Rev. Lett.* 49, 308 (1982).

APPENDIX (A)

A Proposed Gamma-Ray Facility at NSCL

In early September, 1981, a meeting of users interested in gamma-ray physics was held at NSCL and chaired by J.X. Saladin (University of Pittsburgh). Saladin proposed an extensive gamma-ray facility to be constructed and tested at Pittsburgh and then installed at NSCL. His ideas generated favorable responses from both in-house and outside users. During the following months a proposal to the NSF was written by principal investigators, J.X. Saladin, I.Y. Lee and C. Baktash (ORNL), R.A. Sorensen (Carnegie-Mellon University), and W. Benenson, R.A. Blue, and R.M. Ronningen (NSCL). The proposal was submitted to the NSF in the Spring of 1982.

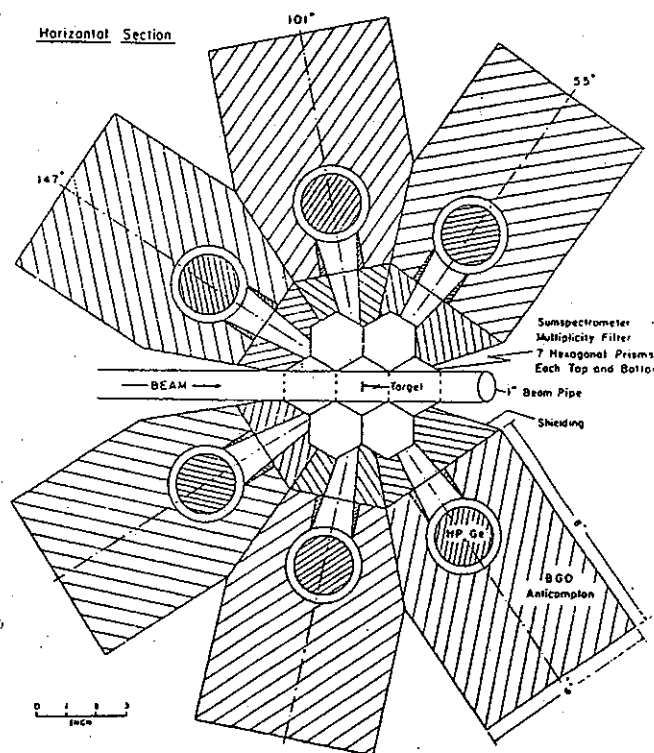


Fig. 1. Horizontal cross sectional view through the detector assembly.

A vertical cross sectional view of a part of the detector facility is shown in Fig. 1 and a horizontal cross section view is shown in Fig. 2. The facility will consist of 14 bismuth-germanate (BGO) scintillator detectors surrounding the target acting as a total gamma-ray energy and gamma-ray multiplicity filter spectrometers, and 6 high purity germanium (Ge) detectors each with an anti-Compton shield made from BGO. BGO is used because its density is over twice that of sodium iodide allowing a more compact configuration and hence larger solid angles to be achieved. The geometry of the Ge detectors shown in the illustrations has a total acceptance solid angle of $\varnothing.89\%$ of 4π . The multiplicity-sum spectrometer subtends $8\varnothing\%$ of 4π .

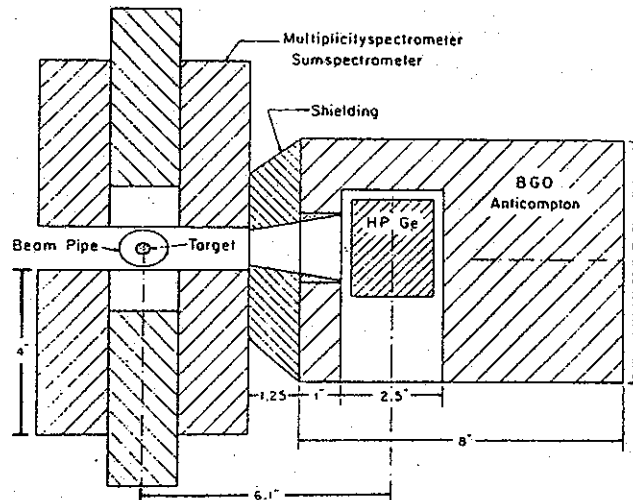


Fig. 2. Vertical cross sectional view through the detector assembly.

Saladin has performed Monte-Carlo calculations on the performance of such anti-Compton shielded Ge detectors using the computer code of F. Avignone (University of South Carolina). He finds, using 1.5 MeV γ -rays for example, a peak-to-total ratio of $\varnothing.77$ for the suppressed spectrum compared to $\varnothing.2$ for the unsuppressed spectrum; the overall suppression factor is about 21.

Although BGO has a photopeak resolution about half that of NaI (its light output is about 10% that for NaI) the peak-to-total ratio is twice that of NaI. This property, coupled

with high efficiency, makes the 14 BGO detector array an excellent total γ -ray energy detector. For 1.5 MeV γ -rays the FWHM of the measured energy distribution is 20% of E for a multiplicity of 25. The resolution for this multiplicity value is 27%.

APPENDIX (B)

Improvements and Innovations in γ -Ray Detectors

The Cyclotron laboratory here at MSU has had a long history of innovations in γ -ray spectroscopy. These have ranged from our early studies on anti-Compton and pair spectrometers¹⁾, through the introduction of new computer techniques such as the digital sum-coincidence method²⁾ to our recent introduction of the "pulse-height correction technique".^{3,4)} In this last method we make use of computer/electronics corrections to compensate for the varying completeness of charge collection in different portions (e.g., damaged vs undamaged, or center vs edge) of a Ge detector. It is most straightforward when applied to a planar detector³⁾, but it also works for coaxial detectors, as can be seen in Fig. 1. Here the energy resolution and the peak-to-Compton ratio for a neutron-damaged detector were improved by more than 50% each without any significant loss in detector efficiency.

Recently there has been a great deal of activity in proposing and constructing large arrays of NaI(Tl) or BGO ("bismuth germanate") detectors in "crystal balls"⁵⁾ or anti-Compton and multiplicity filters.^{6,7)} It is expected that a great deal of new and worthwhile data will be forthcoming from these instruments. At the same time, however, it is also worth while investigating alternative methods for improving the resolution, peak-to-background ratios, and versatility of γ -ray experiments. In particular, we would seek ways of pushing the possibilities of discrete-line spectroscopy up into regions of higher excitation and spin. Two distinct paths look promising enough to warrant at least initial excursions: the use of InSb for γ -ray detectors and

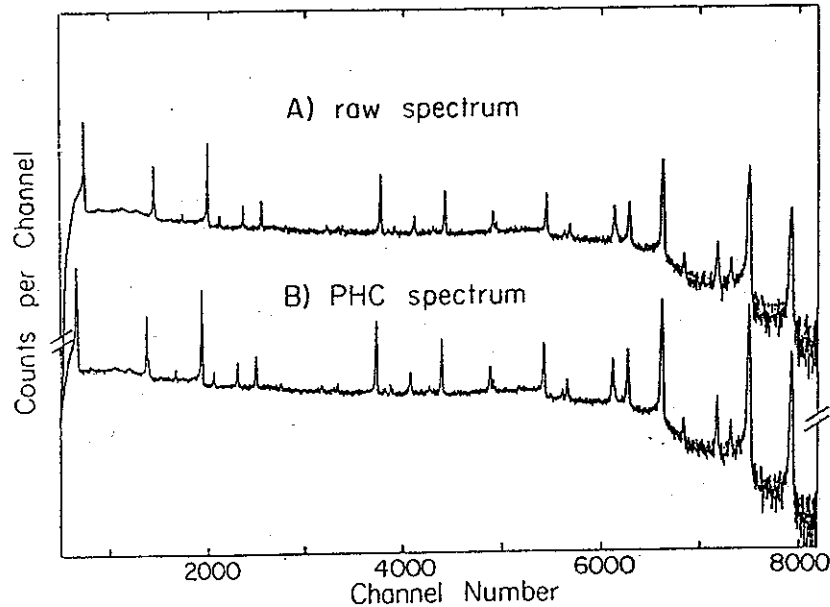


Fig. 1 γ -ray spectra for $^{60}\text{Co} + ^{137}\text{Cs} + ^{152}\text{Eu}$ sources taken with a $\sim 16\%$ -efficient true-coaxial Ge(Li) detector. A) The raw spectrum, with energy resolution of 4.92 FWHM for the ^{60}Co 1332.513-keV peak. B) Pulse-height corrected spectrum, with the energy resolution improved to 2.91 keV FWHM and the peak-to-compton ratio improved by about 43%, all without significant loss in detector efficiency. (From Ref. 4)

the use of Ge as its own anti-Compton shield (at least for close, transverse geometries). Neither of these would have been at all feasible only a few years ago, but improvements in both semiconductor and computer technologies have reached the point that each appears on the threshold of success today. We propose an initial investigation into each, leaving further, detailed development to commercial interests.

InSb as a material for γ -ray detectors

Of all the reasonably common semiconductors, InSb appears to be the best for γ -ray detectors. Its properties are compared with those of Si, Ge, and GaAs in Table I, and from these it can be seen that it would make an almost ideal γ -ray detector--on paper. With its effective Z of 50, it is more efficient than Ge by a factor of almost 10 for the photo-electric effect, even without taking into account its somewhat greater density.

Table I. Semiconductor Properties at 290 K.

	Si	Ge	GaAs	InSb
Effective Z	14	32	32	50
Band Gap (eV)	1.106	0.67	1.35	0.17
Lattice Constant (Å)	5.42	5.65	5.65	6.48
Electron Mobility (cm ² /V·sec)	1350	3900	6800	80,000
Hole Mobility (cm ² /V·sec)	480	1900	680	4,000

Also, with its very small band gap of 0.17 eV, it has the potential for attaining extraordinarily high resolution. On the other hand, at the time Li-drifted Ge (and Si) detectors were being developed, it seemed out of the question that a drifted InSb detector could be produced. First, because of its extraordinarily large electron mobility (as compared with its hole mobility), it is next to impossible to obtain p-type InSb, making drifting with Li⁺ out of the question. Instead, one would have to drift n-type InSb with an anion, probably with F⁻, inherently a slower, less satisfactory process because of the size of the anion. Second, because of the tiny band gap, at the temperatures required for finite-speed drifting, InSb will undoubtedly become conducting and stop the drift. Thus, the properties of InSb, though excellent on paper, were never investigated.

Now just as in the last several years Ge can be produced in pure enough form to construct "intrinsic" Ge detectors, so InSb has been produced for infra-red detectors. We propose to acquire the largest InSb "infra-red" detector feasible and to test its behavior as a γ -ray detector. If it proves promising, we then propose to contract with a commercial manufacturer to produce a larger, more practicable InSb γ -ray detector or to initiate a collaboration with a laboratory such as LBL, which has a large detector fabrication effort already underway. (For example, during the early days of Ge(Li) detectors, C. Gruhn was here at MSU, and we constructed many Ge(Li) detectors together; he is now at LBL in the detector fabrication business.)

Ge as its own anti-Compton shield.

When Ge(Li) detectors were first becoming popular, a number of studies were made of their Compton-scattering properties, and for a short time a "Duode" detector was available commercially (from Nuclear Diodes, Inc.), which made use of summing the Compton signals from two small detectors (actually, two electrically-isolated halves) to achieve a better peak-to-Compton ratio. However, these were necessitated by the extreme smallness of Ge(Li) detectors then available, and, as larger detectors with better resolution and better peak-to-Compton ratios became available, such methods and detectors were quickly forgotten, other than the occasional use of several Ge detectors as a polarimeter. One of the few Ge-Ge Compton-scattering studies made in subsequent years was one done by us,⁸⁾ and it was directed more at the problems encountered in Ge-Ge γ - γ coincidence experiments rather than at improving the peak-to-Compton ratios per se. A better peak-to-Compton ratio is not only of interest for high resolution spectroscopy but also for continuum γ -ray studies, such as in the γ -ray transition energy correlation technique.⁹⁾ Thus, Compton events are part of the unwanted background. Methods using NaI detectors¹⁸⁾

show promise for reducing Compton events and perhaps can be adaptable for large arrays.

One of the major problems encountered in designing the new 4π anti-Compton and multiplicity filters^{6,7)} is the tight geometry. This has led to the use of BGO with its greater density instead of NaI(Tl) for anti-Compton shields, even though in many other respects NaI(Tl) would be preferable. As a result we have reconsidered the use of Ge as its own anti-Compton shield, at least in those positions of close, tight geometry where NaI(Tl) is not practicable. Because of the expense involved, one would want to continue to use NaI(Tl) (or even BGO) in the outer layer of such a "ball" detector system, but Ge could be used as its own anti-Compton shields to fill in the "sides" between the major detectors. Of course, the last thing one desires in a coincidence experiment is cross-talk between the Ge detectors, but computers (and computer programs developed for multi-array detectors) have now reached the point that such problems can not only be handled reasonably efficiently, but also exploited: for example, one can now perform simultaneous coincidence, anti-coincidence, sum coincidence, and correlation experiments between and among various detectors. Thus, what would be unthinkably cumbersome a few years ago now appears to be feasible.

One can perform various calculations, such as Monte Carlo Compton scattering calculations, but the most straightforward procedure seems to be to construct a single representative detector array and to determine its advantages and disadvantages experimentally. Thus, we propose to obtain a single "rosette", consisting of a high-quality (cylindrical) Ge detector surrounded by seven secondary (probably trapezoidal) Ge detectors, all mounted in a single cryostat. (Any small interstitial spaces will not count, to first order, for Compton scattering, except to lower the overall solid angle.) Even at the very worst, such a detector array should prove more efficient than any comparably-

priced detector (if a comparably efficient detector were available), and it can always be used in simple coincidence as a single detector. On the other hand, should it prove as flexible and useful as we anticipate, it can form the first prototype section of a 4π "metal ball" anti-Compton multiplicity filter that could prove more flexible and versatile than those presently in use or under construction.

The projects described above are of an exploratory nature, and the ultimate costs of both will depend on how much we can cooperate and collaborate with other laboratories and with commercial suppliers. We plan to explore these possibilities in the future. If either or both show promise we expect to submit separate, independent proposals at a later date.

References

- 1) R.L. Auble, D.B. Beery, G. Berzins, L.M. Beyer, R.C. Etherton, W.H. Kelly, and Wm.C. McHarris, Nucl. Instr. and Meth. 51, 61 (1967).
- 2) G.C. Giesler, K.L. Kosanke, R.A. Warner, Wm.C. McHarris, and W.H. Kelly, Nucl. Instr. and Meth. 93, 211 (1971).
- 3) N. Matsushita, Wm.C. McHarris, R.B. Firestone, J. Kasagi, and W.H. Kelly, Nucl. Instr. and Meth. 179, 119 (1981)
- 4) N. Matsushita, J. Kasagi, and Wm.C. McHarris, Nucl. Instr. and Meth. 201, 433 (1982).
- 5) D. Sarantites, paper presented at Intl. Conf. on Nucleus-Nucleus Collisions, East Lansing, MI, 26 Sept-1 Oct 1982.
- 6) R.M. Diamond and F.S. Stephens, "High Resolution Ball", proposal submitted to DOE, 1981.
- 7) J.X. Saladin, C. Baktash, S.Y. Lee, W. Benenson, R. Blue, R. Ronningen, and R.A. Sorensen, "Proposal for a Multi-Detector Gamma Ray Facility", submitted to NSF, March 1982.

- 8) G.C. Giesler, Wm.C. McHarris, R.A. Warner, and W.H. Kelly, Nucl. Instr. and Meth. 91, 313 (1971).
- 9) O. Andersen, J.D. Garrett, G.B. Hagemann, B. Herskind, D.L. Hillis, and L.L. Riedinger, Phys. Rev. Lett. 43, 687 (1979).
- 10) J. Kasagi and R.M. Ronningen, MSU Cyclotron Laboratory Annual Report 1979-1980, p. 60.

(b) Continuum Gamma-Ray Studies

R.A. Blue, D.J. Morrissey and R.M. Ronningen

The contributions of discrete gamma-ray spectroscopy to the elucidation of nuclear structure are well known and well developed in this laboratory. In recent years many discrete line studies have been aided, and in some cases made possible, by the exploitation of the information inherent in the sheer numbers and the total energy of gamma-rays. The continuum gamma-rays are used primarily to identify those reactions that lead to nuclei with the highest spins. We are using continuum gamma-rays as part of a study of the statistical decay of a reaction system that we have studied in some detail.

A detailed study of the fusion-evaporation process in a well known system can provide a stringent test of statistical model descriptions. We have undertaken such a study in collaboration with Khoo's group at Argonne National Laboratory¹⁾ using neutron evaporation as a probe of the early stages of the evaporation process. The reaction studied was $^{64}\text{Ni} + ^{92}\text{Zr}$ at 233 MeV (≈ 46 MeV excitation and $l_{\text{max}} \approx 37\hbar$ in the compound nucleus ^{156}Er).

A neutron counter at 0° to the beam detected neutrons in coincidence with two large NaI detectors which acted as a gamma-ray sum-energy detector. Gamma multiplicity information was obtained with large NaI detectors at 0° and 90° and discrete lines were observed in a Ge(Li) detector. Fig. 1 shows neutron spectra for different γ -sum energy slices (i.e. spin slices). Spectra coincident with higher sum energies, corresponding to the decay of higher angular momentum states, are characterized by lower temperatures, hence these nuclei are "cooler" and lie nearer the yrast line. Statistical model calculations reproduce the temperature of the total neutron spectrum but underpredict (by a

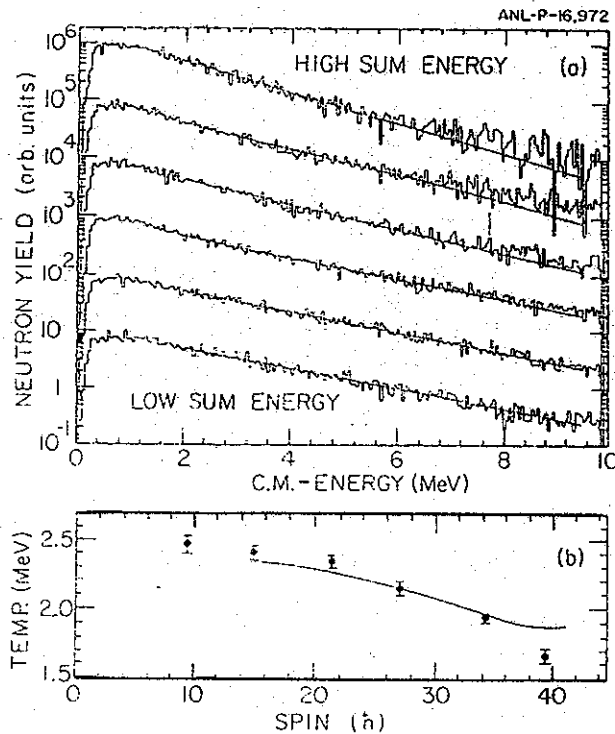


Fig. 1. (a) Neutron spectra, measured at 0° , for six different gamma ray sum energy slices. The straight lines represent fits with an exponential function. (b) Temperatures, derived from the fits in Fig. 1a, as a function of entry line spin corresponding to the different sum slices. The solid line represents results from CASCADE calculations using a "super-deformed" yrast line.

factor of about thirty) the observed 2n-to-3n channel decay ratio, indicating a preference for γ -ray decay. There must be more energy in rotational motion (~ 10 MeV) which is not available for the emission of a third neutron. Thus the yrast line at these high spins lies higher than expected as would be the case for a "superdeformed" shape with a relaxation time longer than a typical neutron emission time. We plan to continue this study at ANL using other Zr targets as well as different entrance channels leading to the same compound nucleus. Such studies can be easily carried out at NSCL using either the MHRACS facility (see Appendix to Section B3(a)) for a total energy spectrometer (if it is funded), or using the existing four 7.6 cm x 7.6 cm BGO crystals to form a device which would provide limited information on the total energy, but at the same time

reasonable information on the gamma-ray multiplicity.

A new and unique tool for the study of nuclei at high spins and excitation energies has recently been identified by Newton et al.²⁾ The tool is the detection of the giant dipole transitions that deexcite the residual nuclei. The studies to date have identified the presence of the transitions and suggested that the observed widths are representative of the shapes of the emitting nuclei. The experiments are complicated by the low intensity of the gamma-rays and by the problems inherent in detecting high energy gamma-rays ($E \approx 80 A^{-1/3}$). In the original studies a complete fusion reaction was used to prepare the highly excited nuclei²⁾ and in recently reported studies a deep inelastic reaction was used to create nuclei over a range of excitation energies.³⁾

We propose to study the deexcitation of nuclei via the giant dipole transitions. The nuclei should be identified as to their excitation energy and spin, if possible. A particularly intriguing possibility exists for the production of nuclei in the giant dipole region with (d, d') scattering. Such nuclei would have particularly low values of excitation energy and spin and the giant dipole decay would have to go to the ground state of the nucleus. Such transition strengths could be compared to giant transition strengths in more highly excited nuclei created for example in deep inelastic reactions.

The detection of the trigger particles is relatively straightforward. Several heavy-ion telescopes are available at the NSCL, and the S-320 spectrograph would be excellently suited to the alpha scattering experiment. However, the detection of the 10-15 MeV gamma-rays expected in the experiment will be more difficult. The NSCL has a set of 7.6 x 7.6 cm BGO detectors, and even though they have a higher stopping power than the detectors used in the early experiments they will be modified to improve their response function. We can improve the BGO by surrounding it with an anticoincidence shield which is used to reject gamma-ray

interactions that lead to escaping annihilation radiation. In Fig. 2 is shown a comparison between the response function of BGO and NaI(Tl) detectors to a 4.44 MeV gamma-ray. The figure emphasizes the importance of vetoing out the escaping annihilation radiation for high energy gamma-rays. We are exploring prototype shields for the BGO detectors with an existing NaI(Tl) annulus and plastic detectors. It should be possible to design and build a compact and low cost anticoincidence shield for the BGO detectors which will give us a set of high energy gamma-ray detectors that are superior to those used to identify the giant dipole transitions.

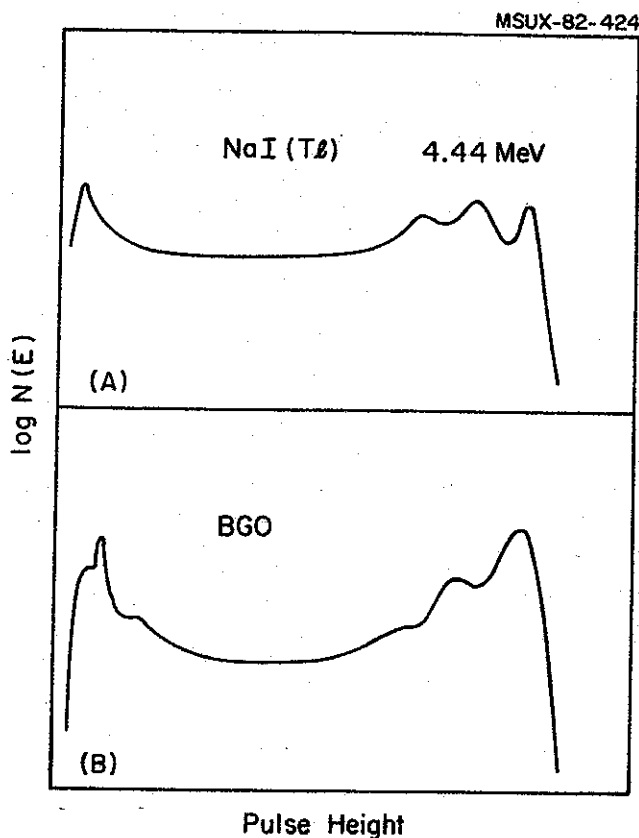


Fig. 2. The pulse height response of 7.6 x 7.6 cm BGO and NaI(Tl) detectors to monoenergetic 4.44 MeV gamma-rays is shown.

References

- 1) W. Kühn, I. Ahmad, P. Chowdhury, R.V.F. Janssens, T.L. Khoo, F. Haas, J. Kasagi, and R.M. Ronningen, *Bull. Am. Phys. Soc.* 27, 475 (1982).
- 2) J.O. Newton, B. Herskind, R.M. Diamond, E.L. Dines, J.E. Draper, K.H. Lindenberg, C. Schuck, S. Shih, and F.S. Stephens, *Phys. Rev. Lett.* 46, 1303 (1981).
- 3) J.E. Draper, J.O. Newton, L.G. Sobotka, H. Lindenberg, G.J. Wozniak, L.G. Moretto, F.S. Stephens, R.M. Diamond, and R.J. McDonald, *Phys. Rev. Lett.* 49, 434 (1982).

(c) Particle Transfer in Nucleus-Nucleus Collisions; the Nuclear Josephson Effect

Wm. C. McHarris

During the past year I have been involved in a collaboration with Stephens, Diamond, and co-workers¹⁾ at LBL for the purpose of looking at two-neutron transfer reactions in heavy nucleus-nucleus collisions. Sometimes referred to as the "nuclear Josephson effect", these reactions show an enhanced cross-section over the single-particle transfer involving the same nuclear combinations, and they may well proceed by a sort of tunneling effect. A very good start has been made at understanding the mechanisms²⁾ involved in such reactions, but much more theoretical work is needed.

The reactions studied thus far at the LBL Super-HILAC involve ^{132}Xe and ^{165}Ho beams on ^{154}Sm and ^{165}Ho targets. Reactions such as $^{132}\text{Xe} + ^{154}\text{Sm} \rightarrow ^{134}\text{Xe} + ^{152}\text{Sm}$, which were detected via their accompanying γ -rays (see below), were found to have surprisingly large cross-sections, considerably larger than single-neutron transfer. The results are quite preliminary, but the reactions appear to be Q dominated, with those reactions producing nuclides closer to stability being the strongest. The same sort of effects were found for the ^{165}Ho beams, but here the spectra were much messier, partly because the projectile γ -rays lie right on top of those of the target and product(s). Thus, a systematic investigation of the reactions with different Xe beams and different deformed lanthanide targets is planned as the more promising initial set of experiments. The variation with the different Xe beams should also yield information about the strength of the pairing force on the transfer, since the Xe beams can range from the closed-shell ^{136}Xe down to soft, almost deformed species.

In addition to the two-neutron transfer reactions, a cursory attempt was made to see the "superallowed" single-proton transfer in the $^{165}\text{Ho} + ^{165}\text{Ho} \rightarrow ^{164}\text{Dy} + ^{166}\text{Er}$

reaction. The ^{165}Ho ground-state is the $7/2^- [523\uparrow]$ proton state, which has lobes on the nuclear surface at about 45° . With the short wave-lengths, i.e., particle nature, of these nuclear collisions, it was hoped that one could obtain a sampling of the nuclear surface in localized regions. Thus, two ^{165}Ho nuclei in a grazing collision at approximately 45° orientation should have an excellent chance of transferring a proton - hence, the "superaligned" sobriquet. In fact, such a transfer has not yet been observed, although the experiments were short and preliminary. This, and other transfer reactions such as d-cluster transfer are wide-open fields, and they should be ripe for investigation, both at the LBL Super-HILAC and with the high-quality, high-resolution heavy-ion beams expected shortly at NSCL.

These two-neutron (and other) transfer reactions require a combination of particle and γ -ray spectroscopy. With such heavy product nuclei, $\Delta E-E$ particle identification is out of the question, and even time-of-flight methods do not have sufficient resolution to identify the desired species from contaminants differing only by a few mass units. On the other hand, Coulomb excitation at large impact parameters completely dominates the γ -ray spectra, effectively obscuring the reactions of interest. This makes it necessary to combine the spatial resolution of position-sensitive particle detectors with the energy resolution (and consequent isotope identification) of Ge γ -ray detectors. The kinematics of the reactions allow one to gate so as to eliminate all but the desired impact parameters, specifically to choose those near the grazing angle for these transfer reactions. In the initial experiments at LBL, it was found desirable to use two position-sensitive particle detectors (at forward and backward angles) to help discriminate between projectile-forward-target-backward and projectile-backward-target-forward scattering, but even one particle detector (because of an angular limitation in the target chamber) was found to clean up the spectra

B 4. NUCLEI FAR FROM STABILITY

- (a) Mass Measurements Far From Stability**
- (b) Studies of Nuclei Far From Stability with the Reaction Product Mass Separator**
- (c) Measurement of β -Decay Halfives of Very Neutron-Excess Nuclei**
- (d) Nuclei Far From Stability Using He Jet Recoil Transport**





sufficiently to glean useful information from the reactions.

Our plans call for a continuation of the collaboration at LBL, also initiating a similar set of studies as a long-range series of studies at NSCL. The detectors and expertise in handling them are already available, and the heaviest beams available from Phase I, e.g., Ar beams, should yield useful complementary studies to those on-going at LBL. Cooperation between these two (and other) laboratories should develop these "exotic" transfer reactions into a useful new field of study.

References

1. F.S. Stephens, R.M. Diamond, A. Machiavelli, M.A. Delaplanque, J.O. Rasmussen, Wm. C. McHarris and others, in progress (1983).
2. M.W. Guidry, T.L. Nichols, R.E. Neese, J.O. Rasmussen, L.F. Oliveira, and R. Donangelo, Nucl. Phys. A361, 275 (1981).



(a) Mass Measurements of Nuclei far from Beta Stability

W. Benenson, E. Kashy, R.M. Ronningen and B.H. Wildenthal

The ground state mass of a nucleus is one of its basic properties, and yet there remain thousands of species for which the mass is either unknown or very poorly known. Knowledge of these masses is of great significance in testing models of nuclear structure and for extrapolations to nuclei of unusual Z/N ratio and the superheavy region. Existing mass formulas and relations do a fair job of fitting the known nuclei, but their extrapolation to the unknown is not always valid and can never predict new phenomena such as the intrusion of a new region of deformation. To improve these models precise data are needed both near and far from the valley of beta stability. Q -value measurements, although not of universal applicability offer the best hope for high precision mass measurements, which in several cases, however, are for nuclei right on the edge of particle stability.

In this section of the proposal we outline our plans to make mass measurements by means of Q -value determinations in spectrographs with light and heavy ion beams. Work of this type has been an important component of this lab's nuclear structure research for the past 15 years.¹⁾ The techniques which were developed²⁾ allowed precise measurements of approximately 50 new nuclei, and are now widely used by other research groups. The possibilities for continuing this work with the K500 and several other accelerators look very promising. Our plans include projects at Indiana, Brookhaven and MSU, using beams of both light and heavy ions.

The (p, π^-) reaction on a proton rich target can lead to an unknown or poorly known final nucleus. We recently completed the first mass measurement of this type with the Indiana Cyclotron. A precision of 40 keV was obtained for

the mass of ^{59}Zn in spite of the high beam energy and low cross section (0.080 nb/sr). An article on this work has been submitted for publication.³⁾ ^{59}Zn completes the highest mass mirror pair known, and its Coulomb energy shows the persistence of the Nolen-Schiffer anomaly⁴⁾ beyond the $f_{7/2}$ shell. Two more nuclei will be run this summer, ^{65}Ge and ^{93}Ru , which are important in deriving Gamow-Teller strength distributions from beta-delayed particle spectra.

At Brookhaven we will be joining forces with C.E. Thorn, P.S. Bond, E.K. Warburton and S. Raman (of Oak Ridge) to utilise the unique combination of high energy ^{14}C beams and the large solid-angle Q3D to measure a whole variety of masses including several on the line of particle stability. The targets will be ^{36}S and ^{48}Ca , and the main goal of the project is to measure ^{14}Be , which may be just unbound and decay via two neutrons to ^{12}Be . In Table I we give a list of some of the nuclei which may be accessible with these targets and a ^{14}C beam. Groups of as many as six new nuclei may be measurable in a single run. A precision of 50 keV should be feasible. Most of the final nuclei listed have unknown masses, and all have uncertainties of 100 keV or more.

At MSU there are a whole variety of possible mass measurements. With beams of ^4He , ^6Li , ^7Li , and ^{12}C on a few targets one will be able to produce the nuclei listed in Table II. A unique advantage of the K500 cyclotron is that it can produce beams at optimum energies for these experiments without going to high charge states. For example, in the case of Li single and double charged ions are all that is required. These beams should be stable and intense enough to obtain high resolution which we found to be crucial to precise mass measurements. The experiments will be carried out either in the S320 or the Enge magnetic spectrographs depending on the rigidity of the outgoing particle. The list given in Table II is arbitrarily cut off. There are at least as many examples of possible reactions omitted as included,

and the actual projects which are undertaken will depend on the availability of the various beams from the K500 cyclotron, our initial experience with the various types of reactions at these energies, and, of course, our success in convincing the P.A.C. of the value of these experiments. Particularly interesting nuclei in the list of Table II are ^{57}Cu , a closed shell plus one proton nucleus which is completely unknown, ^{41}Ti which completes a mass quartet, and ^{22}Al which is right on the proton decay line. In this table the final nuclei all have mass uncertainties of 100 keV or more, but most are unknown. The experiments will also give accurate information on the low lying levels of many unstable nuclei which will be valuable for shell model studies and for identification of exotic decays in the RPMS.

References

- 1) W. Benenson and E. Kashy, Revs. Mod. Phys. 51, 527 (1979).
- 2) E. Kashy, W. Benenson and D. Mueller, Atomic Masses and Fundamental Constants, J.H. Sanders and A.H. Wapstra eds., Plenum Press, N.Y. 1975.
- 3) B. Sherrill et al., Phys. Rev. C, to be published.
- 4) J.A. Nolen and J.P. Schiffer, Ann. Rev. Nucl. Sci., 19, 471 (1969).

Table I. Experiments with ^{14}C Beams.

Reaction	Q-Value
$48\text{Ca}(^{14}\text{C}, ^{14}\text{Be})^{48}\text{Ti}$	-33.7
$48\text{Ca}(^{14}\text{C}, ^{14}\text{O})^{48}\text{Ar}$	-26.1
$48\text{Ca}(^{14}\text{C}, ^{15}\text{O})^{47}\text{Ar}$	-18.5
$48\text{Ca}(^{14}\text{C}, ^{17}\text{F})^{45}\text{Cl}$	-23.6
$48\text{Ca}(^{14}\text{C}, ^{18}\text{F})^{44}\text{Cl}$	-22.0
$48\text{Ca}(^{14}\text{C}, ^{19}\text{F})^{43}\text{Cl}$	-16.6
$48\text{Ca}(^{14}\text{C}, ^{20}\text{F})^{42}\text{Cl}$	-16.8
$48\text{Ca}(^{14}\text{C}, ^{18}\text{Ne})^{44}\text{S}$	-34.5
$48\text{Ca}(^{14}\text{C}, ^{19}\text{Ne})^{43}\text{S}$	-29.5
$48\text{Ca}(^{14}\text{C}, ^{20}\text{Ne})^{42}\text{S}$	-17.7
$48\text{Ca}(^{14}\text{C}, ^{21}\text{Ne})^{41}\text{S}$	-17.6
$48\text{Ca}(^{14}\text{C}, ^{11}\text{C})^{51}\text{Ca}$	-18.3
$48\text{Ca}(^{14}\text{C}, ^{10}\text{C})^{52}\text{Ca}$	-24.8
$36\text{S}(^{14}\text{C}, ^{14}\text{O})^{36}\text{Si}$	-22.2
$36\text{S}(^{14}\text{C}, ^{15}\text{O})^{35}\text{Si}$	-15.7
$36\text{S}(^{14}\text{C}, ^{17}\text{F})^{33}\text{Al}$	-20.3
$36\text{S}(^{14}\text{C}, ^{18}\text{F})^{32}\text{Al}$	-17.1
$36\text{S}(^{14}\text{C}, ^{18}\text{Ne})^{32}\text{Mg}$	-31.2
$36\text{S}(^{14}\text{C}, ^{19}\text{Ne})^{31}\text{Mg}$	-25.5
$36\text{S}(^{14}\text{C}, ^{20}\text{Ne})^{30}\text{Mg}$	-10.9
$36\text{S}(^{14}\text{C}, ^{11}\text{C})^{39}\text{S}$	-15.3
$36\text{S}(^{14}\text{C}, ^{10}\text{C})^{40}\text{S}$	-20.8
$36\text{S}(^{14}\text{C}, ^{13}\text{N})^{37}\text{P}$	-13.9
$36\text{S}(^{14}\text{C}, ^{12}\text{N})^{38}\text{P}$	-30.4

Table II. Partial List of Experiments with K500 Beams.

Reaction	Q-Value
$40\text{Ca}(7\text{Li}, 8\text{He})39\text{Sc}$	-37.5
$58\text{Ni}(7\text{Li}, 8\text{He})57\text{Cu}$	-29.1
$64\text{Zn}(7\text{Li}, 8\text{He})63\text{Ge}$	-26.0
$24\text{Mg}(6\text{Li}, 8\text{He})22\text{Al}$	-49.7
$28\text{Si}(6\text{Li}, 8\text{He})26\text{P}$	-50.3
$32\text{S}(6\text{Li}, 8\text{He})30\text{Cl}$	-48.4
$36\text{Ar}(6\text{Li}, 8\text{He})34\text{K}$	-46.3
$40\text{Ca}(6\text{Li}, 8\text{He})38\text{Sc}$	-47.9
$46\text{Ti}(6\text{Li}, 8\text{He})44\text{V}$	-37.8
$58\text{Ni}(6\text{Li}, 8\text{He})56\text{Cu}$	-37.8
$64\text{Zn}(6\text{Li}, 8\text{He})62\text{Ga}$	-31.8
$28\text{Si}(12\text{C}, 12\text{Be})28\text{S}$	-50.7
$58\text{Ni}(12\text{C}, 12\text{Be})58\text{Zn}$	-43.0
$64\text{Zn}(12\text{C}, 12\text{Be})64\text{Ge}$	-36.6
$40\text{Ca}(12\text{C}, 8\text{Li})44\text{V}$	-17.9
$40\text{Ca}(12\text{C}, 9\text{Li})43\text{V}$	-41.8
$64\text{Zn}(12\text{C}, 9\text{Li})67\text{As}$	-34.3
$58\text{Ni}(12\text{C}, 9\text{Li})61\text{Ga}$	-37.4
$54\text{Fe}(12\text{C}, 9\text{Li})57\text{Cu}$	-33.6
$48\text{Ca}(4\text{He}, 8\text{B})44\text{Cl}$	-44.7
$64\text{Zn}(4\text{He}, 8\text{B})60\text{Mn}$	-34.7
$76\text{Ge}(4\text{He}, 8\text{B})72\text{Cu}$	-33.7
$26\text{Mg}(7\text{Li}, 10\text{C})23\text{F}$	-20.4
$36\text{S}(7\text{Li}, 10\text{C})33\text{Al}$	-22.1
$40\text{Ar}(7\text{Li}, 10\text{C})37\text{P}$	-16.8
$48\text{Ca}(7\text{Li}, 10\text{C})45\text{Cl}$	-27.5
$40\text{Ca}(12\text{C}, 8\text{He})54\text{Cr}$	-52.9
$40\text{Ca}(12\text{C}, 8\text{Li})44\text{V}$	-31.9
$40\text{Ca}(12\text{C}, 9\text{Li})43\text{V}$	-41.8
$40\text{Ca}(12\text{C}, 11\text{Li})41\text{V}$	-72.3
$40\text{Ca}(12\text{C}, 12\text{Be})40\text{Ti}$	-50.8
$40\text{Ca}(12\text{C}, 13\text{B})39\text{Sc}$	-37.3
$40\text{Ca}(12\text{C}, 14\text{B})38\text{Sc}$	-54.0
$40\text{Ca}(12\text{C}, 15\text{B})37\text{Sc}$	-66.8

(b) Studies of Nuclei Far From Stability With The RPMS

W. Benenson, B.A. Brown, L. Harwood, J. Nolen, R.M. Ronningen
and B.H. Wildenthal

The prototype RPMS, which will be operational by mid-1983, will be ideally suited to lifetime measurements of neutron-rich light isotopes such as ^{15}B , ^{17}C , and ^{19}N . We plan to begin these studies with the fragmentation of $^{22}\text{Ne}^{5+}$ beams with energies per nucleon in the 20-27 MeV range. For the reaction $^9\text{Be} + ^{22}\text{Ne}$ in this energy range a reasonable estimate of the cross section for the production of ^{17}C is $1\mu\text{b}$. This cross section, a beam current of 100 ena, an effective target thickness of 40 mg/cm^2 , and an RPMS geometrical acceptance of 20% of the 0° cone will produce a count rate of fifty ^{17}C ions/sec in a 1 cm diameter spot on the RPMS focal plane. The ions will be identified by and stopped in a ΔE - ΔE -E solid state telescope. The telescope will be surrounded by an 8"x8" NaI(Tl) annular detector and/or an array of 4 BGO scintillators to detect the gamma rays following the β -decays of the ^{17}C nuclei. In this way the lifetime can be measured and, at the same time, preliminary information about the decay scheme can be obtained. The background radiation environment for this experiment should be very clean because the ^{22}Ne beam can be stopped in the target (15 meters away from the counters) without significantly slowing down the ^{17}C fragments. Contamination from the possibly prolific $^{17}\text{N}^{6+}$ ions will be eliminated by stopping them in the second of the two ΔE detectors while the ^{17}C ions stop in the third Si detector. This detector will be separated a few centimeters from the ΔE detectors. The range at a given velocity of the ^{17}C ions is 36% larger than that of the ^{17}N ions. Another ion with an m/q similar to that of $^{17}\text{C}^{6+}$ is $^{15}\text{B}^{4+}$. However, since the m/q values differ by 1.2% and the base-to-base resolving power ($m/\Delta m$) of the RPMS is calculated to be 200, these ions should be stopped on a slit

before entering the detectors. The rate in the γ -ray counters from sources outside the E detector will be minimized with lead shielding.

The mass of ^{17}C has been measured via the $^{48}\text{Ca}(^{18}\text{O}, ^{17}\text{C})$ reaction at 102 MeV¹⁾, but no other properties of ^{17}C are currently known. We have made shell model calculations of the low-lying levels of ^{17}C and find that the $1/2^+$, $3/2^+$, and $5/2^+$ states are not well separated, i.e., it is possible for any of these states to actually be the ground state of ^{17}C . Hence, we have made predictions of the lifetime and decay scheme of this nucleus for all three possible ground state configurations. The predictions for the $5/2^+$ state are shown in Fig. 1. The gamma ray signatures for the $3/2^+$ and $5/2^+$ states are somewhat different, whereas that of the $1/2^+$ state is unique.

In conjunction with the ^{17}C measurements we will make yield measurements of other fragments which should also be produced by the reaction $^9\text{Be} + ^{22}\text{Ne}$, e.g., ^{14}Be , ^{15}B , ^{16}B , ^{17}B , ^{18}C , and ^{19}N . The yields of ^{15}B and ^{19}N should be comparable to ^{17}C so that lifetime and decay scheme measurements should be easily carried out. Again ^{15}B and ^{19}N have only their masses known^{2,3)}. (The reported lifetime of ^{19}N has been retracted^{4,5)}). Shell model calculations for ^{19}N have already been completed, while calculations for ^{15}B are planned for the near future. Quantitative measurements on ^{14}Be , ^{16}B , ^{17}B , and ^{18}C will be more difficult because of their expected lower yields. (^{16}B may be particle unstable.) If intense $^{22}\text{Ne}^{6+}$ beams with energies per nucleon above 30 MeV are developed the yields of these isotopes should be significantly increased and detailed measurements should be possible.

In parallel with these measurements, observations of yields in deep-inelastic type reactions away from 0° will be investigated. Typical reactions to be considered will be ^{18}O and ^{22}Ne beams on neutron rich targets such as ^{48}Ca , ^{100}Mo , and ^{232}Th . The energy and angle dependence of

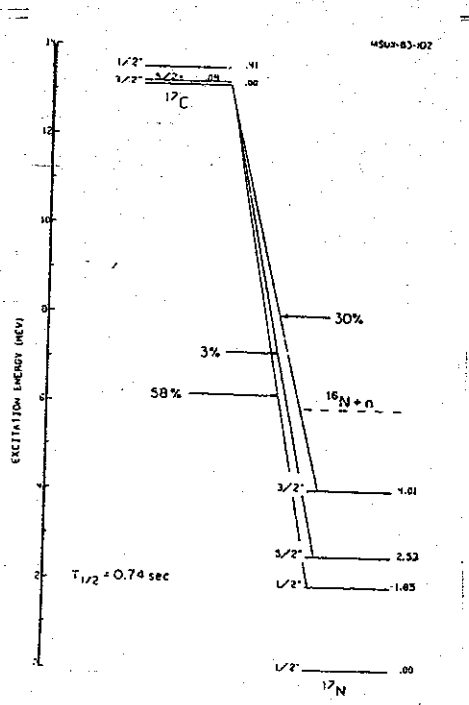


Fig. 1. Shell model prediction of the decay scheme and half-life of ^{17}C assuming the $3/2^+$ state to be the ground state.

neutron rich isotopes for beam energies per nucleon between 10 and 30 MeV will be measured and compared with results we obtained previously for ^{40}Ar beams at 210 MeV/u with a ΔE -E-TOF telescope.⁶⁾ It should be possible to establish the optimum production method for any given isotope, and to determine the extent to which further detailed structure measurements are feasible. These measurements are all preliminary to further studies in Phase II when a larger variety of beams at much higher energies will be available. An important part of research with the RPMS will be the detection of beta-decayed gamma cascades of previously unobserved nuclei. This will require a detector of high resolution and efficiency, such as a hyper-pure germanium detector with 18%

efficiency (relative to 3"x3" NaI(Tl)) and better than 1.9 KeV resolution. We propose buying such a detector specifically for out-of-beam experiments. The current cost is about \$15,000. An additional \$2,000 is needed for solid state detectors.

References

- 1) J.A. Nolen, T.S. Bhatia, H. Hafner, P. Doll, C.A. Wiedner, and G.J. Wagner, Phys. Lett. 71B 314 (1977).
- 2) T.S. Bhatia, H. Hafner, J.A. Nolen, Jr., W. Saathoff, R. Schumacher, R.E. Tribble, G.J. Wagner, and C.A. Wiedner, Phys. Lett. 76B 562 (1978).
- 3) C. Detraz, F. Naulin, M. Langevievin, P. Roussel, M. Bernas, F. Pougheon and J. Vernotte, Phys. Rev. C15 1738 (1977).
- 4) Guillaume, P. Fintz, F. Jundt, I. Ordonez, A. Gallmann, D.E. Alburger and K.W. Jones, Nucl. Phys. A233, 357 (1974).
- 5) David Alburger, private communication.
- 6) L.H. Harwood, T.C. Awes, C.K. Gelbke, J.A. Nolen, W. Bohne, K. Grabisch, and C. Morgenstern, to be published.

(c) Measurement of Beta-Decay Halflives of Very Neutron-Rich Nuclei
Produced by Fragmentation of Beams with Energies > 200 MeV/Nucleon

L.H. Harwood and G.D. Westfall

(i) Scientific Motivation

The study of the properties of neutron-rich nuclei far from the valley of stability provides valuable information basic to many problems in nuclear physics and astrophysics. The combination of measured masses and lifetimes allows the matrix elements of β -decay to be studied while β -decay lifetimes control the progress of stellar evolution and nucleosynthesis. The fragmentation of high energy heavy ions has proved to be a powerful method of producing neutron rich light nuclei with sixteen new nuclei being observed near the limit of stability.^{1,2)} This technique has been further extended to the measurement of β -decay halflives using the fragmentation of a 285 MeV/n ^{40}Ar beam where the previously unknown halflives of ^{22}O and ^{32}Al were found to be 910 ± 350 msec and 35 ± 5 msec respectively.³⁾

(ii) Current Experiments

We have recently performed similar measurements using a 300 MeV/nucleon ^{56}Fe beam of approximately 10^7 particles/sec from the LBL Bevalac. The target was a ≈ 1 g/cm² Be and the resulting neutron-rich projectile fragments were detected in the zero-degree spectrometer with an angular acceptance of 1 msr. The fragments were stopped in an eight element silicon detector telescope located on the focal

plane of the spectrometer. The half-lives of the neutron-rich fragments were measured by recording the time of arrival of the fragment, clamping the beam from the Bevalac, raising the gain of the preamplifiers by a factor of 100 to allow the detection of the β -decay of the neutron-rich fragments, and recording the time of all decays before the next pulse was ready from the Bevalac (≈ 3 sec.). Preliminary analysis indicates that several new half-lives were observed including ^{31}Mg . An example of decay curves for several nuclei is shown in Fig. 1 where the exotic nuclei were produced from ^{40}Ar fragmentation.

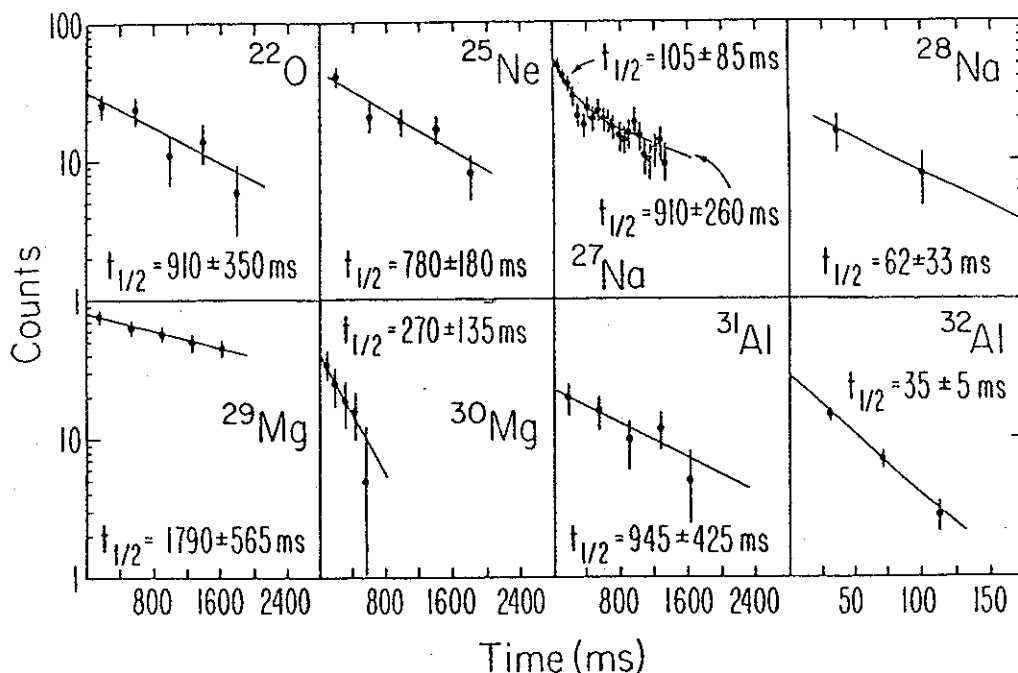


Fig. 1. β -decay half-life curves observed in fragmentation of ^{40}Ar . The curves are least squares fits to the data.

(iii) Future Experiments

We have an approved experiment at the Bevalac to produce exotic nuclei and to measure their decay properties using the HISS spectrometer in conjunction with heavy beams such as Kr. The method will be 21000 times more sensitive than the previous method and should allow the determination of the limits of nuclear stability for all light nuclei up to Ne and perhaps up to Ca.

We also plan to add a velocity filter to the existing zero degree spectrometer. The E x B separator already exists at the Bevalac and its implementation will be straightforward. This device will be able to exploit the high energy (above 200 MeV/nucleon) and very heavy beams (heavier than xenon) available from the upgraded Bevalac. The study of the decay properties of large numbers nuclei on the neutron-rich side of the valley of stability then becomes feasible.

References

- 1) T.J.M. Symons, Y.P. Viyogi, G.D. Westfall, P. Doll, D.E. Greiner, H. Faraggi, P.J. Lindstrom, and D.K. Scott, Phys. Rev. Lett. 42, 40 (1979).
- 2) G.D. Westfall, T.J.M. Symons, D.E. Greiner, H.H. Heckman, P.J. Lindstrom, J. Mahoney, A.C. Shotter, D.K. Scott, H.J. Crawford, C. McParland, T.C. Awes, C.K. Gelbke, and J.M. Kidd, Phys. Rev. Lett. 43, 1859 (1979).
- 3) M.J. Murphy, T.J.M. Symons, G.D. Westfall, and H.J. Crawford, Phys. Rev. Lett. 49, 455 (1982).

(d) Nuclei Far from Stability Using He-Jet Recoil Transport

Wm. C. McHarris

Most of the research at NSCL on short-lived nuclei far from stability will undoubtedly center around the Recoil-Product Mass Spectrometer, as detailed in those sections covering it. However, there will be occasions when the He-jet recoil-transport (HeJRT) system will be used, both when the RPMS is tied up with other uses and at times as the system of choice. We have had a great deal of experience with developing and using the HeJRT system, having been the first to develop a modular, flexible apparatus,¹⁾ the first to perform fast (a few seconds) aqueous chemical separations with a HeJRT system²⁾, and the first to introduce and investigate "plasma chemistry" (making use of chemical effects of the beam plasma on the molecular "clusters" formed in the jet chamber) with a HeJRT system³⁾. In addition, we have had considerable experience with the study of nuclei far from stability, ranging from extensive studies of β^+/ϵ decay to high-lying multi-particle multiplets⁴⁾, to the production of heavy $T = 1/2$ mirror nuclei and the study of their superallowed decay⁵⁾, to the first observation of very high multipolarity (E6 and M5) γ -transitions⁶⁾. Thus, our studies have demonstrated that experiments on a nuclide far from stability can yield more than "just another decay scheme" -- chosen carefully, such nuclides can provide important information on both structure and transition probabilities that can be obtained by no other means.

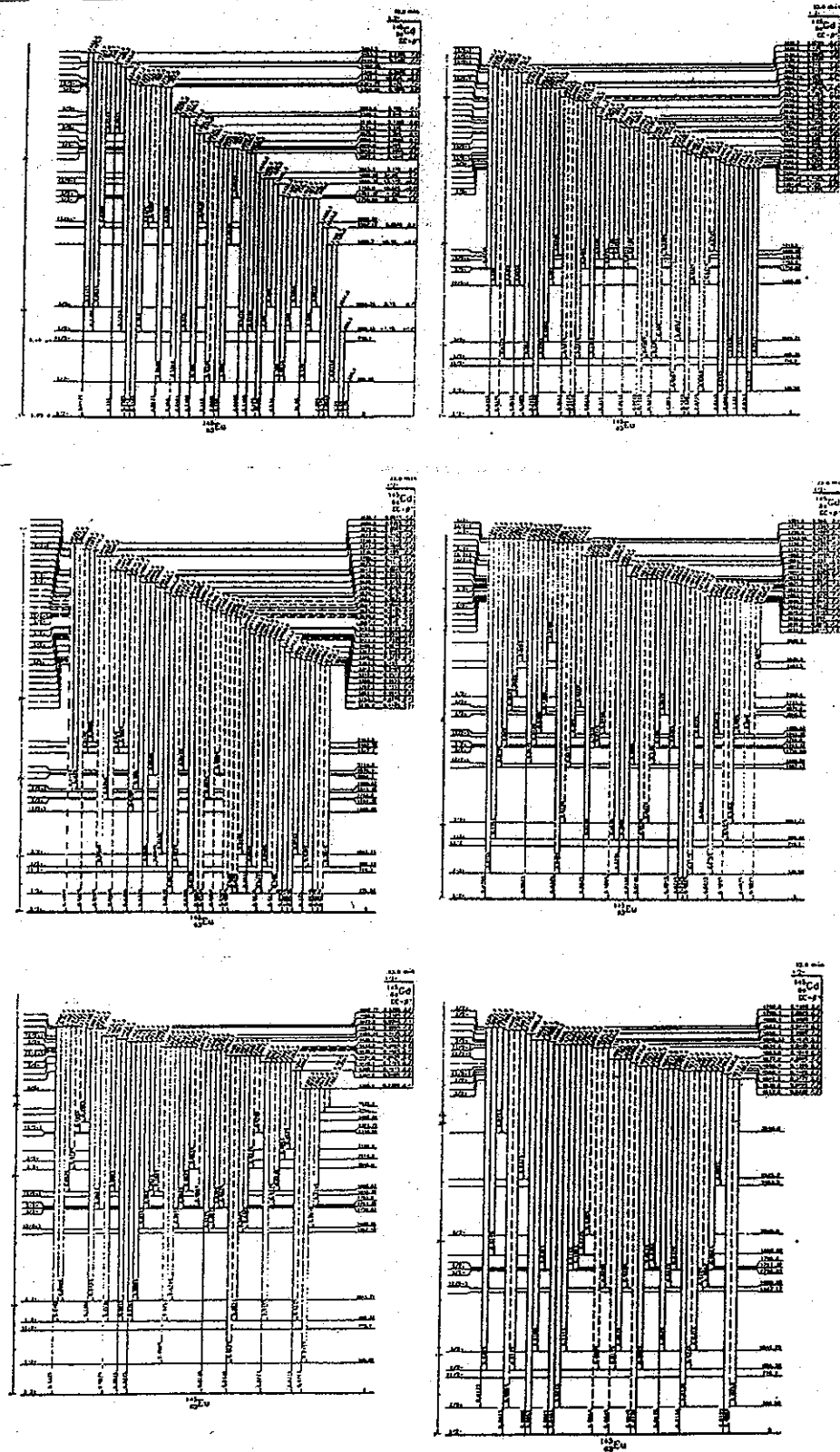


Fig. 1. Decay scheme (in six parts) of $^{145}\text{Gd}^g$; from Ref. 7).

Just as studies of nuclei far from stability have reached new levels of sophistication, unfortunately, so have they reached new levels of complexity and effort. As an example, in Fig. 1 we show the decay scheme of 23.0-min $^{145}\text{Gd}^g$, taken from our paper⁷⁾ published last year. To the best of our knowledge, this is the most complex decay scheme ever published, with 326 γ -rays placed in the scheme, deexciting 136 energy levels. However, if it were merely "the most complex decay scheme", it would scarcely have been worth doing. But it answers several important questions: 1) it puts to rest the questions of $\beta/\bar{\epsilon}$ -branching-ratio anomalies in this nucleus [although they definitely exist in some lighter nuclei, where they can be explained by second-order corrections⁸⁾]; 2) it answers definite structural questions about multi-particle and weak-coupled high-lying states; and 3) perhaps most important it settles the question once and for all as to whether or not β -decay can be represented by a simple statistical model--it cannot, as can be seen by the pronounced structure in the strength function shown in Fig. 2.

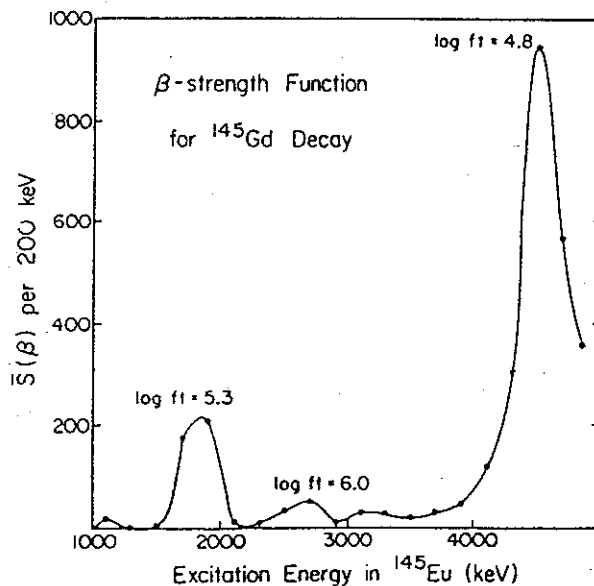


Fig. 2. β -strength function for $^{145}\text{Gd}^g$ decay, showing pronounced structure.

It is anticipated that not all or even most decay schemes of nuclei far from stability will reach the complexity of $^{145}\text{Gd}^g$, yet we must be prepared to deal with such nuclei with a different level of care than has been true in the past. The nuclei just below the closed shell at $N = 82$ should be particularly suited for study, combining as they do straightforward shell-model and collective degrees of freedom.

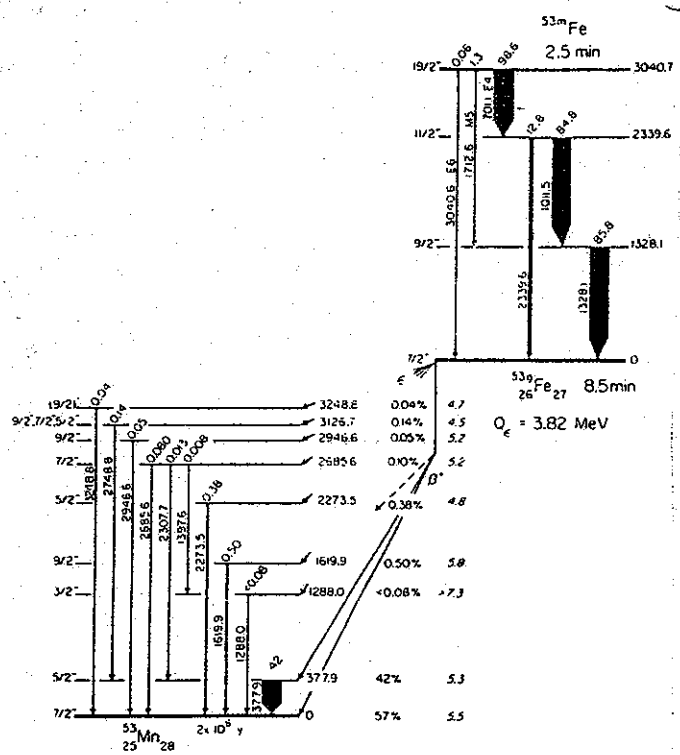


Fig. 3. The decays of $^{53}\text{Fe}^m$ and $^{53}\text{Fe}^g$, showing the first observation of E6 and M5 multipolarities; from Ref. 6).

A final example of the intriguing questions that can be raised by radioactive decay is the recent renewed interest in our work on the E6 transition in ^{53}Fe . As can be seen in Fig. 3, this transition is significantly retarded⁶⁾. Other E6 transitions have been excited in nuclei in this same

general region by means of inelastic electron scattering, and they show very similar retardations. But, to explain a reduced effective charge for such an electric multipole is no trivial matter, and this has led to a number of new types of calculations, both group theoretical and shell model, and some of these are beginning to show successful results⁹⁾.

References

- 1) K.L. Kossanke, M.D. Edmiston, R.A. Warner, R.B. Firestone, Wm. C. McHarris, and W.H. Kelly, Nucl. Instr. and Meth. 124, 365 (1975).
- 2) K.L. Kossanke, Wm.C. McHarris, R.A. Warner, and W.H. Kelly, Nucl. Instr. and Meth. 115, 151 (1974).
- 3) K.L. Kossanke, M.D. Edmiston, R.A. Warner, Wm.C. McHarris, M.F. Slaughter, and W.H. Kelly, Nucl. Instr. and Meth. 125, 253 (1975).
- 4) R.B. Firestone, R.A. Warner, Wm.C. McHarris, and W.H. Kelly, Phys. Rev. C 17, 718 (1978).
- 5) M.D. Edmiston, R.A. Warner, Wm.C. McHarris, and W.H. Kelly, 3rd Intl. Conf. on Nuclei Far from Stability, Cargese, Corsica, 1976, Proceedings, p. 258 (CERN Report 76-13).
- 6) J.N. Black, Wm.C. McHarris, W.H. Kelly, and B.H. Wil-denthal, Phys. Rev. C 11, 939 (1975).
- 7) R.B. Firestone, R.C. Pardo, R.A. Warner, Wm.C. McHarris, and W.H. Kelly, Phys. Rev. C 25, 527 (1982).
- 8) R.B. Firestone, Wm.C. McHarris, and Barry R. Holstein, Phys. Rev. C 18, 2719 (1978).
- 9) L. Zamick, delivered at Summer School on Nuclear Dynamics, Pearson College, Victoria, B.C., 1982; to be published in proceedings.

C. NUCLEAR STRUCTURE THEORY AND ANALYSIS OF SPECTROSCOPIC DATA

C 1. INTRODUCTION

C 2. NEW SHELL MODEL WAVE FUNCTIONS

- (a) A = 17-39 Nuclei**
- (b) N = 82 Isotones**
- (c) Particle-Hole States near O and Ca**
- (d) Future Developments**

C 3. SUGGESTIONS FOR NEW EXPERIMENTS

- (a) Transverse Excitations**
- (b) Pion Reactions**
- (c) Nuclei with Large Neutron Excess**

C 4. SYSTEMATIC ANALYSIS OF SPECTROSCOPIC DATA

- (a) M1 and Gamow-Teller Data**
- (b) E2 and E4 Data**
- (c) Nuclear Sizes and Shapes**
- (d) Nucleon Transfer Data**

C 5. FUNDAMENTAL PROCESSES

- (a) Parity Non-Conserving Transitions**
- (b) Charge-Dependent and Charge Asymmetric Interactions**
- (c) Recoil-order Matrix Elements for Beta Decays**
- (d) Double-Beta Decay**

NUCLEAR STRUCTURE THEORY AND THE ANALYSIS OF
SPECTROSCOPIC DATA

B. A. Brown and B. H. Wildenthal

1. INTRODUCTION

Our research in nuclear structure has four principal themes. One is the expansion in scope and the refinement in precision of shell-model representations of nuclear wave functions. The second is the exploration of these model wave functions in search of features which suggest new directions for experimental research. The third is the utilization of these wave functions in systematic analyses of existing nuclear structure data. The aim in these analyses is to extract from the complexities associated with the individual many-body structures of the various initial and final nuclear states the precise characterizations of the fundamental shell-model parameters such as effective charges and g factors. The fourth is the use of these shell model wave functions in the analysis of nuclear data which bear on fundamental processes such as parity non-conservation and double beta-decay. Background continuo to these major themes is provided by continuing work in improving the technology of shell-model calculations and collaborations, at varying levels of formality, with experimental groups whose interests and needs intersect with our own.

2. NEW SHELL MODEL WAVE FUNCTIONS

Our research in the area of formulating new shell-model wave functions emphasizes the incorporation of as many nuclei into the calculation as possible and the validation of the theoretical results by comparison with experiment for as great a range of states and for as many different types of phenomena as feasible. We think that only in this context is it possible to consider seriously either the "normality"

or the "aberrancy" of an observed effect relative to theoretical expectations. Our recent work in creating improved shell-model descriptions of nuclear wave functions has focussed on the $A = 17-39$ region and the $N = 82$ isotone chain.

(a) $A = 17-39$ Nuclei

For the $A = 17-39$ region, working always within the context of complete $0d_{5/2}-1s_{1/2}-0d_{3/2}$ spaces, we have been able to devise a single formulation of the one- plus two-body Hamiltonian which accounts for the energies of the $(sd)^n$ -type levels of every nucleus in the range $8 < N, Z < 20$ with an rms deviation of about 150 keV (Ref 1). This is a significant advance over the stage we had previously reached with the so-called "Chung-Wildenthal" Hamiltonians (Ref 2, Ref 3).

The key to this advance has been the incorporation of a simple A -dependence into the two-body matrix elements to mock up the effects of increasing nuclear size upon the matrix elements of a constant-strength interaction via an $(18/A)^{0.3}$ uniform scaling factor. Previous calculations have traditionally utilized A -independent two-body matrix elements. With the constraint of A -independence, it is impossible to find a single set of two-body matrix elements of the Hamiltonian for the sd -shell model space which yields acceptable agreement simultaneously with experimental energy level spectra at the lower and upper ends of the shell. The introduction of the simple A -dependence we have utilized allows this simultaneous treatment of the entire sd shell to be accomplished. Hence we were able to use level energy data from throughout the $A = 17-39$ range in determining the optimum values of the sixty six parameters of the sd - shell Hamiltonian.

The empirical Hamiltonian we have found yields, in terms of agreement between theoretical and experimental level energies, as good or better results than those of

Chung and Wildenthal in the region $A = 18-25$, where the older calculations were most successful, appreciably better results for $A = 32-38$ and very much better results for the region $A = 26-31$, where the older calculations, extrapolating several mass units beyond the region for which the A -independent Chung-Wildenthal Hamiltonians had been optimized, only qualitatively reproduced experimental spectra. Hence, we not only have better results nucleus by nucleus than have been achieved in previous calculations but also the additional improvement of establishing a genetic relationship between all sd -shell systems. The quality with which the new Hamiltonian accounts for global trends in energies can be judged from Figure 1, which shows the two-neutron separation energies for all isotope chains in the shell and Figure 2, which shows the variations with A of the excitation energies of the first and second $2+$ states and of the first $4+$ states in the doubly-even nuclei. The accuracy with which the details of the spectra of excitation energies in specific nuclei are reproduced is illustrated in Figure 3. We are now engaged in many investigations which utilize the steadily incrementing library of wave functions for sd -shell states generated from this Hamiltonian.

(b) $N = 82$ isotones

In collaboration with H. Kruse of MSU we have made extensive explorations of seniority and occupation-number truncation schemes for the $N = 82$ isotones and have found a composite truncation algorithm which allows us to work with almost complete freedom in the $0g_{7/2}-1d_{5/2}-1d_{3/2}-2s_{1/2}-0h_{11/2}$ orbit space and accurately reproduce exact complete-space results for the excitation energy regions of experimental importance (Ref 4). Within this model space we have optimized an unconstrained one-body plus two-body Hamiltonian using the techniques of Chung (Ref 2), proceeding from the starting values of the surface-delta interaction (Ref 5). The data base for the optimization of the

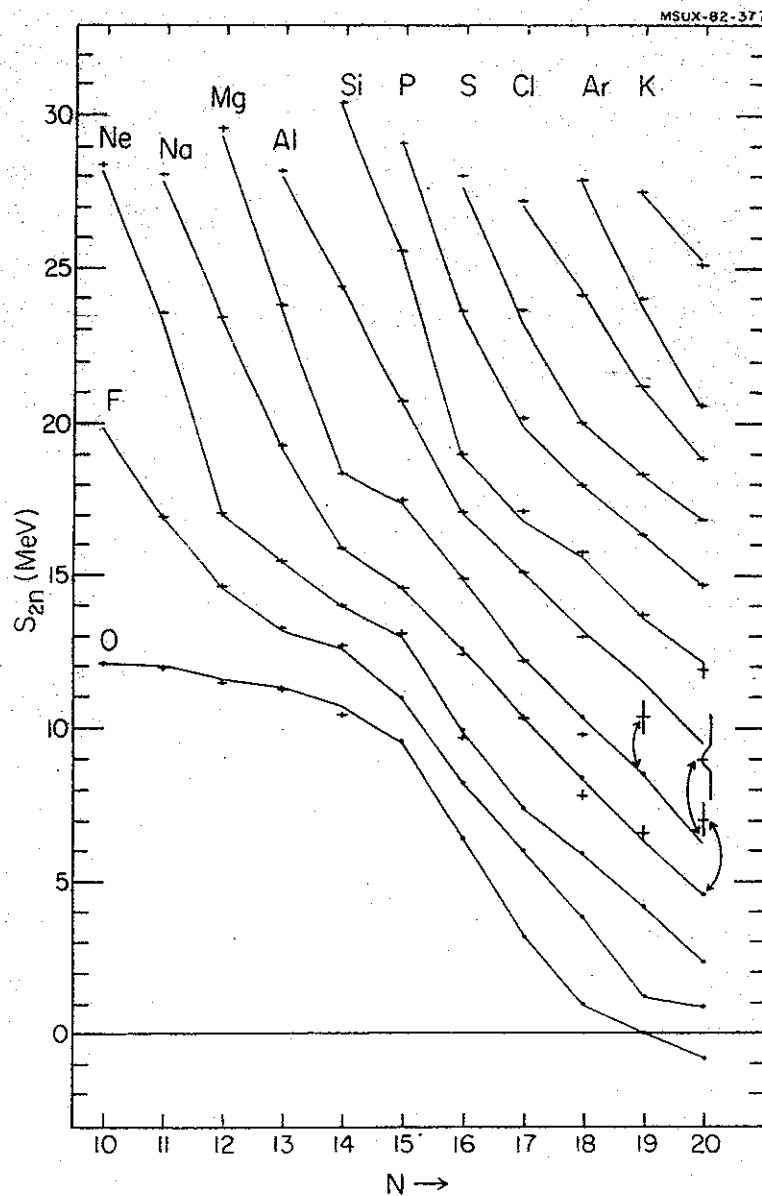


Fig. 1. Two-neutron separation energies for sd shell nuclei. The theoretical values are connected by lines. Experimental uncertainties are indicated when they are larger than a few hundred keV.

Hamiltonian consists of level energies taken in nuclei from $A = 134$ through 146 and from $A = 148$. The eigenvalues from the converged Hamiltonian give an accurate and complete accounting of the levels of the even- A nuclei up to about 3 MeV excitation energy. The results for ^{140}Ce are shown in Figure 4.

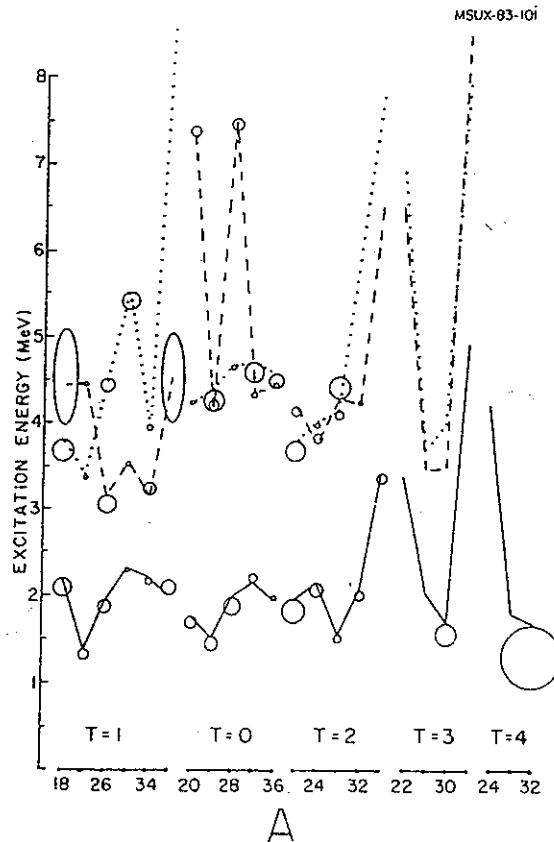


Fig. 2. Excitation energies of the first and second $2+$ and first $4+$ states in even-even sd shell nuclei. The theoretical values are connected by lines and the differences between experiment and theory are indicated by the sizes of the circles.

Many levels below 2 MeV excitation energy in the odd-A nuclei have no assigned spin-parity value and the existence of some are perhaps not yet established. This situation was a handicap in extracting the empirical matrix elements of the Hamiltonian and likewise makes it difficult to evaluate the accuracy of the predicted odd-A spectra. At the least, agreement between experiment as it is known and theory is not bad up through 2 MeV. In particular, the location and detailed fragmentation of the $1d_{3/2}$, $2s_{1/2}$ and $0h_{11/2}$ single-particle transfer strength is well accounted for with the model.

Most of the recent experimental interest in the $N=82$ systems has centered on states of high spin and excitation

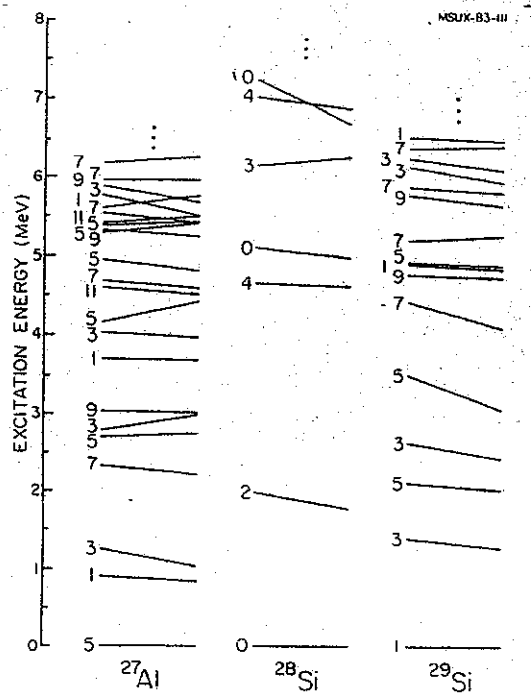


Fig. 3. Energy levels of ^{27}Al , ^{28}Si and ^{29}Si . The lines connect experimental values on the right to theoretical values on the left. The deviations of the slopes of these lines from the horizontal is thus indicative of the magnitude of the disagreement between experiment and theory.

energy and on the very proton rich systems above $A = 145$. The $A = 146$ system, with 64 protons, nominally corresponds to the minor shell closure occasioned by the filling of the $0g_{7/2}$ and $1d_{5/2}$ proton orbits. Its observed spectrum exhibits several features characteristic of shell closure (Ref 6). The systems above $A = 146$ can be treated successfully in the $(0h_{11/2})^n$ approximation (Ref 7). Our model space and Hamiltonian are formulated such that our calculations should translate smoothly from the $0g_{7/2}$ - $1d_{5/2}$ region below $A = 145$ over the "closed" $A = 146$ system into the $0h_{11/2}$ region of $A = 147, 148, 149$ and 150 . We find that our model results reproduce the features of each of these regions but that the underlying structure of the wave functions changes less dramatically in traversing the "shell closure" than might have been suspected (Ref 8). The existence of both experimental data and a unified shell model for the nuclei below, on and above a shell closure gives us a unique chance to study in detail the actual dynamics associated with this fundamental aspect of nuclear structure.

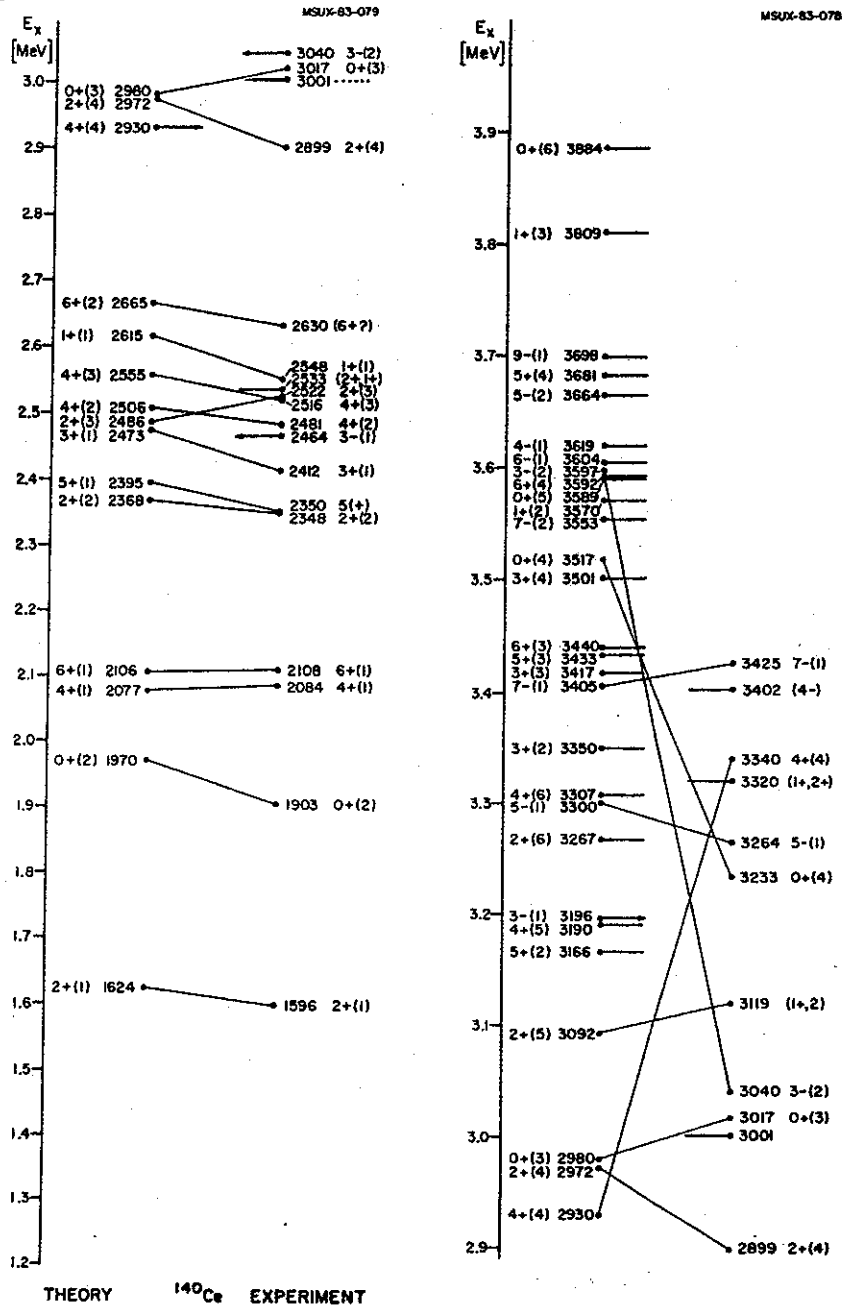


Fig. 4. Energy levels of ^{140}Ce . The lines connect experimental values on the right to theoretical values on the left. Note the suppression of 0 MeV and the different scales for the lower (left hand) and higher (right hand) portions of the spectrum.

(c) Particle-hole states near ^{16}O and ^{40}Ca

The excited states in the closed shell nuclei ^{16}O and ^{40}Ca have proved particularly difficult to describe quantitatively in the shell model. Calculations which use the full space available from a restricted set of orbits, such as the $\text{0p}_{1/2}$ - $\text{0d}_{5/2}$ - $\text{1s}_{1/2}$ (ZBM) orbit space for nuclei near ^{16}O (Ref 9), are able to account for many of the observed features of the spectra, in particular for the "many-particle many-hole" states. In collaboration with O. Avila-Aquirre of Oxford we have incorporated new energy level data for nuclei near ^{16}O into an improved Hamiltonian for the ZBM model space and this has led to some new speculations on the nature of the "2p-2h" states in ^{16}O which are currently the subject of several experimental studies (Ref 10, Ref 11).

The ZBM space cannot be expected to describe features for which the $\text{0p}_{3/2}$ and $\text{0d}_{3/2}$ orbits are intrinsically essential, such as the "lp-lh" 4^- states and the M1 transitions to the "2p-2h" 1^+ states in ^{16}O . We have recently shown that the ground state to 1^+ state B(M1) values calculated in the full 2p-2h space with the existing interactions are completely inconsistent with experiment (Ref 12). We are working in collaboration with I. Towner of Chalk River and D. J. Millener of Brookhaven to understand the reasons for this failure.

For the ^{40}Ca region, we recently have made calculations within the $\text{0d}_{3/2}$ - $\text{0f}_{7/2}$ model space in an attempt to describe the B(M1) and B(GT) strengths observed experimentally in ^{40}Ca and ^{42}Ca (Ref 13) We plan to extend this approach to the calculation of the (p,p') cross sections for the Ca isotopes which have been obtained in the MSU-Orsay collaboration. The main thrust of our future work in this area will be on obtaining improved truncation schemes and effective interactions for these cross-shell excitation in nuclei near ^{16}O and ^{40}Ca .

subset of the interaction terms calculated from a universal G-matrix. This sort of capability is a practical necessity for the utilization of spaces with hundreds of two-body matrix elements, an almost universal characteristic of realistic spaces for regions above the sd-shell.

3. SUGGESTIONS FOR NEW EXPERIMENTS

We are presently engaged in exploring the predictions of the new sd-shell model Hamiltonian in search of features which suggest fruitful experimental projects. One aspect of these explorations involves studying the wave functions by calculating elements of the various one-body density matrices between pairs of initial and final states and combining these results with a variety of operators. Our aim is to determine if there are features embedded in the wave functions which might manifest themselves as dominant concentrations of strength in the response of the nucleus to a particular probe. These concentrations would be analogous to the well-known instances of the concentration of 0^+ longitudinal-electric quadrupole strength in the lowest 2^+ states of doubly-even nuclei and the concentrations of M1 and Gamow-Teller strength which are observed in back-angle (e,e') and 0° -degree (p,n) reaction studies.

(a) Transverse Excitations

We have found that there are significant concentrations of the strength of the transverse E4 operator which should be excited in the inelastic scattering from 0^+ targets to higher-lying 4^+ states. These concentrations correspond to excitations of "stretched" $0d5/2$ hole- $0d3/2$ particle configurations which are analogous to the "stretched" $0d5/2$ hole- $0f7/2$ particle 6^- configurations already identified in inelastic electron and proton scattering (Ref 17, Ref 18). Current (e,e') experiments may have observed examples of such strength (Ref 19). There are, in general, remarkably few data available on transverse-electric inelastic electron

scattering. We are analyzing these data to determine if their strengths can be correlated with the same sort of shell-model--effective-charge factorization scheme which is so successful for the the longitudinal-electric strength.

Available evidence (Ref 20, Ref 21, Ref 22) suggests that the strength of the M3 (unique first-forbidden beta decay) operator is dramatically quenched in sd-shell nuclei. More electron scattering experiments, both inelastic and elastic, are needed to clarify this issue. We are calculating the M3 form factors for cases of practical experimental interest and are conferring with experimental groups who have interests in this field. Concurrently, we are calculating M5 form factors. Evidence suggests, contrary to expectations, that the M5 operator is not quenched. In the course of these calculations we have found that significant concentrations of $\Delta J^{\pi} = 5^{+}$ strength are predicted for low-lying 5_{1}^{+} inelastic excitations. These should be identifiable in large-momentum-transfer (p,n) reaction cross sections. Their experimental study could yield both information of the general issue of the quenching of spin-type transitions and on the basic parameters of configuration mixing in the sd shell.

We are studying the details of the M1 electron scattering form factors in several contexts (Ref 23). We find that the configuration mixing within the sd-shell space can produce a wide variety of form-factor shapes and that, hence, extrapolations to the photon point on the basis of only a few data must be treated with caution. It seems clear from our studies that more detailed experimental data on M1 form factors would pay significant dividends in our knowledge of nuclear structure.

(b) Pion Reactions

The interaction of pions with nuclei is both a topic of fundamental interest in itself and the source of a particularly sensitive probe of the isovector component of electric quadrupole and hexadecupole transitions (Ref 24). The unique

(d) Future developments

Our plans for the next stage of our work in this area of our research include expanding the scope of the $N = 82$ calculations to incorporate excitations of one and two neutron particles and holes and modifying our basic sd-shell model to incorporate $0p-0f, 1p$ excitations. We also plan to derive an alternative Hamiltonian for the Ca isotopes to the one now current (Ref 14) and to make a variety of exploratory ventures into the region between $A = 70$ and 90 .

For shell-model spaces larger than that of the sd shell it is a lengthy and difficult process to extract an unconstrained empirical Hamiltonian from a fit to experimental data. We are investigating whether it is possible to base the empirical Hamiltonian on G-matrix elements, derived from a nucleon-nucleon interaction such as the Paris potential (Ref 15). Those elements of the G-matrix which are most important in determining shell-model eigenvalues would be adjusted to their optimum values relative to experimental energies and those elements to which the shell-model values are quite insensitive would be held fixed. The adjustments obtained in such fits would yield the optimal core-polarization corrections as well as corrections for errors introduced by approximations made in calculating the G matrix.

Essential to this approach is the representation of the Hamiltonian in a scheme which efficiently separates "important" from "unimportant" terms. Work has been initiated on this project in collaboration with W. Richter of Stellenbosch University (Ref 16). We have decomposed the jj-coupled sd shell two-body matrix elements into central, tensor, spin-orbit and antisymmetric spin-orbit components and, within this scheme, we have compared empirical interactions with various G matrix and renormalized G matrix calculations. From such comparisons we hope to identify a technique by which a Hamiltonian can be derived for any shell-model space by making a relatively few empirical adjustments to a

spin characteristics of the pion also contribute to its importance as an alternative to the electron and the nucleon as a scattering probe. We are working with several experimental groups at LAMPF and SIN in the analysis of existing data and the design of new experiments. Goals are to better understand the double-charge-exchange reactions ($\pi^{+/-}, \pi^{-/+}$), the ratios of π^{+} to π^{-} inelastic scattering strengths and the general pattern of pion scattering strengths versus those extracted from electron, proton, deuteron and alpha projectile experiments.

It has recently been discovered (Ref 25) that the (p, π^{-}) reaction, unlike the (p, π^{+}) , populates specific nuclear states in an apparently comprehensible and selective fashion. In collaboration with H. Toki and O. Scholton of MSU we have initiated studies attempting to understand the few currently known data from this reaction and to predict what new experiments might help clarify our present understanding. In the beginning stage of this study we have only dealt with the nuclear structure aspects of the phenomena. The (p, π^{-}) and (π^{-}, p) processes are assumed to formally correspond to the application of a product of three one-body operators to the target state, two creation and one annihilation in the case of (p, π^{-}) , two annihilation and one creation in the case of (π^{-}, p) .

In full generality, the strengths of these processes would be calculated by evaluating all possible paths of this sort and then projecting out the weighting of these contributions appropriate to these particular reactions. We are presently employing a heuristic approximation to this scheme which is motivated by the assumption that the large momentum mismatches inherent in these reactions will emphasize those paths which are characterized by the maximal momentum transfer. Under this assumption we evaluate the matrix elements of the maximum momentum transfer charge exchange process possible within the model space of our nuclear wave functions ($\Delta J = 5$ in the sd shell, $\Delta J = 7$ in the fp shell)

in combination with the largest orbital angular momentum transfer available from single nucleon creation or annihilation. We utilize the result for the path through the single intermediate state which gives the largest value for the strength to the final state.

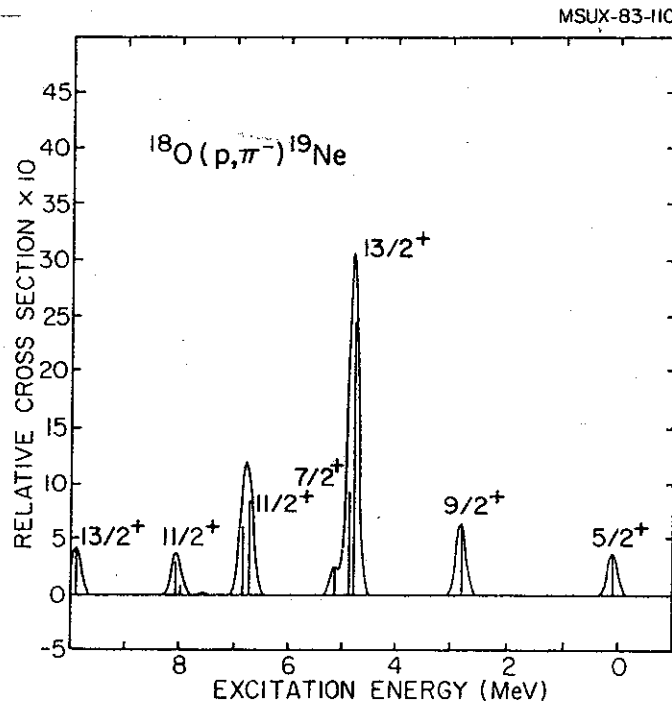


Fig. 5. Calculated relative strengths for the $^{18}\text{O}(p, \pi^-)^{19}\text{Ne}$ reaction. With the assumptions of the calculation, these strengths are proportional to the spectroscopic factor for stripping of a $d_{5/2}$ proton onto the 5^+ state of ^{18}F . The discrete states are indicated by vertical lines and the smooth curve is a 200-keV Gaussian average over these states.

We are working on making the obvious improvements to this procedure. Even this very rudimentary model yields very suggestive predictions, however. The dominant features of the experimental (p, π^-) spectra obtained on ^{18}O and the nuclei around ^{48}Ca are strikingly well reproduced by applying this algorithm to our sd -shell and $(f_{7/2})^n$ wave functions. The ^{18}O case is shown in Fig. 5. Studies with the sd -shell wave functions indicate that the inverse (π^-, p) reaction should have the doubly interesting characteristics of leading to very neutron rich nuclei and, within these

less well known systems, populating states of spins so high as to be in practice invisible to more conventional reactions. In Fig. 6 we show our predictions for $^{24}\text{Mg}(\pi^-, p)^{23}\text{Ne}$. The strengths are smaller than predicted for the $^{18}\text{O}(p, \pi^-)^{19}\text{Ne}$ case but the selectivity, both to high-spin states in general and, in more detail, to specific states among the several possibilities, remains very high.

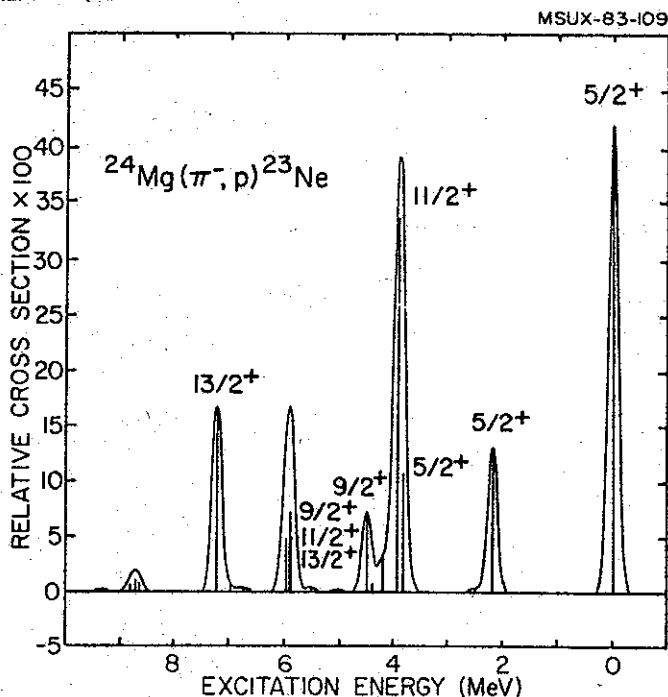


Fig. 6. Calculated relative strengths for the $^{24}\text{Mg}(\pi^- p)^{23}\text{Ne}$ reaction. Note that the strengths have been multiplied by a factor of ten relative to those in Fig. 5. With the assumptions of the calculation, these strengths are proportional to the M5 (n,p) transition strengths between the lowest $5/2^+$ state of ^{23}Na and states in ^{23}Ne . The discrete states are indicated by vertical lines and the smooth curve is a 200-keV Gaussian average over these states.

(c) Nuclei with Large Neutron Excesses

Study of very neutron rich nuclei has the potential to significantly advance our knowledge of the fundamentals of nuclear structure. The discoveries of the unexpected regions of stability in the heavy Na isotopes and near $A = 100$ are

examples. This field should be a focus of vigorous activity in the operations of the K=500 cyclotron. We are making detailed predictions of the masses, spectra and decay properties of sd-shell nuclei (Ref 26) which have large neutron excesses and have proposed several experiments to test these predictions. Measurements of ground state masses, excited-state energies and beta-decay half-lives are all both feasible and of immediate interest in evaluating the limits of validity of the present theories for light nuclei. A combination of experimental advances and extensions of the present shell-model calculations to include fp-shell configurations should make it possible to understand the origins of the still puzzling Na results and the general phenomena associated with crossing of a shell closure. Similarly, expansions of our older work at the juncture of the sd and p shells should make possible better analyses of the structure of the very neutron rich nuclei whose proton structures are rooted in the p shell (Ref 27).

4. SYSTEMATIC ANALYSIS OF SPECTROSCOPIC DATA

One aim of this research is to establish the range, in terms of masses, excitation energies and size of matrix elements, over which the shell model yields an accurate factorization of the many-body nuclear structure problem into state-dependent, intra-model-space terms and state-independent, mass-independent, shell-wide renormalizations, in which the effects of the shell-model truncation are expressed as modifications of the properties of the various spectroscopic operators. Coupled to this is the aim of empirically establishing what the values of these renormalizations are, in order to provide the most secure experimental values against which to evaluate theoretical predictions for such renormalizations. In the process of such analyses we often are able to provide timely theoretical values with which newly available experimental data can be compared.

(a) M1 and Gamow-Teller Data

We have utilized the results of the new sd-shell calculations as they have become available to analyze the existing reservoir of data on Gamow-Teller beta decay transitions and magnetic dipole moments. This project will next be extended to encompass $B(M1)$ values from lifetime measurements and M1 strengths from inelastic electron scattering. Our first aim in these analyses is, of course, to check that the wave functions yield, at least qualitatively, the phenomena found experimentally. This being accomplished, we then wish to determine if a detailed analysis of the data of low-energy spectroscopy reveals evidence that the effective Gamow-Teller and M1 operators in finite nuclei are different from those inferred from the properties of the free neutron and proton.

Such an analysis of a smaller data base with the preceding ("Chung-Wildenthal") generation of sd-shell model wave functions yielded the prediction (Ref. 28) that the average strength of Gamow-Teller transitions in the sd-shell should be quenched by a factor of 0.6 from the value expected on the basis of normalization to the half-life of the free neutron. This quenching factor is, of course, very close to that deduced from recent studies of the full response of the nucleus to the Gamow-Teller probe via the (p,n) reaction. Use of the new wave functions and all of the data available from the sd shell yields a quenching factor of, again, 0.6, but with considerably smaller uncertainty and orbit-dependent variation. The results for the sums of G-T strength in sd shell decays are shown in Fig. 7. The consistency of this renormalization of the Gamow-Teller strength over a range of 20 MeV excitation energy is shown in Figure 8, for example, by comparison of the model predictions to data from the $^{26}\text{Mg}(p,n)^{26}\text{Al}$ reaction (Ref. 29).

These renormalizations of the Gamow-Teller operator are being compared with the results of a similar analysis of the magnetic moments of $T = 0$ states and mirror pairs (Ref. 30).

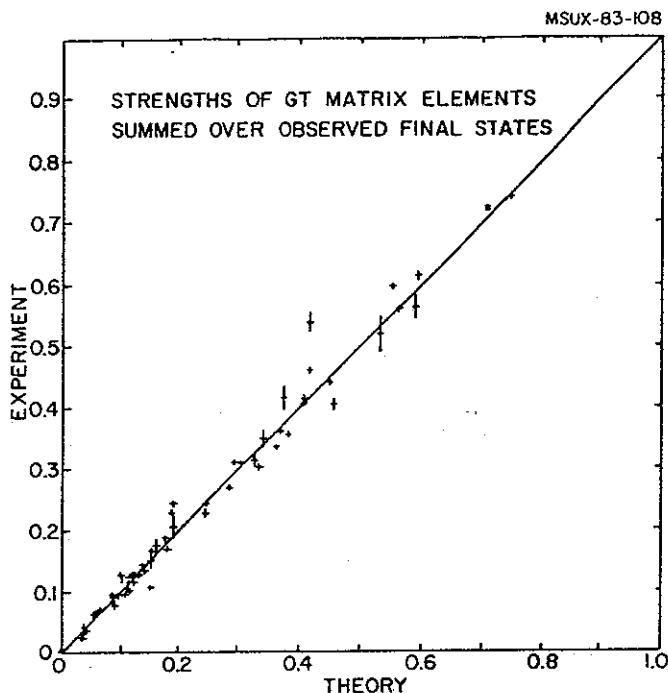


Fig. 7. Summed Gamow-Teller strengths for sd shell nuclei. The sum for $B(GT)$ runs over all final states whose matrix elements have been experimentally determined to better than 10% accuracy. Each beta-unstable nucleus in the sd shell is represented by one point in the figure, with experiment plotted on the y axis and theory on the x axis. The values plotted are obtained by taking the square roots of the summed strengths after they have been divided by a factor proportional to the $(N-Z)$ sum rule. Thus, the square of the value given on the plot indicates the fraction of the $B(GT-) - B(GT+)$ sum rule exhausted with the observed data. The theoretical values were obtained with transition densities calculated with the new sd shell wave functions in combination with empirical values for the five single-particle matrix elements for the G-T process which were obtained from a least square fit to all sd-shell data.

The magnetic moment analysis yields the analogous renormalizations of the isoscalar and isovector single-nucleon matrix elements. The isoscalar renormalizations principally give insight into the importance of the admixtures of many small contributions from distant shells into the explicit model space. The isovector renormalizations can be related to the GT results by extracting the contributions of the orbital term from the M1 values. Comparison of the equivalent GT and

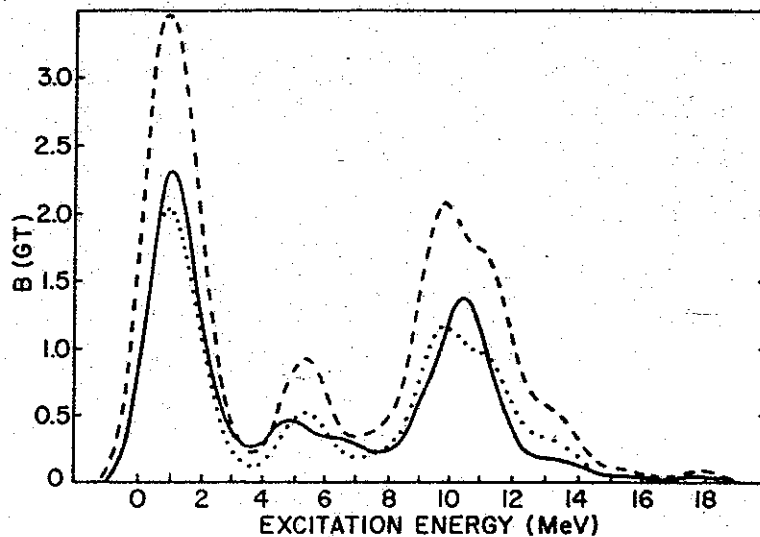


Fig. 8. The $B(GT)$ Strength function for transitions from the ^{26}Mg ground state to the 1^+ , $T=0$, 1 and 2 states of ^{26}Al . In order to emphasize the gross features of the distributions, both experiment and theory have been averaged over a Gaussian with $\text{FWHM} = 1.5$ MeV. The solid line gives the experimental results deduced from the (p,n) reaction data of Ref 29. The dashed line shows the theoretical prediction obtained with the new sd shell wave functions using the free nucleon GT operator. The dotted line is the theoretical prediction multiplied by 0.6.

$M1$ values then yields information on the relative importance of the various non-nucleonic sources of renormalization.

(b) E2 and E4 data

Our last major project with the Chung-Wildenthal wave functions was the extraction from the electromagnetic data of the sd shell of the isovector E2 effective charge (Ref 31). This project is related to the study of the relative inelastic scattering probabilities of π^+ , π^- , proton, electron, deuteron and alpha projectiles. We are collaborating in several experimental projects which have the aims of better understanding both the underlying isovector structure of the nuclear states and of the reaction mechanisms of the probes with the targets.

We are repeating our previous analysis with the new wave functions. The most significant change we have

identified is that the isovector/isoscalar mixtures in the first and second 2^+ states in doubly-even nuclei are quite different with the new wave functions. In most cases the new matrix elements seem to be in better accord with experiment. In a particular instance, the relative sign between the proton and neutron components of the second 2^+ in ^{30}Si predicted by the Chung-Wildenthal calculation is reversed by the new calculations. Recent measurements (Ref 32) have suggested that this case in ^{30}Si represented the only known contradiction to the Chung-Wildenthal predictions with respect to these relative signs.

We plan to continue studying this subject in detail, examining in particular the case of ^{26}Mg , where the latest electromagnetic data (Ref 33) are in contradiction to the shell-model predictions as well as earlier π^+/π^- and $(p,p')/(e,e')$ results. An important element of the analysis of the nucleon scattering data is the consideration of coupled-channel effects which involve intermediate states. The consistent and complete description of the low-lying spectrum of states which we have available with our wave functions permits a coherent analysis of this aspect of the problem along with the neutron-proton nature of the initial and final states. Another area in which the capability to make a complete and self-consistent analysis of nucleon inelastic scattering should yield interesting results involves the extraction of excited-state quadrupole moments from scattering of polarized deuterons (Ref 34).

We have completed a review of the data on longitudinal electric E2 and E4 electron scattering from the doubly-even sd shell nuclei in comparison with the predictions of the new sd-shell wave functions (Ref 35). In this study we have taken some pains to thoroughly explore various options to the formulation of the single-nucleon wave functions and of the effective-charge transition density. This study establishes the systematic near identity between the $B(E2)$ values obtained from the proper extrapolations of the electron

scattering data and from life-time measurements and the insensitivity of the E2 and E4 effective-charge renormalizations to the value of the transferred momentum in the range $q = 0.4$ to 2.5 fm^{-1} . With isolated exceptions, such as the very weakly excited first 4^+ in ^{24}Mg , the shell-model predictions explain the shapes of the observed form factors and, with q - and A -independent effective charges, the absolute magnitudes as well. Typical results are shown in Fig. 9.

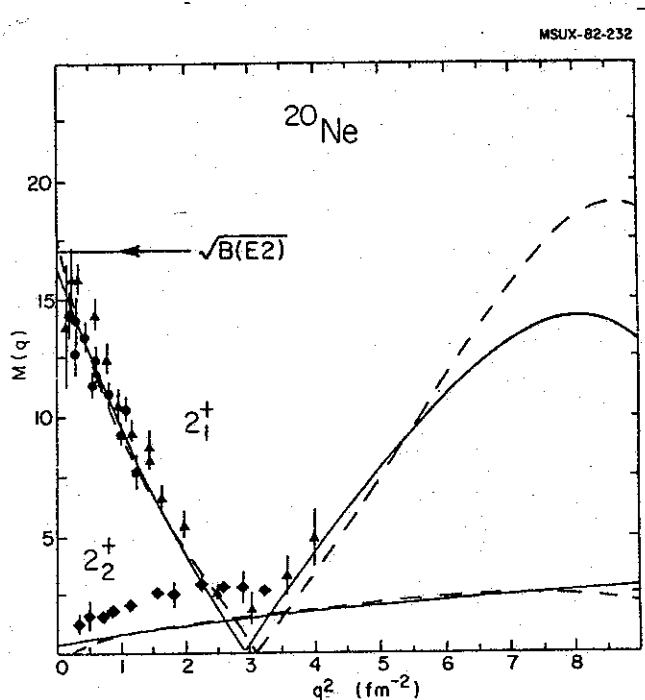


Fig. 9.

The longitudinal form factors for the transitions from the 0^+ to the first and second 2^+ states in ^{20}Ne . We plot the square root of the form factors divided by a q -dependent function chosen so that in the limit of small q the curves go to the square root of the $B(E2)$ values and for finite q are approximately linear in q^2 . The theoretical curves were obtained with the new sd shell wave functions together with a q -independent effective charge based on the Tassie model. The isoscalar effective charge at $q=0$ is $1.7e$ (compared to the free-nucleon value of $1.0e$). The solid curve was obtained with harmonic-oscillator wave functions and the dashed curve with Woods-Saxon wave functions.

Our calculations suggest many extensions of the presently existing data to higher (and lower) values of momentum transfer and to higher excitation energies. The new generation of electron accelerators have the energy and energy-resolution capabilities to perform these needed measurements and we are working together with experimental groups to see that they are made and analyzed. Our plans are to extend our systematic study of longitudinal electric scattering to odd-A targets, which offer a greater variety of structural features for exploration, while simultaneously pursuing the issue of transverse electric and magnetic scattering, as mentioned earlier. Presently we are collaborating with C. Williamson of MIT in analysis of data on ^{19}F and ^{29}Si .

(c) Nuclear Sizes and Shapes

The theoretical description of many features of nuclear structure, such as Gamow-Teller and M1 rates, do not depend explicitly upon the description of the radial dependence of the shell-model wave functions. Other properties, such as the calculated electron scattering form factors, do depend explicitly on the model chosen for the radial wave functions. Historically the models and parameters for the radial potentials have been obtained from analyses of the longitudinal elastic form factors and the associated rms radii. In recent years we have carried out such analyses with harmonic-oscillator (Ref 36), Woods-Saxon (Ref 31, Ref 37) and self-consistent Hartree-Fock potentials (Ref 38, Ref 39). In particular we have discussed the physics needed to understand the density oscillations in the nuclear interior of ^{208}Pb (Ref 39), the isotope shifts of light nuclei (Ref 38) and the isotope shifts of the Pb and Sn isotopes (Ref 40). The latter of these studies involves collaborations with the Laser group at Karlsruhe lead by H. Rebel (Ref 41). This work is continuing in collaboration with P. Hodgson of Oxford. We are making a comprehensive comparison of all

measured rms charge radii with Hartree-Fock theory and with global parameterizations such as the Woods-Saxon potential model and the droplet model. This work will be important in connection with possible future experiments at the NSCL which would use laser spectroscopy to study the exotic nuclei separated in the RPMS spectrometer. Continuation of these studies will be an important part of our future research.

(d) Nucleon Transfer Data

A preliminary survey of the spectroscopic factors for single-nucleon transfer from $J = 0^+$ targets predicted from the new sd-shell wave functions suggests that they uniformly reproduce the existing experimental values to within the commonly accepted uncertainties in the final experimental quotations. A similar survey of transfer on odd-A targets is underway, but the suggestion as of now is that the uncertainties in experimental spectroscopic factors must be reduced if they are to offer any further critique to the present stage of shell-model calculations. One avenue to accomplishing a contraction of experimental uncertainties is to concentrate on relative values and attempt to establish an empirical chain of values tied to the closed-shell values. One such attempt, focussing on the ($^3\text{He}, d$) reaction, is being pursued in collaboration with J. Vernotte of Orsay.

Two-nucleon transfer studies in which the Chung-Wildenthal wave functions were used in the analysis of the observed differential cross sections yielded mixed conclusions about the efficacy either of the wave functions or of the more general context of the analysis (Ref 42, Ref 43). Most qualitatively obvious experimental features were explained in terms of the structure of the wave functions but the quantitative accuracy of the agreement between experiment and theory was uneven. We are collaborating with H. Nann of Indiana and H. T. Fortune of Pennsylvania in investigations with the new sd-shell wave functions, in

comparison with both new and existing data, to determine whether better results can be obtained than was previously the case.

5. FUNDAMENTAL PROCESSES

(a) Parity Non-Conserving Transitions

Our initial work in this area has involved the development of the theory and the computer programs needed to calculate matrix elements of the parity non-conserving (PNC) two-body transition densities between large-basis shell model wave functions (Ref 44). The results obtained with the most recently developed PNC interaction (Ref 45) for the cases of interest in ^{16}O , ^{18}F , ^{19}F and ^{21}Ne have lead to some interesting constraints on the PNC interaction (Ref 46). Our present interest in this area consists of using the existing wave functions to make predictions for cases of interest. Current work includes collaborations with R.G.H. Robertson (Los Alamos) on the PNC forbidden α -decay width of the 0^+ T=1 state of ^6Li and with E. Adelberger (Seattle) on the observables connected with the $0^{+/-}$ and $2^{+/-}$ T=1 doublets in A=14 nuclei. The A=14 PNC are sensitive to the iso-tensor PNC which may be connected to the anomalously large result obtained in the $n+p \rightarrow d+\gamma$ experiment of Labashov. We feel that major progress in this area relies on the improvements in the shell-model wave functions which will come out of the research proposed in the previous sections.

(b) Charge-Dependent and Charge-Asymmetric Interactions

Our research into this area has been divided into two rather distinct areas. One is a study of the systematics of the displacement energies of mirror nuclei which display the well known but poorly understood Nolen-Schiffer anomaly. We have developed a model which analytically displays the dependence of the Coulomb displacement energy upon the core and valence rms radii. To this we have added analytic terms

for the various proposed corrections, including the core-compression effect and the charge asymmetric interaction (Ref 48). With harmonic oscillator radial wave functions, the core-compression effect accounts remarkably well for all displacement energies between $A=17$ and 55 except for those states which are loosely bound. We have used this model to make predictions for the binding energies of proton rich nuclei for a $^{58}\text{Ni}(p,\pi^-)^{59}\text{Zn}$ experiment recently carried out at the IUCF (Ref 49) and several experiments proposed for the NSCL, including $^{58}\text{Ni}(^7\text{Li}, ^8\text{He})^{57}\text{Cu}$.

Our second area of investigation concerns the extraction of the effective charge-dependent and charge-asymmetric interactions from the b and c coefficients in the isobaric mass multiplet equation (IMME). The approach here is essentially the same as that involved in obtaining the effective shell-model Hamiltonian from fits to the "a" coefficient of the IMME and has proved to be quite successful in the $1f7/2$ shell (Ref 50). Currently work is in progress to extend our treatment to larger shell-model spaces where we hope that the extracted two-body matrix elements can be more directly related to the fundamental interactions (in collaborations with E. Adelberger of the University of Washington and E.Ormand of MSU). Our results are being used to calculate isospin mixing between excited nuclear states which have been measured for example by π^+/π^- reactions and to calculate the isospin mixing corrections to Fermi decays which are needed in order to discuss such things as the mean quark charge of the nucleon (Ref 51).

(c) Recoil-Order Matrix Elements for Beta Decays

Various experiments have been performed in nuclei in order to set limits on the presence of second-class currents. The analysis of these experiments requires the calculation of the nuclear matrix elements involved in the recoil-order corrections to beta decay (Ref 52). Using the recent sd shell wave functions, we propose to make several

new calculations in order to make a systematic comparison with recent experiments (in collaboration with F. Calaprice of Princeton and T. Girard of the Univ. of Michigan).

(d) Double-Beta decay

Because of the very different phase space factors for two-neutrino and neutrino-less double-beta decay, this decay in nuclei is very sensitive to the properties of the neutrino such as its mass (Ref 53). The degree to which this sensitivity can be exploited depends upon the accuracy with which the nuclear two-body density can be calculated (Ref 54). We have not previously made calculations for this process, but our recent work in calculating two-body transition densities and calculating Gamow-Teller strength distributions (the intermediate states in double beta decay from $J=0^+$ nuclei are the 1^+ states), make it logical to extend our program to include research on this topic. The extensions of our shell-model wave function research mentioned in Section 2d are in part motivated by this interest.

References

1. B. H. Wildenthal, Bull. Am. Phys. Soc. 27, 725 (1982).
2. W. Chung, PhD Thesis, Michigan State University, 1976.
3. B. H. Wildenthal, "Elementary Modes of Nuclear Excitation", edited by A. Bohr and R. Broglia, Soc. Italiana de Fisica, Bologna (1977) p. 383.
4. H. G. W. Kruse and B. H. Wildenthal, Bull. Am. Phys. Soc. 27, 533 (1982).
5. B. H. Wildenthal, Phys. Rev. Lett. 22, 1118 (1969).
6. P. Kleinheinz, R. Broda, P. J. Daly, S. Lunardi, M. Ogawa and J. Blomqvist, Z. Phys. A290, 279 (1979).
7. H. Helppi, Y. H. Chung, P. J. Daly, S. R. Faber, A. Pakkanen, I. Ahmad, P. Chowdhury, Z. W. Grabowski, T. L. Khoo, R. D. Lawson and J. Blomqvist, Phys. Lett. 115B, 11 (1982).

8. H. G. W. Kruse and B. H. Wildenthal, *Bull. Am. Phys. Soc.* 27, 725 (1982).
9. B. S. Reehal and B. H. Wildenthal, *Particles and Nuclei* 6, 137 (1973).
10. E. Adelberger, private communication.
11. R. Sherr, P. Kutt and R. Kouzes, private communication.
12. K. A. Snover, E. G. Adelberger, P. K. Ikossi and B. A. Brown, to be published in *Phys. Rev. C*.
13. B.A. Brown, D. J. Horen, B. Castel and H. Toki, submitted to *Phys. Lett. B*.
14. J. B. McGrory and B. H. Wildenthal, *Phys. Lett.* 103B, 173 (1981).
15. N. Anantaraman, H. Toki and G. F. Bertsch, to be published in *Nucl. Phys. A*.
16. B. A. Brown and W. Richter, *Bull. Am. Phys. Soc.* (Baltimore Meeting, 1983).
17. H. Zarek, B. O. Pich, T. E. Drake, D. J. Rowe, W. Bertozzi, C. Creswell, A. Hirsch, M. V. Hynes, S. Kowalski, B. Norum, and R. A. Lindgren, *Phys. Rev. Lett.* 38, 750 (1977).
18. G. S. Adams, A. D. Bacher, G. T. Emery, W. P. Jones, R. T. Kouzes, D. W. Miller, A. Picklesimer and G. E. Walker, *Phys. Rev. Lett.* 38, 1387 (1977).
19. R. A. Lindgren, M. A. Plum, R. L. Huffman, R. S. Hicks, X. K. Muruyama, A. D. Bacher, C. Olmer, D. F. Geesaman and B. H. Wildenthal, *Bull. Am. Phys. Soc.* 27, 697 (1982).
20. M. V. Hynes, H. Miska, B. Norim, W. Bertozzi, S. Kowalski, F. N. Rad, C. P. Sargent, T. Sasanuma, W. Turchinets and B. L. Berman, *Phys. Rev. Lett.* 42, 1444 (1979).

21. E. K. Warburton, G. T. Garvey and I. S. Towner, *Annals of Physics*, 57, 174 (1970).
22. B. A. Brown, S. E. Massen, W. Chung, B. H. Wildenthal and T. A. Shibata, *Phys. Rev. C* 22, 842 (1980).
23. B. A. Brown and B. H. Wildenthal, *Bull. Am. Phys. Soc.* 27, 725 (1982), and in press, *Phys. Rev. C*.
24. B. A. Brown and B. H. Wildenthal, *Phys. Rev. C* 21, 2107 (1980).
25. S. E. Vigdor, T. G. Throwe, M. C. Green, W. W. Jacobs, R. D. Bent, J. J. Kehayias, W. K. Pitts and T. E. Ward, *Phys. Rev. Lett.* 49, 1314 (1982).
26. B. H. Wildenthal, M. S. Curtin and B. A. Brown, submitted for publication.
27. M. S. Curtin, B. H. Wildenthal and B. A. Brown, *Bull. Am. Phys. Soc.* 27, 696 (1982).
28. B. A. Brown, W. Chung and B. H. Wildenthal, *Phys. Rev. Lett.* 40, 1631 (1978).
29. R. Madey, B. D. Anderson, J. W. Watson, A. R. Baldwin, B. S. Flanders, C. Lebo, C. C. Foster, S. M. Austin, A. Galonsky and B. H. Wildenthal, *Bull. Am. Phys. Soc.* 27, 731 (1982).
30. B. A. Brown and B. H. Wildenthal, *Bull. Am. Phys. Soc.* 27, 726 (1982).
31. B. A. Brown, B. H. Wildenthal, W. Chung, S. E. Massen, M. Bernas, A. M. Bernstein, R. Miskimen, V. R. Brown and V. A. Madsen, *Phys. Rev. C* 26, 247 (1982).
32. R. A. Miskimen, A. M. Bernstein, B. Quinn, S. A. Wood, M. V. Hynes, G. S. Blanpied, B. G. Ritchie and V. R. Brown *Bull. Am. Phys. Soc.* 27, 730 (1982).
33. T. K. Alexander, G. C. Ball, W. G. Davies, J. S. Forster, I. V. Mitchell and H. B. Mak, *Phys. Lett.* 113B, 132 (1982).

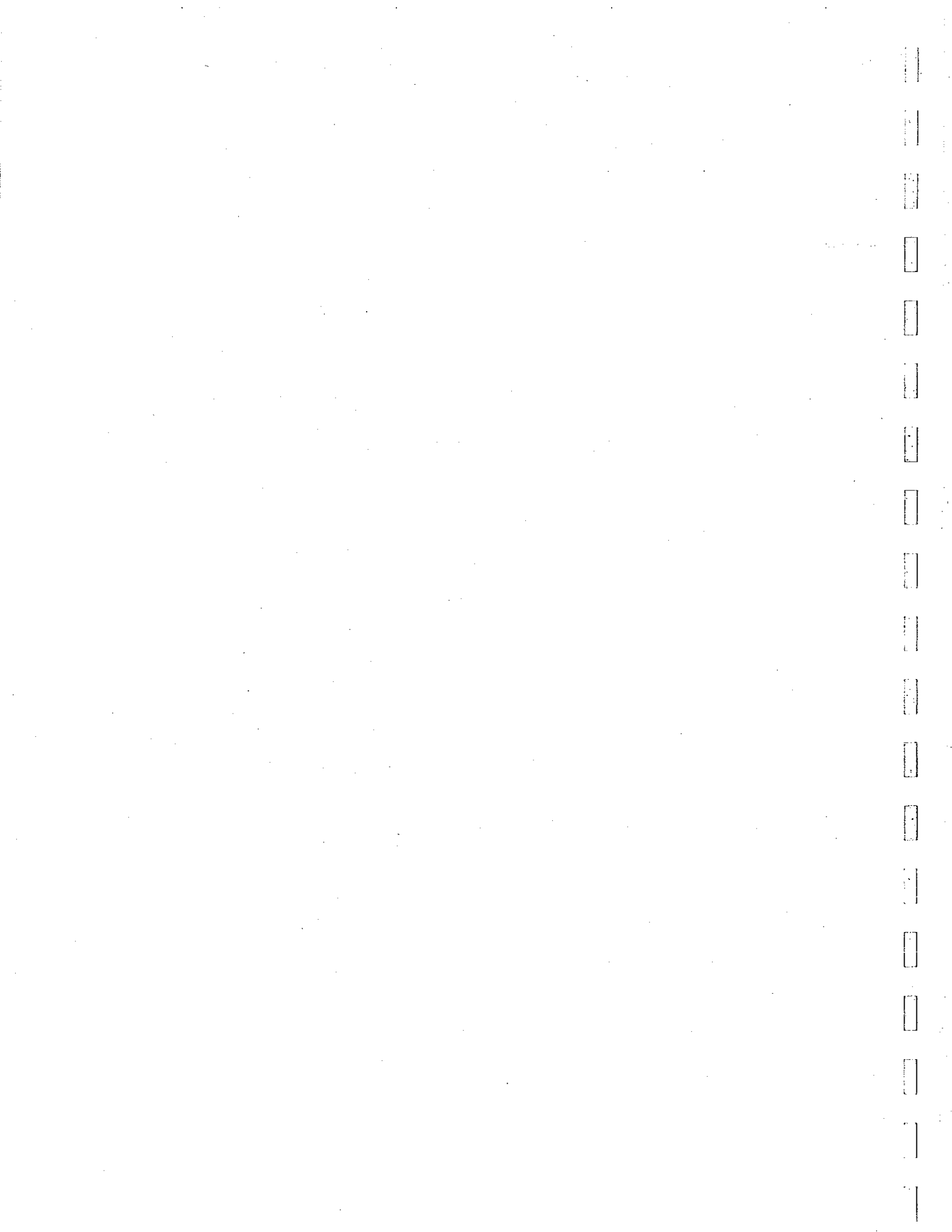
34. H. Clement, R. Frick, G. Graw, P. Schiemenz, N. Seichert and S. T. Hsun, Phys. Rev. Lett. 45, 599 (1980).
35. B. A. Brown, R. Radhi and B. H. Wildenthal, submitted for publication.
36. B. A. Brown, W. Chung and B. H. Wildenthal, Phys. Rev. C22, 774 (1980).
37. J. Streets, B. A. Brown and P. E. Hodgson, Jour. Phys. G8, 839 (1982).
38. B. A. Brown, S. E. Massen and P. E. Hodgson, Jour. Phys. G5, 1655 (1979).
39. B. A. Brown, S. E. Massen, J. I. Escudero, P. E. Hodgson, G. Madurga and J. Vinas, Jour. Phys. G to be published.
40. J. B. McGrory and B. A. Brown, in Lasers and Nuclear Spectroscopy (ed by C. E. Bemis and H. K. Carter, Harwood Academic Pub. 1982) p. 455.
41. R. C. Thompson, M. Anselment, K. Bekk, S. Goring, A. Hanser, G. Meisel, H. Rebel, G. Schatz, and B. A. Brown, Jour. Phys. G to be published.
42. H. Nann, A. Saha and B. H. Wildenthal, Phys. Rev. C23, 606 (1981).
43. H. T. Fortune, L. Bland, R. Middleton, W. Chung and B. H. Wildenthal, Phys. Lett. 87B, 29 (1979).
44. B. A. Brown, W. A. Richter and N. S. Goodwin, Phys. Rev. Lett. 45, 1681 (1980).
45. B. Desplanques, J. F. Donoghue and B. R. Holstein, Ann. Phys. 124, 449 (1980).
46. J. F. Donoghue and B. R. Holstein, Phys. Rev. Lett. 46, 1603 (1981).
47. K. R. Lassey and B. H. J. McKellar, Nucl. Phys. A260, 413 (1976).

48. S. Shlomo, Rep. Prog. Phys. 41, 957 (1978)
49. B. Sherrill, K. Beard, W. Benenson, B. A. Brown, E. Kashy, W. E. Ormand, H. Nann, J. J. Kehayias, A. D. Bacher, and T. E. Ward, submitted to Phys. Rev. C.
50. B. A. Brown and R. Sherr, Nucl. Phys. A, 61 (1979).
51. D. H. Wilkinson, A. Gallmann and D. E. Alberger, Phys. Rev. C 18, 401 (1978).
52. F.P. Calaprice, W. Chung and B.H. Wildenthal, Phys. Rev. C15, 2178 (1978).
53. H. Primakoff and S. Rosen, Ann. Rev. Nucl. Sci. 31, 145 (1981).
54. W. Haxton, G. Stephenson and D. Strottman, Phys. Rev. D25, 2360 (1982).

D. FUNDAMENTAL INTERACTIONS AND ASTROPHYSICS

D L. WEAK INTERACTIONS

- (a) Superallowed β -decay**
- (b) Measurements of Gamow-Teller Strength for Double-Beta Decaying Nuclei**



(a) Superallowed Beta Decay

B.A. Brown, L. Harwood, J. Nolen and B.H. Wildenthal

During the past 10 years or so much experimental work has been done in an attempt to measure, in as many cases as possible, precise values of the ft values for superallowed Fermi beta decay transitions. Recent summaries of the data have been made by Towner and Hardy¹⁾ and by Wilkinson²⁾. We began working in this area during the last years of operation of the K50 cyclotron when P.H. Barker spent a sabbatical leave at MSU. The Z -dependence of the well-known ft -values as summarized by Wilkinson in 1977²⁾ is reproduced in Fig. 1. The entire Z -dependence shown in this figure is determined by the ^{14}O and $^{26}\text{Al}^m$ values. However, the ^{14}O mass which we reported in 1977³⁾ is in disagreement with the Munich⁴⁾ and Auckland^{5,6)} measurements which Wilkinson used in this figure. Our measurement would raise the ^{14}O ft -value enough to almost completely eliminate the Z -dependence shown in Fig. 1. In Auckland, New Zealand, White et al., have put much effort into measuring the ^{14}O transition energy^{5,6)}. The value obtained is between the MSU and Munich values, but is still over two standard deviations from our measurement. Hence, we feel that the ^{14}O mass is still somewhat in question and further measurements are appropriate. We plan to carry out this work in collaboration with Calaprice and Kouzes using the Q3D spectrograph and cyclotron at Princeton University. Using momentum matching and kinematic techniques developed at MSU during the last years of the K50 cyclotron, we believe that an independent measurement of the ^{14}O mass can be done at Princeton with an uncertainty of ± 100 eV. In addition to the justification given above for this remeasurement, there is an additional incentive related to recent measurements at Chalk River by

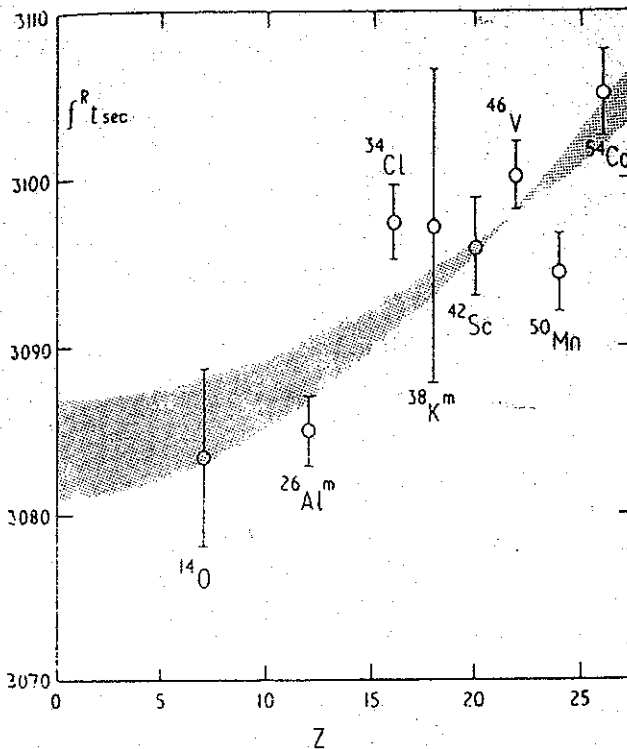


Fig. 1. Plot of ft -values published by Wilkinson (ref.2).

Hardy et al.⁷ They have reported a new improved measurement of the $^{26}\text{Al}^m$ mass relative to that of ^{14}O . Hence, any new measurement which moves the ^{14}O transition energy will also move that of $^{26}\text{Al}^m$.

We also plan to carry out related work at MSU using the RPMS as a mass separator. Our initial measurements in this area will be on the branching ratio for the ^{10}C (0^+ , $T=1$) to ^{10}B (0^+ , $T=1$) decay. Since ^{10}C has the lowest Z of all superallowed beta decays, it would be a very interesting point to add to the systematics shown in Fig. 1. The recent Auckland⁸⁾ work on the ^{10}C transition energy seems to be on firm ground since the experiments did not have the target problems in this measurement which they did for ^{14}O . The lifetime of ^{10}C is also well known, but the branching ratio to the $T=1, 0^+$ state of ^{10}B is not known well enough at this time (see Fig. 2). We plan to use either the $^{12}\text{C}^{3+}$ beam at an energy per nucleon of about 30 MeV or the $^{12}\text{C}^{4+}$ beam with

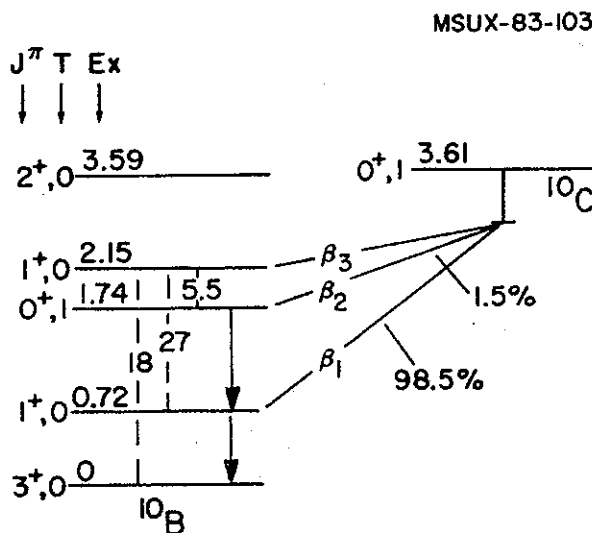


Fig. 2. Decay scheme of ^{10}C showing the 1.5% superallowed transition. (from ref. 9).

E/A of about 40 MeV for this measurement. The ^{10}C nuclei will be produced via fragmentation of the ^{12}C beam on a ^9Be target and collected at 0° in the focal plane of the RPMS. The mass-separated ^{10}C samples collected in this way will be transported via a rabbit-type apparatus to a shielded counting area. Two intrinsic Ge detectors will be used to count the 0.72 MeV and 1.02 MeV gammas (see Fig. 2). The gamma rays counted in the previous measurement by Robinson, et al.⁹⁾ are shown in Fig. 3. Our setup will be improved over that of Robinson et al. in two ways: firstly, the mass separation afforded by the RPMS will eliminate the ^{11}C positron background, and secondly, an array of BGO scintillators will be used in coincidence with the Ge detectors to reduce the effect of 511 keV pileup.

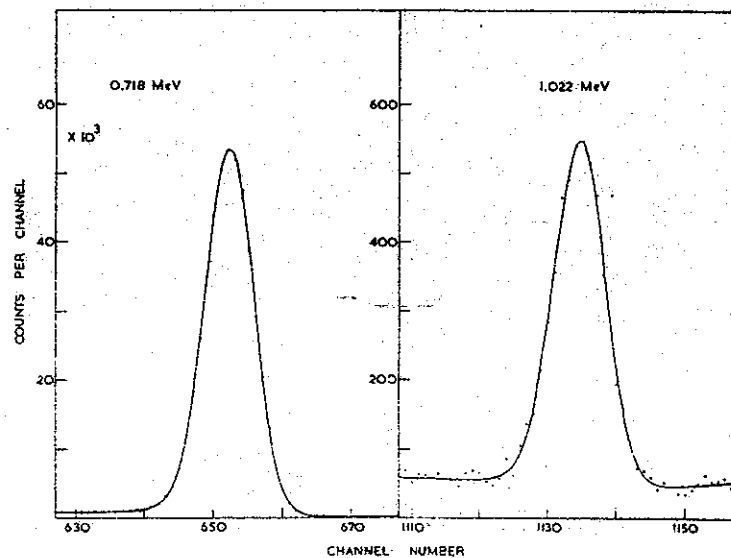


Fig. 3. Data from Robinson et al.⁹⁾ showing the two gamma peaks of interest in the decay of $^{10}\text{C } ^{10}\text{B}$.

References

- 1) J.C. Hardy and I.S. Towner, Nucl. Phys. A254, 221 (1975); I.S. Towner and J.C. Hardy, Phys. Lett. 73B, 20 (1978).
- 2) D.H. Wilkinson, Phys. Lett. 67B, 13 (1977).
- 3) P.H. Barker and J.A. Nolen, Proceedings of the International Conference on Nuclear Structure, 1977, Contributed papers, p. 155.
- 4) H. Vonach, et al., Nucl. Phys. A278, 189 (1977).
- 5) P.H. Barker, et al., AMCO-6, p. 233 (1979).
- 6) R.E. White, H. Naylor, P.H. Barker, D.M.J. Lovelock, and R.M. Smythe, Phys. Lett. 105B, 116 (1981).
- 7) J.C. Hardy, V.T. Koslowsky, R.E. Azuma, G.C. Ball, E.T.H. Clifford, W.G. Davies, E. Hagberg, H. Schmeing, U.J. Schrewe and K.S. Sharma, BAPS 27, 696 (1982).
- 8) P.H. Berker, Private Communication.
- 9) D.C. Robinson, J.M. Freeman and T.T. Thwaites, Nucl. Phys. A181, 645 (1972).

(b) Measurements of Gamow-Teller Strength for Double-Beta Decaying Nuclei

N. Anantaraman, S.M. Austin, B.A. Brown and B.H. Wildenthal

Double β decay (denoted $\beta\beta$ decay)¹⁾ can occur in two modes:

$$(Z,A) \rightarrow (Z+2,A) + e_1^- + e_2^- + \bar{\nu}_1 + \bar{\nu}_2 \quad (2\nu)$$

$$(Z,A) \rightarrow (Z+2,A) + e_1^- + e_2^- \quad (0\nu)$$

The first of these modes can be thought of as a second order process, a sequence of two normal β decays passing through (virtual) intermediate states of the nucleus $(Z+1,A)$. The second is of great interest since it does not conserve lepton number.

Recently there has been a renewed interest in these decays because limits on the (0ν) branch for ^{82}Se and ^{76}Ge decay have been used to place limits on the masses of Majorana neutrinos²⁾ and because the first direct electron counting experiment³⁾ has been performed for $^{82}\text{Se} \rightarrow ^{82}\text{Kr} + 2e^- + 2\bar{\nu}$, yielding a lifetime of $1.0 \pm 0.4 \times 10^{19}$ years. This is about a factor of thirty shorter than the lifetime obtained by geochemical methods. A detailed model calculation of the (2ν) lifetime has been performed²⁾ and is in good agreement with the direct counting result but not with the geochemical results. Other analyses based on the experimental ratio of the lifetimes for ^{128}Te and ^{130}Te indicate that the non-lepton conserving 0ν process may have been observed. The argument involves only the assumption⁴⁾ that the $\beta\beta$ matrix elements for ^{128}Te and ^{130}Te are the same. Theoretical shell model calculations⁵⁾ bear out this assumption but also greatly overestimate the strength of the transition, weakening the conclusion about the ratio.

In an attempt to provide constraints on the calculations we⁶⁾ have used the neutron time-of-flight system at the Indiana University Cyclotron Facility to obtain (p,n)

spectra at 0° , 4° and 8° for ^{76}Ge , ^{82}Se and $^{128,130}\text{Te}$ with an energy resolution of 360 KeV. The $L=0$ strength at 0° (low q) is closely proportional to the Gamow-Teller (GT) strength to the (virtual) intermediate states of the $\beta\beta$ process. Strength is observed to the giant GT resonance region and to narrow low lying structures populated with $\sim 10^{-2}$ of the strength of the giant resonance. The spectrum for ^{82}Se is shown in Fig. 1.

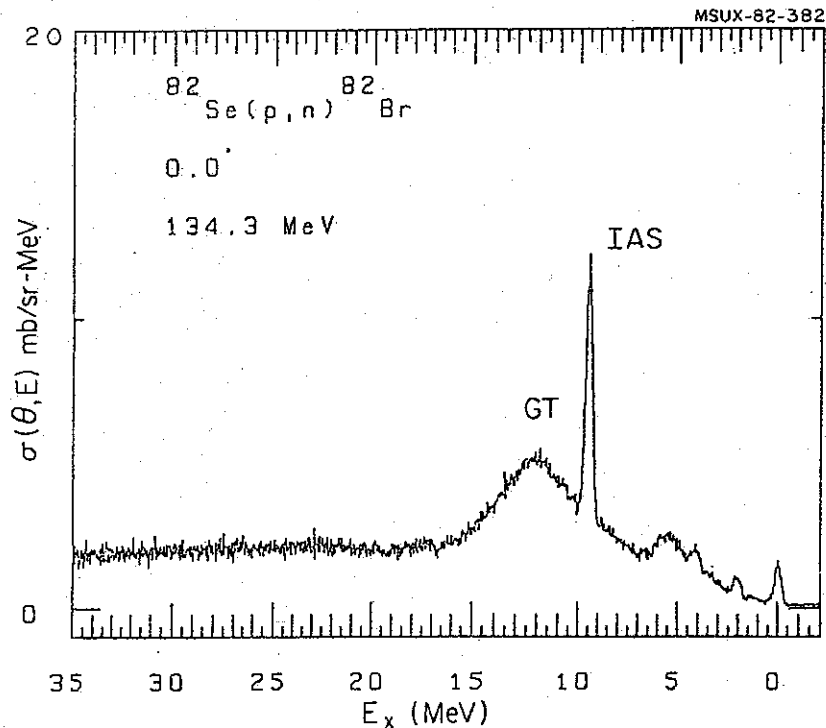


Fig. 1. Spectrum for $^{82}\text{Se}(p,n)$ at 0° and $E_p=134$ MeV.

The results for $^{128,130}\text{Te}$ are simplest to interpret, since the $\beta\beta$ decay analysis assumes only that the matrix elements are the same. Since the Fermi-like ($L=0, S=0$) transition to the isobaric analog state (IAS) is proportional to $(N-Z)$ for the target, an estimate of the differences in the GT strengths, independent of many systematic errors, can be obtained by normalizing the spectra so the IAS yield is proportional to $N-Z$. This has been done for the spectrum shown

in Fig. 2 where we plot the quantity

$$\frac{Y(^{130}\text{Te}) - Y(^{128}\text{Te})}{Y(^{130}\text{Te})}$$

Here the Y's are the yields for the noted nuclei normalized as discussed above. To the extent that only $L=0$ GT strength is observed at 0° , a good approximation in the neighborhood of the giant Gamow-Teller resonance, the plotted ratio is also the fractional difference of the allowed ($L=0$) GT strength for ^{128}Te and ^{130}Te . We see that this difference is less than 15% in the neighborhood of the giant resonance. At low excitation the GT strengths differ markedly. Although a rather small portion of the total strength is involved and the low lying strength is mostly $L>0$ which does not contribute to the $\beta\beta$ process, for reasons given below this may lead to a substantial uncertainty. Several further measurements appear important:

1). $^{128,130}\text{Te}$: Because of the $\frac{1}{E}$ energy dependence of the matrix elements for 2β decay, even the rather small amount of $L=0$ strength which might lie low in ^{128}Te and ^{130}Te could be important. Unfortunately, with the 360 keV resolution obtained in the (p,n) measurements, this strength is obscured by $L>0$ strength. We will repeat these measurements with better resolution in an attempt to resolve any $L=0$ strength using the (^6Li , ^6He) reaction at MSU (see section DII 2(a)) or if that probe proves ineffective, with lower energy (p,n) reactions at the IUCF. These measurements should also simplify comparison with the low lying strength in these nuclei predicted by theoretical models.

2). $^{76}\text{Se}(^{12}\text{C}, ^{12}\text{N})^{76}\text{As}$: Having the GT strength leading to the ^{76}As intermediate system from ^{76}Se , this proposed measurement from the ^{76}Se side should allow us to place a limit

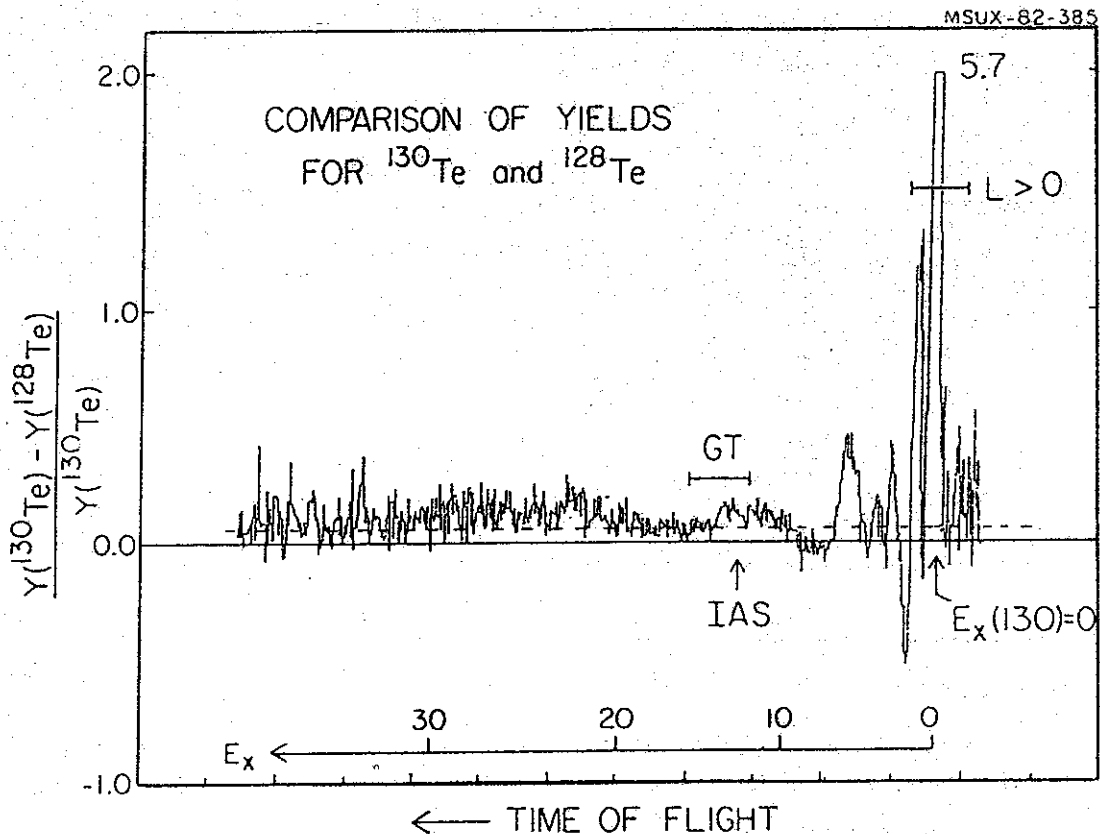


Fig. 2. Normalized fractional difference in yields for ^{128}Te and ^{130}Te at $E = 134$ MeV. The positions of the IAS and GT giant resonances are indicated.

on the total strength of the $^{76}\text{Ge} \rightarrow ^{76}\text{As} (\text{virtual}) \rightarrow ^{76}\text{Se}$ decay. Since we don't determine the phases of the GT amplitudes, but only their magnitudes, our limit will assume the amplitudes are all in phase. Hence it will be meaningful only if the transition is quite collective. Fortunately this appears to be the case,^(2,7) so we may hope to determine whether the theoretical estimates are reasonable. Related experiments with the (p,p') reaction are discussed in section B1(a).

References

- 1) D. Bryman and C. Picciotto, Rev. Mod. Phys. 50, 11 (1978).

- 2) W.C. Haxton, G.J. Stephenson and D. Strottman, Phys. Rev. Lett. 47, 153 (1981).
- 3) M.K. Moe and D.D. Lowenthal, Phys. Rev. C22, 2186 (1980).
- 4) B. Pontecorvo, Phys. Lett. 26B, 630 (1968).
- 5) W.C. Haxton, Comments on Nuclear and Particle Physics XI, 41 (1983) and references therein.
- 6) Sam M. Austin, R. Madey, J.W. Watson, B.D. Anderson, A. Baldwin, B.S. Flanders, C. Lebo and C.C. Foster, unpublished.
- 7) L. Zamick, preprint.

D 2. NUCLEAR ASTROPHYSICS

- (a) The Reaction ${}^3\text{He}(\alpha, \gamma){}^7\text{Be}$ and the Solar Neutrino Problem**
- (b) The Creation of the Light Elements**
- (c) Spallation Cross Sections for Cosmic Ray Astrophysics**
- (d) β^- Strength Functions in Astrophysics**
- (e) β^+ Strength Functions in Astrophysics**

(a) The Reaction ${}^3\text{He}(d, \gamma){}^7\text{Be}$ and the Solar Neutrino Problem.¹⁾S.M. Austin, P. Dyer, and R.G.H. Robertson

The reaction ${}^3\text{He}(d, \gamma){}^7\text{Be}$ is a link in the chain of reactions leading to the production of ${}^8\text{B}$ in the sun. Since ${}^8\text{B}$ is the major source of neutrinos observable in Davis' experiment,²⁾ there was great interest in the experiment of Krawinkel, et al.;³⁾ these authors reported cross sections for the reaction almost a factor of two lower than found in previous work, substantially reducing the discrepancy between the predicted and observed solar neutrino fluxes. Since only the normalization of the cross section was in doubt, all measured energy dependences being essentially similar, we have measured the cross section at a single energy (~ 900 keV) using activation techniques. Details are presented in ref. 1. The results of this measurement are shown in Fig. 1; they are inconsistent with the results of Krawinkel, et al., but consistent with other results. The solar neutrino problem remains: the measured neutrino flux from the sun is a factor of 2-4 below theoretical predictions.

(b) The Creation of the Light Elements.

S.M. Austin and D. Morrissey

While most of the elements we see about us are synthesized in stars, those lighter than ${}^{12}\text{C}$ do not share this origin. Indeed, most of these elements are so fragile (in the sense that they are rapidly destroyed by proton-induced reactions at the temperatures found in stellar centers) that stellar processing leads rather to their destruction. A cooler and/or less dense environment must then be the site of light element synthesis. Our laboratory has been involved for some time in measurements of spallation and fusion cross sections related to this problem.⁴⁾

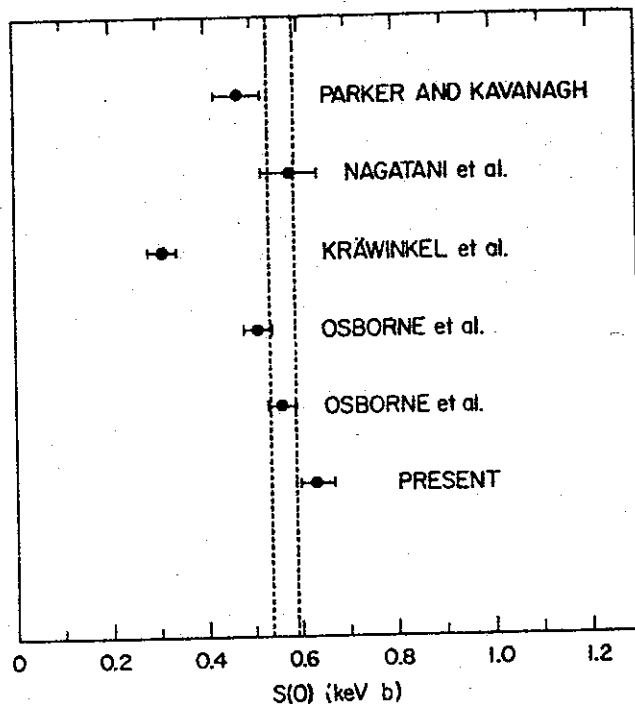


Fig. 1. Graphical representation of $S(0)$ from various experiments. The band represents $1-\sigma$ limits from the recommended value. Further uncertainty is contributed by the choice of theoretical extrapolation. The data in this figure have all been reduced to zero energy with the aid of the Tombrello-Parker theory. (From Ref. 1).

Over the past decade an elegantly simple model⁴⁾ has evolved in which these elements are created in the Galactic Cosmic Rays⁵⁾ and in the Universal Big Bang⁶⁾ expansion as is shown in Table I. It appears that ${}^6\text{Li}$, ${}^9\text{Be}$, ${}^{10,11}\text{B}$ result from interactions over the past 10^{10} years of the high energy galactic cosmic rays with abundant elements in the interstellar medium while ${}^2\text{H}$, ${}^{3,4}\text{He}$, ${}^7\text{Li}$ are produced early in the Big Bang when temperatures are near 10^9 K.

TABLE I. Sources of the light elements

Isotope	Galactic Cosmic Rays ^a	Big Bang ^a
² H	No	Yes
³ He	No	Yes
⁴ He	No	Yes
⁶ Li	Yes	No
⁷ Li	10%	Yes
⁹ Be	Yes	No
¹⁰ B	Yes	No
¹¹ B	Yes	No

^a The entry "yes" means the computed yield is in quantitative agreement with observation and "no" that it is hopelessly low.

Only one or two parameters enter this model and these have values that are consistent with what is known from other information. For example, element synthesis in a Big Bang depends on the average Universal density ρ_B of baryons; the four isotopes mentioned above are all produced within their abundance uncertainties at a common value of $\rho_B = 5 \times 10^{-31} \text{ gm/cm}^3$ (See Fig. 2). This value of ρ_B is insufficient to close the Universe which will then continue to expand forever (unless neutrinos have sufficient mass). Strong limits on the allowed number of neutrino species (<4 species; 2 or (probably) 3 are presently known) follow from the ⁴He abundance.

The strength of this picture lies in its simplicity and in that it explains all the abundances in an economical function, involving only mechanisms known from other evidence to exist in nature. There are however two uncertainties in the cosmic ray sector of the theory, involving possible contributions of low energy cosmic rays to the production of ¹¹B and the contributions of the $d + d \rightarrow \text{mass } 6,7$ to production of the isotopes of Li.

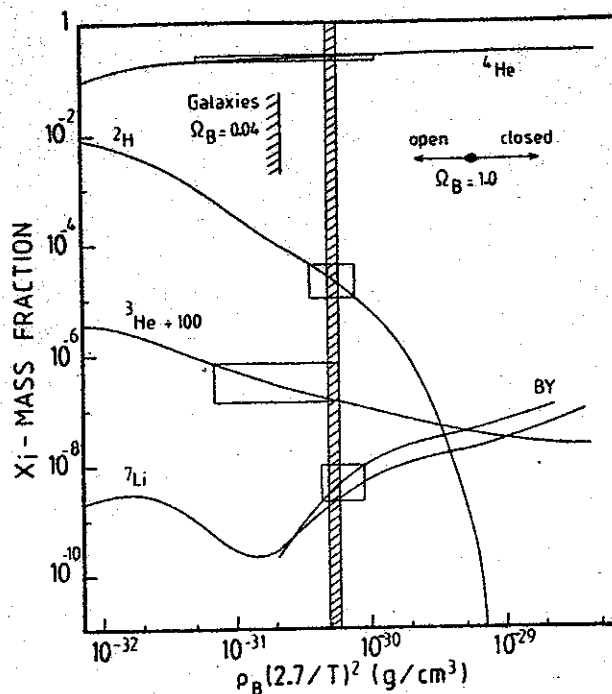


Fig. 2. Determination of the universal baryon density ρ_B from big bang nucleosynthesis. The calculations are mainly from Wagoner (Ref. 6). The curve for ${}^3\text{He}$ has been divided by 100 for display purposes. The long shaded bar at $5.4 \times 10^{-31} \text{ g/cm}^3$ is the resulting concordant density. Also shown are the values of ρ_B corresponding to $\Omega_B = 0.04$, a lower limit on the density in galaxies, and $\Omega_B = 1.0$ which divides closed from open universes. Both are calculated for a Hubble constant $H_0 = 55 \text{ km sec}^{-1} \text{ Mpc}^{-1}$. $\Omega_B = \rho_B / \rho_{\text{crit}}$ where ρ_{crit} just closes the Universe.

The available cross sections^{7,8)} for the $d+d$ reaction are shown in Fig. 3. Since the important energy range for galactic cosmic ray production lies near 1 GeV/nucleon substantial extrapolations to higher energy are required. Nevertheless, the exponential decrease of the mass 7 cross sections makes it likely that the $d+d$ reaction is unimportant for ${}^7\text{Li}$ production. The situation is much less clear for ${}^6\text{Li}$. If one extrapolates along the line labelled "exponential decrease" then $d+d$ is also unimportant for ${}^6\text{Li}$; since this has been assumed in the theories whose results are summarized in Table 1, the situation is in hand. If, however, the cross section for $d+d \rightarrow {}^6\text{Li}+p+n$ remains constant above 140 MeV as is common in reactions leading to three-particle final states, then ${}^6\text{Li}$ will be overproduced and the whole picture of light element creation will be on much less firm ground.

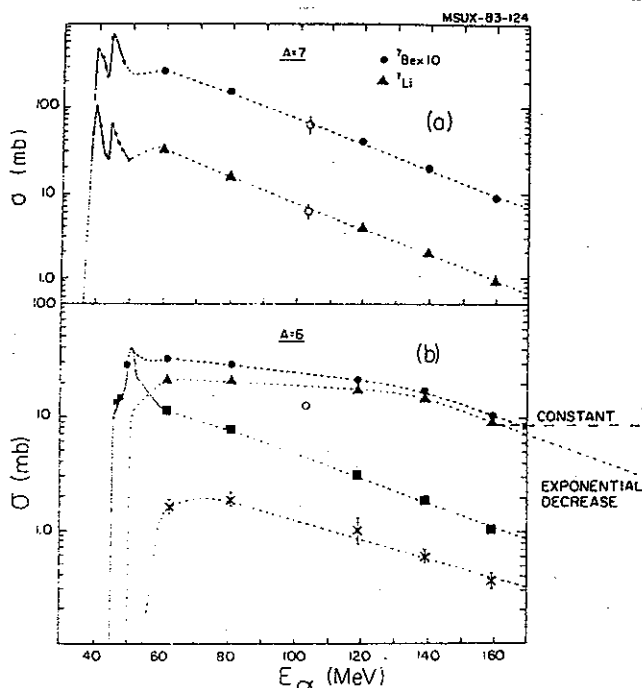


Fig. 3. Excitation functions for production of masses 6 and 7 in the $d+d$ reaction. (a) Be and Li, (b) Various contributions to mass-6: (\bullet , \circ) total production; (\blacktriangle) ${}^6\text{Li}+pn$; (\blacksquare) ${}^6\text{Li}+d$; (x) $\text{He}+2p$. (From Refs. 7, 8).

We propose to measure cross sections for the production of isotopes of mass 6 and mass 7 in the $d+d$ reactions over an energy range from 125 to 320 MeV. These measurements will be done in the 60" scattering chamber using a gas target and standard multielement silicon $\Delta E-E$ detectors to detect the mass 6, 7 products. Cross sections for the $d+d$ elastic scattering channel will be obtained at the same time as a by-product of the study.

The proposed measurements should be sufficient to determine which alternative is correct. Should the exponential decrease continue up to 320 MeV, then the situation can probably be regarded as settled. If the cross section remains relatively constant, then the measurements can be regarded as a first step to the solution; additional measurements extending up to at least 1 GeV/nucleon will be required.

(c) Spallation Cross Sections for Cosmic Ray Astrophysics

S.M. Austin and G.D. Westfall

Recent studies⁹⁾ of the isotope composition of C, O, Ne, Mg and Si for galactic cosmic rays of 100-500 MeV/nucleon can be interpreted in terms of the isotopic composition of the cosmic ray sources; one finds that the source compositions are substantially enriched in the heavy isotopes of a given element as compared to the solar system. Possible explanations include the possibilities that cosmic ray sources are in regions of the galaxy that differ in composition from the galaxy as a whole or that the solar system is atypical of the galaxy, reflecting the mechanisms of the solar birth. Unfortunately, the inferred source abundances are not always on firm ground. Some of them depend sensitively on unmeasured spallation cross sections which determine the modification of the cosmic ray abundances during the flight from their sources to the earth. The most important cross sections are fragmentation of ^{16}O and ^{28}Si by ^1H in the energy range from 200-1000 MeV/nucleon. We intend to measure these cross sections using the HISS spectrometer at the Bevalac.

(d) β^- Decay Strength Functions in AstrophysicsN. Anantaraman, S.M. Austin and A. Galonsky

Many heavy nuclei are produced in a rapid neutron capture process (dynamic r process), the understanding of which depends on the strength functions S_{β} for Gamow-Teller (GT) β -decay. Since little is known about S_{β} , simple structureless forms have been assumed in most calculations. However, shell model arguments lead one to expect local enhancements in decay strength, and such enhancements have recently been seen both in classic β decay experiments and in high energy (p,n) studies done at IUCF (See section B1(a)). If such an

enhancement should occur within the energy window accessible to β decay it would greatly affect the β -decay lifetime and result in changes¹⁰ in the predicted production of elements in the dynamical r-process. Furthermore, the onset of β -delayed fission processes near $A=250$ is expected to affect the production ratio of chronological pairs (e.g. ^{238}U , ^{235}U) and hence the measurements of lifetimes of the elements extracted from them.¹¹⁾

To understand these phenomena one needs accurate information about S_{β} but unfortunately little is known to date. (Some β -delayed neutron experiments bear on this subject (see, for example, Kratz et al.¹²⁾), and Firestone¹³⁾ has observed structure in classical β - γ decay studies of ^{145}Gd).

We are presently involved in a study of GT strength in ^{238}U using the $^{238}\text{U}(p,n)$ reaction at the IUCF (Kent State, Heidelberg, Indiana, MSU collaboration). It is not clear whether the resolution available in (p,n) will permit us to observe low-lying GT strength in this deformed nucleus, but if so, we will extend these studies to other heavy nuclei.

We also intend to search for low lying GT strength with the (^6Li , ^6He) reaction discussed elsewhere in this proposal (Sec. B2(a)). For the present purpose, the main advantages of this reaction are: 1) the higher resolution and, likely, smaller background compared to (p,n). (This will permit one to search for relatively weak transitions) and 2) the possibility of using thin targets of rare isotopes far from stability. Unfortunately, the nuclei along the r-process path are unstable and one must rely on studying a sufficiently wide range of nuclei to fix the parameters of theoretical models well enough to permit an extrapolation into the region of interest.

Initial studies will follow the calibration of the (^6Li , ^6He) reaction discussed earlier and will be concentrated on the medium heavy and heavy nuclei likely to

influence the r process¹¹⁾ and specifically on nuclei in the lead region where dipole ($L=1$) strength may be important. Following this work, it may be profitable to study S_{β} for nuclei farther from stability through observation of β -delayed neutron emission¹²⁾ by neutron rich nuclei made, for example, in the collisions of neutron rich projectiles with heavy targets. Recent studies have shown that either deeply inelastic reactions of ^{48}Ca at low energies (<10 MeV/u) or fragmentation reactions at higher energies (>100 MeV/u) are effective methods for the production of neutron rich nuclei. Projectiles such as ^{22}Ne at 37 MeV/u, which will be available, will combine some advantages of both methods. The reaction product mass filter (see Sec. B4(b)) combined with simple neutron detectors¹²⁾ should be very useful for these purposes.

(e) β^+ Strength in Astrophysics

N. Anantaraman and S.M. Austin

Late in a star's life, following hydrogen and helium burning, the star passes rather rapidly through C, O, and Si burning phases until its core is entirely converted to nuclei near iron. At this point, nuclear energy is exhausted and a gravitational collapse of the core ensues, presumably initiating a supernova explosion. During these later phases of stellar evolution, electron capture transitions in nuclei in the upper-sd and fp shells affect nucleosynthesis, neutrino cooling and neutronization (conversion of protons to neutrons by e^- capture) in the stellar interior.¹⁴⁾ The nature of the supernova explosion itself is sensitive to these rates.¹⁴⁾

Unfortunately little information is available on electron capture (β^+) transition rates in the important nuclei. The collective Gamow-Teller (GT) strength is not energetically accessible to β decay in $N>Z$ nuclei and charge exchange reactions such as (n,p) or $(t, ^3\text{He})$ ¹⁵⁾ present

formidable experimental and reaction mechanism problems. Should the ($^{12}\text{C}, ^{12}\text{N}$) reaction discussed in Section B2(a) prove feasible it will be a powerful tool for these investigations. The first experiment would study the $^{56}\text{Fe} (^{12}\text{C}, ^{12}\text{N}) ^{56}\text{Mn}$ reaction as a prototype of these reactions and as one which is itself important¹⁴⁾ for the supernova problem.

References

1. R.G.H. Robertson, P. Dyer, T.J. Bowles, R.E. Brown, N. Jarmie, C.J. Maggiore and Sam M. Austin, Phys. Rev. C27, 11 (1983).
2. See J.N. Bahcall, W.F. Huebner, S.H. Lubow, P.D. Parker and R.K. Ulrich, Rev. Mod. Phys. 54, 767 (1982) for details.
3. H. Krawinkel, H.W. Becker, L. Buchmann, J. Gorres, K.U. Kettner, W.E. Kieser, R. Santo, P. Schmalbrock, H.P. Trautvetter, A. Vlieks, C. Rolfs, J.W. Hammer, R.E. Azuma and W.S. Rodney, Z. Physik A304, 307 (1982).
4. An up to date discussion of this model is given by Sam M. Austin, Progress in Particle and Nuclear Physics 7, 1 (1981). See also the recent paper by F.Spite and M.Spite, Astron., Astrophys. 115, 357 (1982).
5. H. Reeves, W.A. Fowler and F. Hoyle, Nature 226, 727 (1970).
6. R. Wagoner, Astrophys. J. 173, 343 (1973).
7. C.H. King, S.M. Austin, H.H. Rossner and W.S. Chen, Phys. Rev. C16, 1712 (1977).
8. B.G. Glagola, G.J. Mathews, H.F. Brewer, V.E. Viola, P.G. Roos, A. Nadasen and S.M. Austin, Phys. Rev. Letts. 41, 1698 (1978).

9. See for example M.E. Wiedenbeck and D.E. Greiner, Paper OGl.2-4, Proceedings 17th Int'l Cosmic Ray Conf., Paris, 1981; R.A. Mewaldt, E.C. Stone and M.E. Medenbeck, Sci. Am. 247, 108 (1982) and references therein.
10. H.V. Klapdor and C.O. Wene, Ap. J. 230, L113 (1979).
11. H.V. Klapdor, Proceedings of Conf. on Nuclear Spectroscopy and Structure of the Nucleus, Rega 27-30 March 1979. MPI report H-1979-V13, Heidelberg.
12. K.L. Kratz, W. Rudolph, H. Ohm, H. Franz, M. Zendel, G. Herrmann, S.G. Prussin, F.M. Nuh, A.A. Shihab-Eldin, D.R. Slaughter, W. Halverson and H.V. Klapdor, Nucl. Phys. A317, 335 (1979).
13. R. Firestone, R.C. Pardo, and Wm C. McHarris, Phys. Lett. 89B, 36 (1979).
14. G.M. Fuller, W.A. Fowler and M.J. Newman, Ap.J. 252, 715 (1982); G.M. Fuller, Ap.J. 252, 741 (1982).
15. E.R. Flynn, F. Ajzenberg-Selove, R.E. Brown and J.W. Sunier, Bull Am. Phys. Soc. 27, 731 (1982).

E. NUCLEAR RESEARCH BUDGET



E. NUCLEAR RESEARCH BUDGET

This section summarizes the costs associated with the staff research program described in previous subsections. Table IV.1 gives a summary of the projects, listed in the order which they appear in the previous subsections. Research staff are listed at the top of the Table, and each researcher is identified by an X where the research project constitutes a major component of his/her research interest. The remaining columns of the Table show, respectively, the distribution of Post-doctoral Research Associates and Graduate Students (in FTE) over the projects, the estimated cost of outside user travel, the cost of specialized detectors, electronics and targets necessary for the work. The majority of special targets are required in studies of nuclei far from stability and giant resonance research, whereas the major expenses in detectors and electronics fall in the category of nuclear reactions. The largest fraction of Post-doctoral Research Associates and Graduate Students is concentrated in nuclear reactions, partly because many of the proposals in this category contain several different experiments, and also because the analysis and interpretation of the multiparameter data is highly manpower intensive.

The totals for all projects are listed at the bottom of Table IV.1, and these numbers are also entered in Table IV.2, which is a summary of the total budget request for Nuclear Research. In addition to the items already discussed, the Table shows the requested NSF contribution to salaries of all staff and support personnel required to carry out the research, according to the percentage distribution of the effort in the laboratory set out in Table II of the Proposal Introduction. The other items are largely self-explanatory. A total of 26 graduate students are currently receiving training in research at NSCL and the number will continue to be in force during FY84 (an

additional 2 graduate students are associated with accelerator physics). Undergraduates equivalent to 5 FTE are also associated with the research projects. There is a specific item for magnetic tapes, since all users, whether in-house or outside, will be charged for tapes.

In considering the requested level of support for MSU staff research at other facilities, a further relevant consideration is the role of the in-house staff in keeping the NSCL facility at the forefront in instrumentation. Most major instrumentation efforts in final analysis depend on the in-house staff for primary conceptual ideas and leadership drive. In order for this group to be in real frontline contact with new ideas and directions, it is essential that the in-house research effort itself be at the cutting edge of the research field. Work at other laboratories is a key factor in the important process of maintaining desired close contact with new developments at these laboratories so that these developments can be utilized at NSCL when appropriate, and such work also has an additional important value in giving the MSU staff continuing direct experience as to what it is like to do experiments in the outside user mode. Actual experience as an outside user at other facilities is then, in total, extremely valuable in enhancing the effectiveness of the in-house staff in their important role of guiding the technical evolution of the NSCL facility in directions which give a continuing frontier capability in the instrumentation systems of the Laboratory while at the same time maintaining an essential sensitivity to the important issue of preserving a viable human interface in the presence of the added handicaps associated with being an outsider, away from home institution support.

TABLE IV.1

DISTRIBUTION OF EFFORT AND EXPENDITURES FOR MSU RESEARCH
(FY 84)

		NUCLEAR SCIENCE RESEARCH STAFF																																															
SECTION	PROJECT	SUB-SECTION	Arantaraman	Abstin	Berenson	Blue	Brown	Crawley	Galonsky	Galbke	Harwood	Kasby	McHarris	Morrissey	Nolen	Ronningen	Scott	Westfall	Widenthal	Zeller	Post Docs	Grad Studs	Ditside KS	User Travel	Specialized Equipment KS	Targets	KS																						
REACTIONS A	FUSION/FISSION	1(a)						X	X													0.75	2.0	6.0	-	-																							
	DEEP INELASTIC	1(b)						X					X									0.75	1.5	2.0	3.0	-																							
	FRAGMENTATION	1(c)								X												-	0.5	3.0	3.0	-																							
	TWO-PARTICLE CORREL.	2(a)							X													0.75	1.0	-	35.0	-																							
	LIGHT/HEAVY COINC.	2(b)							X							X						0.25	1.0	-	-	-																							
	COMPOSITE PARTICLES	3(a)					X		X							X	X					0.5	2.5	8.0	20.0	-																							
	STREAMER CHAMBER	3(b)	X					X								X	X					-	1.0	7.0	-	-																							
	MULTIPLICITY ARRAY	3(c)					X		X									X				0.5	2.0	-	3.0	-																							
	PION PRODUCTION	4(a)		X								X										0.25	1.0	2.0	-	-																							
	ANDMALONS	4(b)											X									0.25	1.0	2.0	-	-																							
TOTALS FOR REACTIONS																						4.0	13.5	30.0	64.0	-																							
NUCLEAR STRUCTURE B	MI GIANT RESONANCE	1(a)	X				X	X													0.25	0.5	-	-	2.0																								
	GIANT RESONANCE	1(b)		X			X			X			X									0.65	1.0	-	10.0	2.0																							
	PARTICLE RESPONSE FUNC.	1(c)					X			X														1.0	-	-																							
	Ca + Ca REACTIONS	1(d)														X						0.25	1.0	-	-	-																							
	CHARGE EXCHANGE	2(a)	X	X				X	X									X				0.25	1.0	1.0	-	-																							
	PION PRECURSOR	2(b)	X																			-	0.5	1.0	-	2.0																							
	Y SPECTROSCOPY	3(a)			X							X		X					X			-	0.5	1.0	-	-																							
	CONTINUUM γ	3(b)			X								X	X								-	-	1.0	-	-																							
	NUCLEAR JOSEPHSON	3(c)											X									-	1.0	-	-	-																							
	MASS MEASUREMENTS	4(a)		X						X									X			0.75	2.0	2.0	-	5.0																							
EXOTIC NUCL. RPHS	4(b)								X				X	X							0.25	1.0	-	17.0	-																								
NEUTRON EXCESS T ₁	4(c)								X								X				-	0.5	2.0	3.0	-																								
He JET EXOTIC NUCL.	4(d)										X										-	0.5	-	-	-																								
TOTALS FOR STRUCTURE																						2.5	9.5	9.0	30.0	11.0																							
C	NUCLEAR STRUCTURE ANALYSIS			X													X				1.5	1.5	4.0	-	-																								
Fundamental and Astrophysics	SUPERALLOWED β DECAY	1(a)			X			X					X				X				-	1.0	5.0	-	-																								
	DOUBLE β DECAY	1(b)	X		X												X				0.25	0.5	1.0	-	-																								
	NUCLEAR ASTROPHYSICS	2	X	X									X								0.25	0.5	2.0	-	-																								
TOTALS FOR FUNDAMENTAL & ASTROPHYS.																						0.5	1.5	8.0	-	-																							
TOTALS FOR ALL PROJECTS																						8.4	26.0	51.0	94.0	11.0																							

TABLE IV.2

NUCLEAR SCIENCE RESEARCH		
	K\$	K\$
PRINCIPAL INVESTIGATORS & CO. PI.'S	267.1	
FACULTY & SENIOR ASSOC	167.7	
OTHER PROFESSIONALS (3.7 FTE)	65.8	
SECRETARIAL AND CLERICAL (2.8 FTE)	39.2	
OTHER (2.3 FTE)	32.5	
	<u>572.3</u>	
LESS MSU CONTRIBUTION	204.2	
NSF CONTRIBUTION TO SALARIES	368.1	368.1
RESEARCH ASSOCIATES (8.4 FTE)		166.6
FRINGE BENEFITS (18.9%)		101.1
GRADUATE STUDENTS (26)		234.0
UNDERGRADUATE STUDENTS (5 FTE)		30.0 +
ADMINISTRATIVE COSTS (60% share of telephone, copying, supplies, postage, etc.)		54.0
PAGE CHARGES		24.0
SEMINARS & CONSULTANTS		13.0
LIBRARY		2.5
TRAVEL (Conferences, Committees)		39.0
TRAVEL FOR EXPERIMENTS (See TABLE IV.1)		51.0
MAGNETIC TAPES		10.0
SPECIAL TARGETS (See TABLE IV.1)		11.0
OVERHEAD (39.5% on non equipment items)		436.2
EQUIPMENT (See TABLE IV.1)		94.0
TOTAL		<u>\$1634.5K</u>

Σ 180.5

V. ACCELERATOR RESEARCH AND DEVELOPMENT

V. ACCELERATOR RESEARCH AND DEVELOPMENT

Development of advanced nuclear instrumentation systems has been a major component of the MSU Cyclotron Laboratory's program from the beginning. The goal of these activities is development of instruments and techniques which will allow study of significant nuclear phenomena which are either not accessible with present techniques or which are substantially more difficult or more costly to study using present techniques.

In the early years the primary objective of this program was development of the isochronous cyclotron as a precision device for study of nuclear phenomena. Techniques for achieving single turn extraction were introduced; the system included a series of slits which gave a sharp time structure in the beam; this time structure then itself allowed a number of significant advances in nuclear studies. Much program effort was also devoted to a number of smaller projects aimed at upgrading overall effectiveness and reliability of the cyclotron system.

Later, major program effort shifted to optimization of the matching of the complete cyclotron, beam transport, and reaction-product-spectrograph system with the goal of increasing the energy resolution of the total system. A number of on-line feedback loops were very successfully introduced; these loops used information from beam pickups in the transport system and spectrograph to stabilize the overall system. These techniques, in combination with the cyclotron's single turn extraction system, gave final lines in the spectrograph focal plane which were direct images of the ion source slit in the cyclotron; the high intrinsic brightness of the source and the absence or cancellation of aberrations gave a powerful system for high resolution studies of nuclear properties.

Another important line of effort provided an absolute energy calibration for the spectrograph system in terms of

accurately known nuclear masses. These calibrations then gave access to a broad spectrum of significant issues hinging on accurate absolute measurements of various nuclear characteristics.

In the early 70's a new major effort was added to the instrumentation program, namely adapting superconducting techniques to cyclotrons. The first goal of this work involved using a superconducting coil of the type which had been developed for large bubble chambers to provide primary excitation for the cyclotron magnet. With such a coil, main magnet power is removed from the family of constraints which define an optimized cyclotron design; this then leads to an approximate tripling of the optimum magnetic field (relative to field strengths typically used in room temperature cyclotrons) and the complete cyclotron becomes much smaller and less costly although somewhat more complicated. The resulting high-field cyclotrons are particularly well matched to the requirements of heavy-ions where relatively low values of the ion charge to mass ratio give beams which are typically extremely rigid and difficult to bend. Computer studies of the characteristics of such a cyclotron led to funding of a prototype magnet project in August of 1975. First full field operation of this magnet occurred in May of 1977 and a grant providing funding for construction of a complete operating cyclotron (using the prototype magnet) was received later in 1977. The K500 cyclotron is then the end result of this project and this cyclotron is the first such "superconducting cyclotron" to come into operation in the world. First internal beam operation of this cyclotron occurred in November 1981; first external beam operation was in August 1982. Four other such cyclotrons are now in construction (one of these being the NSCL K800); an additional ten or so laboratories have made proposals or are actively involved in design studies for such cyclotrons.

A central goal of the MSU cyclotron program from the beginning, and still continuing, is the development of

techniques for making the performance of cyclotrons predictable and calculable. In the early years this effort was based on a computer with a 1024 word memory which was used for orbit tracking in measured magnetic and electric fields, information on the fields coming from operating models. The intervening years have seen an incredible increase in computing power although still not to the point where the complex three dimensional geometry of a cyclotron pole tip can be economically included in a first principles calculation (or at least not at the level of detail needed to accurately predict all the various features of the field which need to be considered in designing for a well behaved family of cyclotron orbits). Fortunately, at high fields, an accurate simplifying approximation can be introduced based on the relatively complete saturation of the ferromagnetic materials in the magnet pole tip; refinement of this approximation has been a central objective of the Laboratory's cyclotron R & D program in recent years and an overall predictive accuracy of about 1 in 1000 can now be achieved in all details of the field. This level of accuracy is comfortably adequate to allow the costly and time consuming magnet modeling process to be completely eliminated. The K500 is then also the first isochronous cyclotron to be designed without the use of magnet models.

At this time the numerical computations effort of the cyclotron R&D group has two main components one associated with the K500 cyclotron the other with the K800.

The present principal goal of K500 computing is a comparison of computed orbit characteristics versus observed characteristics of actual orbits in the cyclotron. The objective of this effort is to identify construction errors in the K500 which are not now accounted for in the numerical calculations. Where these errors have a significant adverse effect on performance, a further objective is to design optimized correction elements. One important construction error which is known to have occurred in the final assembly

of the K500 involved an unintended change in the system which is used to determine main coil position. This error removed the reference points relative to which the coil was positioned in the final field mapping cycle; this then introduces a major uncertainty in the accumulated body of data describing field imperfections, since an uncalibrated shift in the main coil position has a large effect on field imperfections. In order to move ahead with the first experimental program running period, the coil was approximately positioned based on measurement of forces in the coil support system, but this is a relatively inaccurate method and significant unmeasured imperfection components in the magnetic field are therefore probable in the present running situation. This error will be corrected in a planned July 1983 shutdown when an imperfection mapping system will be installed in the cyclotron and accurate reference locations for the coil position will be reestablished. A concurrent intensive orbit computation effort will analyze the effect of measured imperfections on beam behaviour and, where appropriate, correction elements will be designed and installed. The central objective of this effort is to obtain a field which will allow the beam to be accelerated through the main part of the acceleration cycle in orbits which are "well centered". With such a well centered orbit pattern extraction efficiency should improve markedly even when a broad distribution of rf phases is included in the beam. Extraction efficiencies in the vicinity of 80% should be achievable whereas the efficiency in present conditions is typically 35-40%.

Numerical studies of the K800 cyclotron are at this time mainly concerned with the extraction system. This is in response to the difficulty experienced in the K500 with electric fields above 100 keV/cm; this experience clearly indicates the desirability of using lower electric fields in the K800 extraction system. An intensive program of numerical explorations of possible systems is in process.

Computations related to the design of the K800 magnet are at this time complete. When the magnet comes into operation a further sizeable computing effort will be directed toward comparison of computations and measurements; using these results, benefits to be derived from possible correction of observed imperfections will be analyzed.

Another important component of the Laboratory's accelerator R&D effort is the further extension of theoretical analysis of cyclotron orbit phenomena to previously unstudied characteristics. Theoretical analysis of any aspect of cyclotron behaviour has great value in that it provides a basic understanding of the controlling features of the phenomena; with such an understanding the efficiency of detailed numerical design studies is almost always greatly enhanced. Recent theoretical studies have developed a formalism describing primary features of the coupling between longitudinal and transverse oscillations due to spiral accelerating gaps such as are typically used in superconducting cyclotrons. Another recent theoretical study has developed a new Hamiltonian formulation of the equations of motion for particles in cyclotron type fields. This derivation clarifies the limits of validity of several approximate invariants which have been of important use.

The instrumentation research and development program of the Laboratory also involves large non-cyclotron efforts in the design of the beam transport systems and in the design of experimental apparatus.

The primary goal of the beam transport studies at the present time is development and testing of techniques and procedures which will be used in the construction of the superconducting beam transport system for the phase II project. Such a system has an inherent attractive efficiency coming from the combined use of cryogenics for both magnet cooling and vacuum pumping. An important design detail concerns the degree to which the magnet cooling system should be protected or separated from the beam. "Coldbore" magnets

are less costly but also more vulnerable to possible beam excursions and the greater cold mass means slower cool down. Critical features of possible magnet designs are being evaluated in a series of prototype studies. Interestingly, at an early stage, the program arrived at the conclusion that beamline magnets would be easier to construct and less expensive if designed to work at "normal" field levels where field shaping is dominated by the iron rather than by the coils. A similar conclusion is now widely advocated in the high energy accelerator field where the most economical future 20 Tev machine is seen by many to be the "Desertron", namely a machine using a relatively low magnetic field (approximately 2 tesla) located in a region where land and below grade construction are very inexpensive, such as a desert. (It is perhaps useful to clarify that high fields remain a great advantage for cyclotrons due to a basic difference in the scaling laws in a pancake field situation, such as in the cyclotron, versus a linear field situation such as in the bending magnet-- in the cyclotron situation the flux for given maximum magnetic rigidity varies inversely as the field strength and so high fields are strongly advantageous whereas for a linear magnet the flux required to produce a given bend is independent of field strength.)

Instrumentation research and development work related to design of experimental devices at present involves three large projects as well as a number of smaller efforts. The large projects are: 1) the design of the "S800" spectrograph, a high resolution spectrograph with maximum rigidity matched to that of the K800 cyclotron, 2) the design of the "Recoil Particle Mass Spectrometer" a device which filters particles from a nuclear reaction in terms of Q/M, and 3) a "4 π " charged particle detector array with capability for detecting the very complicated sprays of particles which come from central collisions on an event by event basis.

The S800 spectrograph is designed to yield an energy resolution of 1 part in 10^4 with a solid angle of 20 msr and an excitation energy range of 10%. This corresponds to a resolution of 800 keV and an excitation energy range of 800 MeV with the 8 GeV ^{40}Ca beams from the Phase II coupled cyclotron system. We have completed what we believe to be a highly optimized design for this spectrograph and the required beam analysis system. The spectrograph consists of two superconducting quadrupoles followed by two superconducting dipoles. The machined dipole steel (150 tons) is on order and will be delivered by August, 1983 (see photograph in the "Introduction" section). The same is true for the dipole superconductor.

The prototype RPMS is currently under construction and will be in the testing stage by summer, 1983. The prototype was designed to utilize existing surplus components from other laboratories. The design combines a Wien Filter (ExB device) with a magnetic dipole to focus ions to a focal plane with an m/q dispersion of approximately 1 cm per percent, with a resolution $m/\Delta m$ of 200 at a solid angle of 1 msr and a velocity acceptance range of 10%. These parameters are energy dependent, with these numbers being appropriate for 20 MeV/u. We expect this device to be very useful for studying very neutron rich isotopes produced via heavy ion beam fragmentation. This mechanism will be especially prolific at Phase II energies. The prototype RPMS will be upgraded for Phase II by replacing the present conventional quadrupoles with superconducting versions to focus the more rigid reaction products. Other changes in the design may be made based on our experience with the prototype device in Phase I.

In high energy nucleus-nucleus collisions, up to 100 particles can emerge from a single reaction. Most of the previous data in this field has consisted of single-particle inclusive measurements. In many cases one cannot distinguish between radically different theoretical predictions using

single particle data alone and only multi-particle observations are able to disprove or substantiate the disparate calculations. New multi-particle detection systems are then being designed in many laboratories in the world in order to deal with the observed multiplicities of fast charged particles. At NSCL energies one must deal with not only a large number of fast light particles, but also with many slower, highly ionizing particles. A detector system which promises to meet these needs in an effective and economical way involves a multi-layer, multi-detector array consisting of 32 Parallel Plate Avalanche Counters, 32 Bragg Curve Spectrometers, and 192 Calcium Fluoride-Plastic Scintillator telescopes, the entire assembly being housed in a single vacuum enclosure. Such a detector would provide NSCL with a unique device to measure most of the charged particles emerging from high energy nucleus-nucleus reactions ranging from 1 MeV/nucleon $A=100$ fragments up to 300 MeV protons and 100 MeV positive pions and would take full advantage of the unique beams available from the NSCL facility. Prototypes of critical elements of such an array are presently being designed and/or constructed in order to evaluate essential features of the design.

The budget for the first year of the Accelerator Research and Development component of the Laboratory's program (also interchangeably referred to as "instrumentation R & D") is given in Table V.1. In this year (1984) most support for the instrumentation program comes from the Phase II construction budget as indicated in Table I of the Introduction (and with manpower assignments as indicated in Table II of the Introduction). The costs shown in Table V.1 are for the small component of the program which is uniquely related to the K500 cyclotron or to Phase I experimental devices. In the second and third years of the three year period the situation will be very different, since the unusual R & D provision in the construction project line item will have terminated and the full instrumentation R&D effort of the

Laboratory will once again be funded from the operating budget. Table V.2 shows details of the R & D component of the construction budget as it is expected to be in 1984 but with costs presented in terms of 1983 salaries and prices i.e. on the same basis as all tables thus far presented herein. (The discussion of the on-going work and objectives of the instrumentation program in preceding paragraphs was a general review of the whole program including both the component funded from the operating program and the component funded from the construction program--support for this work thus corresponds to the the sum of the expenditures shown in Tables V.1 and V.2). Assuming the same level of effort in 1985 as in 1984, the rate of expenditure will be the same as the total R & D expenditure in 1984 from the construction and operating programs combined, namely 1159K in 1983 dollars.

A strong instrumentation development program is of course in accord with the basic origins and traditions of this Laboratory. It is furthermore clear that optimum progress in advancing scientific frontiers hinges on innovative advances in both direct experimental study and in instrumentation development. One should nevertheless continually address the issue of whether the distribution of resources between the two lines of effort is in an effective equilibrium or is unbalanced in either direction to a point of reduced overall effectiveness.

In the years of principal exploitation of the K50 cyclotron, the ratio of effort in nuclear research to that in instrumentation research was at a level of approximately 3 to 1, whereas the present ratio is in the vicinity of 1.5 to 1. The role of the Laboratory has, however, greatly changed since the years of running the K50 in that the instrumentation effort is now intended to provide forefront capabilities for a broad national group of users rather than for the inhouse group alone. Also traditionally, the starting up years of a major new facility are a time when payoffs

from continued instrumentation development are particularly large; complicated new apparatus has been created in the process of constructing such a facility and full understanding of the intricacies of the equipment generally involves a good many years of intensive further effort. As an example the K50 cyclotron came into operation in 1965 and while its high resolution capability was intrinsically present from the beginning, realization of this capability in an operational sense required a sustained effort extending through 1969 and routine use of the high resolution system was really only achieved in 1970. A similar process typically occurs in almost all new facilities, the Indiana University Cyclotron Facility coming to mind as one of many examples--the present outstanding characteristics of the IU facility are the result of a sustained continued instrumentation effort over a sizable period of years following first operation of the facility. In the relatively immediate future, corresponding to the period covered by this proposal, it is clearly essential to have the instrumentation R&D program continue at basically its present level. Lacking this, the construction effort going into the Phase II program will have severe difficulty in dealing with the debugging phase which will undoubtedly accompany start-up of the Phase II facility. For this combination of general and specific reasons, we then request support for the level of Accelerator R & D effort shown in Table V.1 in the first year and for support of the additional component transferred from the construction program in the second and third years of the three year period covered by this proposal.

TABLE V.1

ACCELERATOR R&D		
	K\$	K\$
PRINCIPAL INVESTIGATORS & CO. PI.'S	17.0	
FACULTY & SENIOR ASSOC	23.2	
OTHER PROFESSIONALS (0.5 FTE)	9.4	
SECRETARIAL AND CLERICAL (0.1 FTE)	1.2	
OTHER (0.2 FTE)	3.5	
	<u>54.3</u>	
LESS MSU CONTRIBUTION	19.7	
NSF CONTRIBUTION TO SALARIES	34.6	34.6
FRINGE BENEFITS (18.9%)		6.5
GRADUATE STUDENTS (2)		18.0
UNDERGRADUATE STUDENTS (0.5)		3.0
ADMINISTRATIVE COSTS (5% SHARE OF TELEPHONE, COPYING, SUPPLIES, POSTAGE, ETC.)		4.5
PAGE CHARGES		1.5
TRAVEL (CONFERENCES, COMMITTEES)		5.0
MAGNETIC TAPES		3.0
OTHER SUPPLIES		2.5
OVERHEAD (39.5% ON NON EQUIPMENT ITEMS)		31.1
TOTAL		<u><u>\$109.7K</u></u>

Σ = 19.5

TABLE V.2

1983 PHASE II ACCELERATOR R&D

	K\$	K\$
PRINCIPAL INVESTIGATORS & CO. PI.'s	40.3	
FACULTY & SENIOR ASSOC.	192.5	
OTHER PROFESSIONALS (2.8 FTE)	46.2	
SECRETARIAL & CLERICAL (0.6 FTE)	11.3	
OTHER (0.6 FTE)	8.2	
	<u>298.5</u>	
LESS MSU CONTRIBUTION	0*	
NSF CONTRIBUTION TO SALARIES	<u>298.5</u>	298.5
FRINGE BENEFITS (18.9%)		56.4
GRADUATE STUDENTS (1)		9.0
UNDERGRADUATE STUDENTS (8)		48.0
CONSULTANTS		14.0
ADMINISTRATIVE COSTS (35% SHARE OF TELEPHONE, COPYING, SUPPLIES, POSTAGE, ETC.)		31.5
PAGE CHARGES		12.0
TRAVEL (CONFERENCES, COMMITTEES)		21.5
MAGNETIC TAPES		7.5
SUPPLIES		125.0
PROTOTYPE DEVICES		180.0
OVERHEAD (39.5% ON NON EQUIPMENT ITEMS)		<u>246.2</u>
TOTAL		<u>\$1,049.6</u>

*MSU provided the Phase I building addition in support of the construction project.

VI. BUDGET SUMMARIES

1
2
3
4
5
6
7
8
9
10
11
12
13
14
15
16
17
18
19
20
21
22
23
24
25
26
27
28
29
30
31
32
33
34
35
36
37
38
39
40
41
42
43
44
45
46
47
48
49
50
51
52
53
54
55
56
57
58
59
60
61
62
63
64
65
66
67
68
69
70
71
72
73
74
75
76
77
78
79
80
81
82
83
84
85
86
87
88
89
90
91
92
93
94
95
96
97
98
99
100

VI. BUDGET SUMMARIES

Each of the preceding five programmatic sections presented detailed and summary budgets describing the need for funds in each programmatic area, all costs being presented in terms of present (1983) salaries and prices. The remaining cost issue is the correction factor for inflation from 1983 to the year of expenditure.

It is of course not possible to predict such economic issues in any reliable way. We therefore elect to use a round number approximately corresponding to the present situation, namely 5% per year. If this is an over estimate, the NSF Program Officer will clearly make an appropriate reduction in the course of the final budget negotiations which take place each year just prior to issuing an actual grant. An underestimate of the inflation effect produces (in our experience) a considerably more cumbersome problem for the NSF because of the limitations set in the National Science Board approval process for large grants. From this aspect it is then advisable to have a conservative estimate of the inflation factor. The assumed figure of 5% per year is perhaps only marginally conservative but its attractiveness as an even round number has led us to the decision to adopt that figure.

In the following pages the summary budgets from the preceding programmatic sections are repeated and their sum is 4323.7K dollars (again noting that this figure is in terms of present salaries and prices). Using the 5% per year inflation assumption the budget request for 1984, stated in terms of expected 1984 salaries and prices, becomes 4539.9K dollars. The budget for 1985 is estimated based on the same level of effort as in 1985 but with the Accelerator Research and Development component transferred from the construction project giving a total budget in terms of 1983 salaries and prices of 5373.7K dollars; this becomes 5924.5K when translated to expected 1985 salaries and pricing; again using the assumed inflation correction of 5% per

year. The budget in the year 1986 is difficult to forecast at this time, but an allowance for a small increase in total effort associated with the start up of the Phase II facility seems prudent, (particularly noting the fact that the Science Board approval process gives the figure presented here the effect of a ceiling). We thus add a programmatic increase of 10% to allow for additional costs associated with operation of the Phase II facility; this gives a 1986 budget of 5911.1K dollars in terms of 1983 salaries and prices and translating this to 1986 salaries and prices with the assumed 5% per year factor gives 6842.8K dollars. Table VI.1 summarizes these figures. Finally Table VI.2 presents these 1984 costs with items arranged according to the categorization of the "Summary Proposal Budget" form of the National Science Foundation.

TABLE I.1

FACILITY OPERATIONS		
	K\$	K\$
PRINCIPAL INVESTIGATORS & CO. PI.'S	62.8	
FACULTY & SENIOR ASSOC	236.4	
OTHER PROFESSIONALS (18.5 FTE)	339.7	
SECRETARIAL AND CLERICAL (1.0 FTE)	15.0	
OTHER (2.6 FTE)	41.4	
	<u>695.3</u>	
LESS MSU CONTRIBUTION	103.8	
NSF CONTRIBUTION TO SALARIES	<u>591.5</u>	591.5
FRINGES (18.9%)		111.8
UNDERGRADUATES (14 @29hrs/week)		85.5
TRAVEL SUPPORT		12.0
ION SOURCE (TABLE I.2)		107.5
CRYOGENICS (TABLE I.3)		102.0
RF UPGRADE (TABLE I.4)		96.0
RF AND DEFLECTOR MAINTENANCE (TABLE I.5)		37.4
CONTROL SYSTEM (TABLE I.6)		21.5
LCW, ELECTRICAL, HYDRAULICS (TABLE I.7)		12.0
UTILITIES		33.3
COMPUTER MAINTENANCE (TABLE I.8)		107.7
COMPUTER SUPPLIES AND SOFTWARE (TABLE I.9)		31.1
BEAMLINES (TABLE I.10)		19.2
K500 EQUIPMENT (TABLE I.11)		34.3
O. H. (39.5% of Non-equipment items)		474.2
TOTAL		<u>\$1877.0K</u>

TABLE II.1

USER SUPPORT		
	K\$	K\$
PRINCIPAL INVESTIGATORS & CO. PI.'S	51.8	
FACULTY & SENIOR ASSOC	155.1	
POST DOCS (.6 FTE)	11.8	
OTHER PROFESSIONALS (4.0 FTE)	72.0	
SECRETARIAL-CLERICAL (.8 FTE)	11.85	
OTHER (.7 FTE)	10.0	
	<hr/> 312.5	
LESS MSU CONTRIBUTION	59.0	
TOTAL	<hr/> 253.6	253.6
FRINGES (18.9%)		47.9
EXPENSES FOR PROGRAM ADVISORY COMM, USER'S EXEC COMM, VISITORS AND UNFUNDED USERS (TABLE II.2)		41.0
ADAPTATION OF BEAMLINES, PROVISION OF BEAMLINE ELEMENTS		14.0
UPGRADE OF ELECTRONICS (TABLE II.3)		146.0
COMPUTER TERMINALS FOR GENERAL USE		6.0
TARGET AND DETECTOR LABS (TABLES II.4 AND II.5)		49.5
OVERHEAD (39.5% on Non-Equipment Items)		144.6
TOTAL		<hr/> <u>\$702.6K</u> <hr/>

TABLE IV.2

NUCLEAR SCIENCE RESEARCH		
	K\$	K\$
PRINCIPAL INVESTIGATORS & CO. PI.'S	267.1	
FACULTY & SENIOR ASSOC	167.7	
OTHER PROFESSIONALS (3.7 FTE)	65.8	
SECRETARIAL AND CLERICAL (2.8 FTE)	39.2	
OTHER (2.3 FTE)	32.5	
	<u>572.3</u>	
LESS MSU CONTRIBUTION	204.2	
NSF CONTRIBUTION TO SALARIES	<u>368.1</u>	368.1
RESEARCH ASSOCIATES (8.4 FTE)		166.6
FRINGE BENEFITS (18.9%)		101.1
GRADUATE STUDENTS (26)		234.0
UNDERGRADUATE STUDENTS (5 FTE)		30.0
ADMINISTRATIVE COSTS (60% share of telephone, copying, supplies, postage, etc.)		54.0
PAGE CHARGES		24.0
SEMINARS & CONSULTANTS		13.0
LIBRARY		2.5
TRAVEL (Conferences, Committees)		39.0
TRAVEL FOR EXPERIMENTS (See TABLE IV.1)		51.0
MAGNETIC TAPES		10.0
SPECIAL TARGETS (See TABLE IV.1)		11.0
OVERHEAD (39.5% on non equipment items)		436.2
EQUIPMENT (See TABLE IV.1)		94.0
TOTAL		<u>\$1634.5K</u>

TABLE V.1

ACCELERATOR R&D		
	K\$	K\$
PRINCIPAL INVESTIGATORS & CO. PI.'S	17.0	
FACULTY & SENIOR ASSOC.	23.2	
OTHER PROFESSIONALS (0.5 FTE)	9.4	
SECRETARIAL AND CLERICAL (0.1 FTE)	1.2	
OTHER (0.2 FTE)	3.5	
	<u>54.3</u>	
LESS MSU CONTRIBUTION	19.7	
NSF CONTRIBUTION TO SALARIES	34.6	34.6
FRINGE BENEFITS (18.9%)		6.5
GRADUATE STUDENTS (2)		18.0
UNDERGRADUATE STUDENTS (0.5)		3.0
ADMINISTRATIVE COSTS (5% SHARE OF TELEPHONE, COPYING, SUPPLIES, POSTAGE, ETC.)		4.5
PAGE CHARGES		1.5
TRAVEL (CONFERENCES, COMMITTEES)		5.0
MAGNETIC TAPES		3.0
OTHER SUPPLIES		2.5
OVERHEAD (39.5% ON NON EQUIPMENT ITEMS)		31.1
TOTAL		<u>\$109.7K</u>

Table VI.1

THREE YEAR COST SUMMARY ASSUMING INFLATION
CORRECTION OF 5% PER YEAR

actual 5.5%
special \$37,500

Year	Requested budget in 1983 dollars	Requested budget in year-of-expenditure dollars
1984	4,323.7K	4,539.9K
1985	5,373.7K	5,924.5K
1986	5,911.1K	6,842.8K
TOTAL		17,307.2K

TABLE VI.2

For period Nov. 1, 1983 - Oct. 31, 1984

(SEE INSTRUCTIONS ON REVERSE BEFORE COMPLETING)

SUMMARY PROPOSAL BUDGET

FOR NSF USE ONLY

ORGANIZATION National Superconducting Cyclotron Laboratory Michigan State University, East Lansing, MI 48824		PROPOSAL NO.		DURATION (MONTHS)	
PRINCIPAL INVESTIGATOR/PROJECT DIRECTOR H.G. Blosser and D.K. Scott		AWARD NO.		Proposed	Granted
				12	
A. SENIOR PERSONNEL: PI/PD, Co-PI's, Faculty and Other Senior Associates (List each separately with title; A.6. show number in brackets)		NSF FUNDED PERSON-MOS.		FUNDS REQUESTED BY PROPOSER	
		CAL. ACADSUMR		FUNDS GRANTED BY NSF (IF DIFFERENT)	
1. (12) See Introduction Table II		28.8		\$137.9K	
2.					
3.					
4.					
5. (20) OTHERS (LIST INDIVIDUALLY ON BUDGET EXPLANATION PAGE)		192		486.3	
6. (28) TOTAL SENIOR PERSONNEL (1-5)				624.2	
B. OTHER PERSONNEL (SHOW NUMBERS IN BRACKETS)					
1. (9) POST DOCTORAL ASSOCIATES		108		187.3	
2. (67) OTHER PROFESSIONALS (TECHNICIAN, PROGRAMMER, ETC.)		320.4		511.2	
3. (28) GRADUATE STUDENTS				264.6	
4. (21) UNDERGRADUATE STUDENTS				124.4	
5. (4.7) SECRETARIAL-CLERICAL				70.7	
6. (5.8) OTHER				91.9	
TOTAL SALARIES AND WAGES (A+B)				1874.3	
C. FRINGE BENEFITS (IF CHARGED AS DIRECT COSTS) 18.9%				280.7	
TOTAL SALARIES, WAGES AND FRINGE BENEFITS (A+B+C)				2155.0	
D. PERMANENT EQUIPMENT (LIST ITEM AND DOLLAR AMOUNT FOR EACH ITEM EXCEEDING \$1,000; ITEMS OVER \$10,000 REQUIRE CERTIFICATION)					
See details in Tables I.1-11, II.1-5, IV.1-2					
TOTAL PERMANENT EQUIPMENT				514.3	
E. TRAVEL 1. DOMESTIC (INCL. CANADA AND U.S. POSSESSIONS) (Including Exec.Users				125.0	
2. FOREIGN Comm. & PAC)-Visitors					
F. PARTICIPANT SUPPORT COSTS					
1. STIPENDS \$ _____					
2. TRAVEL _____					
3. SUBSISTENCE _____					
4. OTHER _____					
TOTAL PARTICIPANT COSTS					
G. OTHER DIRECT COSTS					
1. MATERIALS AND SUPPLIES				377.2	
2. PUBLICATION COSTS/PAGE CHARGES				26.8	
3. CONSULTANT SERVICES includes user & visitor support (Tables II.1,II.2)				44.2	
4. COMPUTER (ADPE) SERVICES Maintenance & Repairs (Tables I.6,I.8)				122.5	
5. SUBCONTRACTS					
6. OTHER (Electricity)				35.0	
TOTAL OTHER DIRECT COSTS					
H. TOTAL DIRECT COSTS (A THROUGH G)					
I. INDIRECT COSTS (SPECIFY) 39.5% of total direct costs except permanent equipment				1139.9	
TOTAL INDIRECT COSTS					
J. TOTAL DIRECT AND INDIRECT COSTS (H + I)				4539.9K	
K. RESIDUAL FUNDS (IF FOR FURTHER SUPPORT OF CURRENT PROJECTS GPM 252 AND 253)				0	
L. AMOUNT OF THIS REQUEST (J) OR (J MINUS K)				\$4539.9K	

PI/PD TYPED NAME & SIGNATURE*	DATE	FOR NSF USE ONLY		
INST. REP. TYPED NAME & SIGNATURE*	DATE	INDIRECT COST RATE VERIFICATION		
		Date Checked	Date of Rate Sheet	Initials - DGC

APPENDICES SEPARATELY BOUND

VOLUME MSUCL-404A